UCLA
UCLA Electronic Theses and Dissertations

Title
Transcriptional Control of Hepatic Metabolism in Physiology

Permalink
https://escholarship.org/uc/item/6ht528rf

Author
Bideyan, Lara

Publication Date
2022

Peer reviewed|Thesis/dissertation

eScholarship.org Powered by the California Digital Library
University of California

UNIVERSITY OF CALIFORNIA

Los Angeles

Transcriptional Control of Hepatic Lipid Metabolism in Physiology

A dissertation submitted in partial satisfaction of the requirements for the degree Doctor of Philosophy in Molecular, Cellular, and Integrative Physiology

by

Lara Bideyan

2022

© Copyright by

Lara Bideyan

2022

ABSTRACT OF THE DISSERTATION

Transcriptional Control of Hepatic Metabolism

in Physiology

by

Lara Bideyan

Doctor of Philosophy in Molecular, Cellular, and Integrative Physiology

University of California, Los Angeles, 2022

Professor Peter John Tontonoz, Chair

Liver is a key regulator of systemic metabolism in physiology and pathology. It maintains cholesterol, triglyceride and glucose homeostasis in response to fasting and feeding. Transcription factors responsive to hormones and nutrients coordinate many of these responses. They regulate gene networks relating to lipid, glucose and amino acid metabolism during fasting and feeding, and factors such as sex, circadian rhythms and dietary content interact with these transcriptional programs, as reviewed in chapter 1. Understanding the different players in these processes and how they interact with each other will be key to develop strategies to combat metabolic diseases. Recent advances in probing the transcriptional landscape, coupled with high throughput sequencing approaches such as assay for transposase accessible chromatin (ATAC-Seq), have enabled the identification of transcriptional regulators of these processes and their interrelationships. In chapter 2, I describe results from a screen using ATAC-Seq and RNA-Seq to profile novel transcriptional regulators of the hepatic response to fasting and feeding. We

determined GATA4 expression and activity to be upregulated by feeding through insulin. Knocking out *Gata4* in adult liver impaired the transcriptional and metabolic response to feeding. Additionally, loss of hepatic GATA4 led to a reduction in HDL cholesterol and to the accumulation of liver triglycerides. These effects were accompanied by the downregulation of genes involved in cholesterol efflux and triglyceride hydrolysis, and the upregulation of genes involved in lipid uptake. Furthermore, hepatic GATA4 colocalized and collaborated with Liver X Receptor (LXR), a key regulator of cholesterol transport. In chapter 3, I investigated the dynamics of hepatic LXRs via ATAC-Seq and RNA-Seq in wild-type and LXRα/β knockout liver. Loss of LXRs in liver changed the transcriptional regulatory landscape by reducing accessibility at enhancers and increasing accessibility at promoters. A broad set of transcription factors that bind enhancers, including nuclear receptors, had reduced activity based on their motif accessibility, showing their reliance on LXRs. Moreover, this investigation demonstrated that LXR also functions as a transcriptional repressor of certain genes. Overall, these studies revealed important functions for GATA4 and LXR within hepatic transcriptional networks, extending our understanding of transcriptional regulation of hepatic lipid metabolism.

The dissertation of Lara Bideyan is approved.

Aldons J. Lusis

Xia Yang

Andrea L. Hevener

Peter John Tontonoz, Committee Chair

University of California, Los Angeles

2022

Table of Contents

Acknowledgements viii

Vita x

Chapter 1 : Hepatic Transcriptional Responses to Fasting and Feeding 1

Abstract 2

Introduction 3

Lipid metabolism 3

Glucose metabolism 9

Other fasting/feeding responsive pathways 13

High throughput sequencing and -omics studies 16

Epigenetics and transcription factor relationships 19

Insulin signaling and insulin resistance 23

Effect of time on fasting and feeding response 24

Effect of diet, exercise and sex on fasting and feeding response 30

Conclusions 33

Figures 35

Figure legends 38

Chapter 2 : Hepatic GATA4 regulates cholesterol and triglyceride homeostasis 40

Abstract 41

Introduction 42

Results 42

Discussion 44

Methods 55

Figures and Tables 66

Figure Legends 82

Chapter 3 : Integrative analysis reveals multiple modes of LXR transcriptional regulation in liver 90

Abstract 91

Significance Statement 92

Introduction 93

Results 96

Discussion 107

Methods 112

Figures and Tables 116

Figure Legends 130

Chapter 4 : Conclusions 136

References 139

Table of Figures and Tables

Figure 1-1-1: Transcription factors that regulate lipid metabolism in fasted and fed state 35

Figure 1-1-2: Transcription factors that regulate glucose metabolism in fasted and fed states.... 36

Figure 1-1-3:Interplay of circadian rhythm and hepatic gene regulation in mice 37

Figure 2-1: GATA4 motif accessibility and expression is upregulated in liver by feeding. 66

Figure 2-2: Loss of Gata4 in liver alters the hepatic and systemic lipid profile in fasting and in feeding..... 67

Figure 2-3: Loss of Gata4 downregulates lipid metabolism pathways in fasting and in feeding. 68

Figure 2-4: GATA4 has common and differential targets in fasted versus refed liver..... 69

Figure 2-5: Loss of Gata4 results in reduction in plasma cholesterol and accumulation of liver triglycerides..... 70

Figure 2-6: GATA4 collaborates with LXR to induce shared transcriptional targets. 71

Figure 3-1:Global chromatin accessibility changes in LXRDKO liver..... 116

Figure 3-2: Correlation of LXR binding, gene expression, and chromatin accessibility. 117

Figure 3-3: Loss of LXR affects chromatin accessibility at other transcription factor binding sites. 118

Figure 3-4: Increased accessibility of NFY motifs in LXR-deficient liver. 119

Figure 3-5:LXR can act as a ligand-dependent and -independent repressor. 120

Figure 3-S3-6: Loss of LXRs reduces motif accessibility of other transcription factors. 126

Figure 3-S3-7: Impact of the loss of LXR on other transcription factor motif activity..... 127

Figure 3-8: Change in accessibility and genomic features at the LXR binding sites in relation to different modes of LXR action. 128

Acknowledgements

I would like to thank everyone who has supported me throughout my scientific journey. Foremost, I would like to thank my advisor, Dr. Peter Tontonoz, for guiding me throughout these years. He provided the calm confidence when the experiments weren't working. He has taught me how to see and communicate the big picture in my projects. Moreover, I would like to extend my thanks to everyone in the Tontonoz laboratory, for listening to my concerns and questions every day for the last 6 years, making it a lot of fun. I would also like to thank my committee members Dr. Jake Lusis, Dr. Andrea Hevener and Dr. Xia Yang for their helpful suggestions throughout my project.

Outside of academia, I would like to thank my mom, dad and my sister for making me the person I am today. I would like to thank my partner Christopher Pavia for the love and support he brings to our home, helping me weather the stress of graduate school. I would like to thank Chris' family for welcoming me into their family. Furthermore, I would like to thank my friends at UCLA both from MCIP and other programs for bringing so much joy into my life. Lastly, I want to show my gratitude to family and friends in California and also in Turkey for keeping me in their heart and messages throughout these years.

Chapter 1 is adapted from a version of a paper published in Genes and Development. Title: Hepatic transcriptional responses to fasting and feeding. Authors: Lara Bideyan, Rohith Nagari, and Peter Tontonoz. L.B. and R.N. wrote the manuscript and P.T. reviewed and edited the manuscript.

Chapter 2 is a adapted from manuscript under review in Genes and Development. Title: Hepatic GATA4 regulates cholesterol and triglyceride homeostasis. Authors: Lara Bideyan,

Maykel Lopez, Christina Priest, John P. Kennelly, An-Chie Feng, Alessandra Ferrari, Prashant Rajbhandari, Peter Tontonoz. L.B. and P.T. designed the study and wrote the manuscript. L.B., M.L. and C.P. conducted the sequencing experiments. L.B., A.C.F, and P.R. analyzed the sequencing data. L.B., C.P., M.L., J.P.K., and A.F. conducted the metabolic phenotyping experiments and L.B. analyzed the data. M.L. conducted the ChIP experiments. P.T. C.P., M.L., J.P.K., and A.F. provided feedback on the data. Additionally, we thank Sergei Tevosian for providing the Gata4 floxed mice.

Chapter 3 is adapted from a version of a paper published in Proceedings of the National Academy of Sciences. Title: Integrative analysis reveals multiple modes of LXR transcriptional regulation in liver. Authors: Lara Bideyan, Wenxin Fan, Karolina Elzbieta Kaczor-Urbanowicz, Christina Priest, David Casero, Peter Tontonoz. L.B., W.F., D.C., and P.T. designed research; L.B., W.F., and C.P. performed research; L.B., W.F., K.E.K.-U., D.C., and P.T. analyzed data; and L.B., D.C., and P.T. wrote the paper. Funding for these projects were provided by grants to P.T. from the NIH (HL136618, DK126779, and DK063491).

Vita

• EDUCATION

PhD University of California, Los Angeles (expected) August 2022
Molecular, Cellular, and Integrative Physiology
Dissertation: GATA4 in Liver Lipid Metabolism: Using ATAC-Seq to Identify New Transcriptional Regulators

BS University of California, Berkeley May 2015
Major: Molecular and Cell Biology
Honors in Molecular and Cell Biology, High Distinction in General Scholarship
Thesis: Acyl-CoA Thioesterase 2 Is a Potential Novel Target for Breast Cancer Aggressiveness

• HONORS AND AWARDS

Dissertation Year Fellowship, UCLA 2021 – 2022

Mangasar M. Mangasarian Scholarship, UCLA 2019 - 2021

UCLA Affiliates Award 2018 - 2020

Graduate Dean's Scholar Award, UCLA 2016 - 2018

I.L. Chaikoff Memorial Award, UC Berkeley 2015
For outstanding achievement and excellence

Dean's Honors, UC Berkeley 2012, 2013

• RESEARCH EXPERIENCE

PhD candidate, UCLA 2017 – present
Advisor: Peter Tontonoz, MD, PhD
Project: Using ATAC-Seq to Identify New Transcriptional Regulators of Lipid Liver Metabolism

Research Lab Technician II, USC 2015 - 2016
The Lawrence J. Ellison Institute for Transformative Medicine of USC
Supervisor: Jonathan Katz, PhD

Undergraduate Researcher, UC Berkeley 2014 - 2015
Advisor: Daniel Nomura, PhD
Project: Investigating the role of acyl-CoA thioesterase-2 (ACOT2) in breast cancer aggressiveness

• TEACHING AND MENTORING EXPERIENCE

Teaching Assistant, UCLA Jan to March, 2018 and 2019
Course: Physiology of Nutrition

Graduate Student Mentor, UCLA 2019 - 2021
Mentored an undergraduate researcher

- **PEER REVIEWED PUBLICATIONS**

Review Articles

Bideyan, L., Nagari, R. & Tontonoz, P. (2021). Hepatic transcriptional responses to fasting and feeding. Genes Dev.

Research Articles

Bideyan, L., López Rodríguez, M., Priest, C., Kennelly, J.P., Ferrari, A., Rajbhandari, P., Feng, A.-C., Tevosian, S.G., Smale, S.T., Tontonoz, P. Hepatic GATA4 regulates cholesterol and triglyceride homeostasis in collaboration with LXRs. Manuscript under review. Genes and Dev.

Priest, C., Nagari, R., **Bideyan, L.**, Lee, S.D., Nguyen, A., Tontonoz, P. (2022) Brap regulates liver morphology and hepatocyte turnover via modulation of the Hippo pathway. PNAS, 119(18). https://doi.org/10.1073/pnas.2201859119

Bideyan, L., Fan, W., Kaczor-Urbanowicz, K.E., Priest, C., Casero, D., and Tontonoz, P. (2022). Integrative analysis reveals multiple modes of LXR transcriptional regulation in liver. PNAS 119(7). https://doi.org/10.1073/pnas.2122683119

Kohnz, R. A., Roberts, L. S., DeTomaso, D., **Bideyan, L**., Yan, P., ... & Nomura, D. K. (2016). Protein Sialylation Regulates a Gene Expression Signature that Promotes Breast Cancer Cell Pathogenicity. ACS Chemical Biology, 11(8), 2131-2139.

- **PRESENTATIONS**

"The Role of GATA4 in Liver Lipid Metabolism: Using ATAC-Seq to Identify New Transcriptional Regulators". Oral Presentation. March 2022 at the Molecular, Cellular and Integrative Interdepartmental PhD Program Annual Retreat, Los Angeles, CA

"Dissecting the Role of GATA4 in Liver Lipid Metabolism". Poster presentation. March 2022 at the annual Deuel Conference on lipids, Monterey, CA.

"The Role of GATA4 in Liver Lipid Metabolism". Poster presentation. March 2021 at the Keystone eSymposia titled "Fatty Liver Disease and Multi-Systems Complications".

"Discovering the Role of Hepatic GATA4 in Lipid Metabolism". Poster presentation. February 2020 at the Molecular, Cellular and Integrative Interdepartmental PhD Program Annual Retreat, Malibu, CA

"GATA4 in Liver Lipid Metabolism: Using ATAC-Seq to Identify New Transcriptional Regulators". Poster presentation. February 2019 at the Molecular, Cellular and Integrative Interdepartmental PhD Program Annual Retreat, Malibu, CA

"ACOT2 is a potential novel target for breast cancer aggressiveness.". Poster presentation. May 2015 at the Molecular Cell Biology Honors Symposia, Berkeley, CA

- Received Outstanding Poster Award.

- **PROFESSIONAL AFFILIATIONS**

American Society for Biochemistry and Molecular Biology
Graduate Women in Science

Chapter 1 : Hepatic Transcriptional Responses to Fasting and Feeding

Lara Bideyan, Rohith Nagari and Peter Tontonoz*

Department of Pathology and Laboratory Medicine, Department of Biological Chemistry and Molecular Biology institute, University of California, Los Angeles, CA 90095 USA

* Version of an accepted manuscript, published in Genes and Development, 2021.

Abstract

Mammals undergo regular cycles of fasting and feeding that engage dynamic transcriptional responses in metabolic tissues. Here we review advances in our understanding of the gene regulatory networks that contribute to hepatic responses to fasting and feeding. The advent of sequencing and -omics techniques have begun to facilitate a holistic understanding of the transcriptional landscape and its plasticity. We highlight transcription factors, their cofactors, and the pathways that they impact. We also discuss physiological factors that impinge on these responses, including circadian rhythms and sex differences. Finally, we review how dietary modifications modulate hepatic gene expression programs.

Introduction

In mammals, the transitions between fasting and fed states are accompanied by complex changes in hepatic gene expression. The liver is a central hub for coordination of fasting-feeding transitions given its roles in maintaining blood glucose levels, processing dietary nutrients, and regulating whole-body energy metabolism (reviewed in Trefts et al. 2017). During fasting the liver is the target of hormones such as glucagon which shift it into an energy production mode [2]. In response, the liver takes up free fatty acids (FFAs) released into the circulation by adipose lipolysis to provide energy for itself and to generate ketones for use by other tissues [3]. It also breaks down glycogen and amino acids to generate glucose for the brain (reviewed in Berg et al. 2002). In the postprandial state–signaled by insulin and the influx of dietary carbohydrates–liver suppresses the production of glucose and switches to utilizing it as its main fuel (reviewed in Rui 2014). Excess glucose is converted into glycogen and fatty acids. Newly synthesized and dietary fatty acids are esterified to generate triglycerides, which are packaged and exported to the circulation (reviewed Alves-Bezerra and Cohen 2017). Transcriptional regulation is fundamental to the execution of each these physiological responses. Regulation of transcription involves the coordinated action of a bevy of transcription factors, co-regulators and chromatin modifying enzymes, all acting downstream of hormonal signaling pathways. Elucidating the complex metabolic changes associated with fasting and feeding and their transcriptional underpinnings is crucial for understanding both normal physiology and metabolic pathologies such as insulin resistance. Given the extent of transcriptional pathways affected, feeding status can be a critical variable in the design of experiments involving animals and humans.

Lipid metabolism

PPAR*α*, fatty acid oxidation and ketogenesis

The nuclear receptor peroxisome proliferator-activated receptor alpha (PPARα) sits atop a crucial node coordinating changes in hepatic lipid metabolism during fasting. Seminal studies by Gonzalez and colleagues showed that PPARα-knockout mice are compromised in fatty acid oxidation and ketogenesis [7,8]. PPARα governs the expression of a battery of genes that coordinates fatty acid uptake and oxidation, ketogenesis, and lipid droplet dynamics during fasting. Regulation of acyl-coA oxidase 1 (ACOX1) by PPARα facilitates peroxisomal long chain fatty acid (LCFA) oxidation. PPARα induces mitochondrial LCFA oxidation through upregulation of carnitine palmitoyltransferase 1a and 2 (CPT1A and CPT2) (which transport LCFA into the mitochondria), malonyl-CoA decarboxylase (which degrades the CPT1 inhibitor malonyl-CoA), and other β oxidation enzymes. PPARα also induces ketogenesis pathway enzymes, including 3-hydroxy-3-methylglutaryl-CoA lyase (HMGCL), acetyl-CoA acetyltransferase 1 (ACAT1), and 3-hydroxy-3-methylglutaryl-CoA synthase 2 (HMGCS2) [9,10]. PPARα regulates phospholipid remodeling as well by influencing expression of choline kinase isotypes a and b (CHKA and CHKB), as well as the acyl-transferases glycerol-3-phosphate acyltransferase 3 (GPAT3) and monoacylglycerol O-acyltransferase 1 (MOGAT1) [11]. Additionally, PPARα induces expression of fibroblast growth factor 21 (FGF21), a liver hormone that promotes β-oxidation and ketogenesis [12]. FGF21 contributes to the upregulation of proliferator-activated receptor γ coactivator protein-1α (PGC-1α) which serves as a transcriptional coactivator of genes in LCFA oxidation and ketogenesis [13].

Importantly, fatty acids and their derivatives are activating ligands for PPARα and thereby help to control their own metabolism [14–16]. During fasting, PPARα has been hypothesized to be activated by the influx of FFA from adipose lipolysis [7,17]. However, Sanderson et al. (2009) suggested that peroxisome proliferator-activated receptor delta (PPARδ)

rather than PPARα is activated by FFA from adipose lipolysis during fasting. Chakravarthy et al. (2005) suggested that PPARα could be activated by hepatic lipid products of fatty acid synthase (FASN). Other studies indicate that PPARα may be activated by lipolysis of locally stored triglycerides [20]. Glucagon, sirtuin 1 (SIRT1), glucocorticoid receptor (GR) and PPARG coactivator 1 alpha (PGC-1α) are known to promote PPARα activity during fasting (Fig 1-1B) [21–24]. Suppression of mechanistic target of rapamycin kinase (mTOR) signaling in fasting was found to be necessary for PPARα ketogenic activity [25]. Additional evidence suggests that SRY-box transcription factor 17 (Sox17) and cyclin dependent kinase inhibitor 1a (p21) might also play roles in activation of PPARα [26,27].

Transcription factors in feeding-induced lipogenesis

In the fed state, liver receives dietary carbohydrates from the portal vein and the excess glucose is converted into fatty acids through de novo lipogenesis. Fatty acids are then esterified to make phospholipids, triglyceride and cholesterol esters. Sterol regulatory element binding transcription factor 1c (SREBP-1c) binds to sterol regulatory elements (SREs) in the regulatory regions of its target gene promoters [28]. SREBP-1c is induced in the fed state and plays a central role in coordinating lipid synthesis.Immature ER membrane-bound SREBP-1c protein is processed in the Golgi and the mature transcription factor subsequently travels to nucleus where it activates its target genes [29]. SREBP-1c induces the transcription of multiple genes in fatty acid biosynthesis. It drives expression of ATP citrate lyase (ACLY) to make acetyl-CoA, and acetyl-CoA carboxylase alpha (ACC1*)* and FASN to convert Acetyl-CoA into palmitate. Regulation of elongation of very long chain fatty acids protein 6 (ELOVL6) and stearoyl-CoA desaturase (SCD-1) by SREBP-1c facilitates the elongation and desaturation of fatty acids, respectively [30,31]. Additional fatty acid desaturase 1 and 2(FADS1 and FADS2), regulated by SREBP-1c, influence polyunsaturated fatty acid (PUFA) generation. SREBP-1c also regulates the expression of genes encoding proteins linked to triglyceride synthesis, including patatin like

phospholipase domain containing 3 (PNPLA3*)*, mitochondrial glycerol-3-phosphate acyltransferase (GPAM*)*, malic enzyme (ME*)*, and glucose-6-phosphate dehydrogenase (G6PD) [32]. Studies have shown that ~ 50% of the hepatic lipogenic response to feeding is abolished in SREBP-1c-knockout mice [33].

Insulin secretion in response to a carbohydrate-rich diet promotes both transcription of *Srebf1* (the gene for SREBP1-c) and processing of immature SREBP-1c protein [34]. Although it is clear from knockout studies that SREBP-1c is a major mediator of insulin's lipogenic actions [35,36], the underlying mechanisms by which insulin controls SREBP-1c activity are incompletely understood. Yamamoto et al. (2010) and Matsumoto et al. (2003) provided evidence that inhibition of protein kinase C beta and lambda (PKCβ and PKCλ) reduces insulin-dependent SREBP-1c activation. Analysis of the *Srebf1* promoter has identified several transcription factors that contribute its insulin responsiveness, including liver x receptors (LXRs), CCAAT enhancer binding protein beta (C/EBPβ) and basic helix-loop-helix family member e40 BHLHE40 (Fig 1-1A) [39–41]. SREBP-1c also induces its own promoter [42].

Multiple studies have shown that feeding increases SREBP-1c processing, and this effect appears to be in part mTORC1-dependent and facilitated by protein kinase B (also known as AKT)phosphorylation [43,44]. Studies have also suggested that SREBP-1c activity may be regulated by phosphorylation and acetylation. Phosphorylation by protein kinase A (PKA) was reported to attenuate SREBP-1c binding at lipogenic promoters [45]. SREBP-1c may be acetylated under high insulin and high glucose conditions by histone acetyltransferase p300 [46]. E4 promoter-binding protein 4 (E4BP4), a transcription factor that is upregulated during feeding by SREBP-1c, physically interacts with mature SREBP-1c and protects it from degradation by promoting its acetylation (Fig 1-1A) [47]. Conversely, the fasting-responsive factor SIRT1 deacetylates SREBP-1c, leading to its degradation [46].

Insulin induced gene proteins (INSIG-1 and INSIG-2) capture SREBP cleavage-activating protein (SCAP) and prevent it from escorting SREBP-1c to the Golgi for cleavage. Regulation of *Insig1* and *Insig2* thereby provides another layer of control for the feeding response of SREBP-1c. Insulin reduces *Insig2a* expression in fed liver, allowing SREBP-1c to be processed [48]. Additionally, dietary PUFAs have

been shown to inhibit refeeding-induced SREBP-1c activation by suppressing processing [49]. Xu et al. (2001) also showed that PUFAs can increase *Srebf1c* mRNA decay. More recently, Kim et al. (2017) showed that inhibiting ACC1 decreased PUFA biosynthesis, which led to increases in *Srebf1c* mRNA expression. Other studies indicate that ER phospholipid composition is a determinant of SREBP-1c activity. In feeding and in obesity, increased levels of polyunsaturated phosphatidylcholine generated by the remodeling enzyme lysophosphatidylcholine acyltransferase 3 (LPCAT3) promote SREBP-1c processing [52]. Further studies are needed to reveal the complex relationship between the effects of free PUFAs and polyunsaturated phospholipids on SREBP-1c activity.

LXRα is a nuclear receptor activated by oxysterols [53]. Although LXRα is required for maximal transcription of *Srebf1* [54], whether or not LXRα itself conveys a feeding signal less clear. Anthonisen et al. (2010) suggested that glucose feeding can activate LXRα via O-linked β-N-acetylglucosamine (*O*-GlcNAc) modification (Fig 1-1A). However, in contrast to *Srebf1*, most other LXRα targets genes in liver are not induced appreciably by feeding (e.g. *Abcg5/8*, *Abca1*). Furthermore, *Srebf1* expression is still induced by feeding in LXRα/β double knockout mice, even though basal levels are reduced [56]. Interestingly, *Lpcat3* expression is also controlled by LXRα in the liver. Induction of LPCAT3-dependent ER phospholipid remodeling thus provides a mechanism whereby LXR can stimulate SREBP-1c processing as well as transcription [52].

Upstream transcription factor 1 (USF-1) is another factor important in the lipogenic response. USF-1 is necessary for the full activation of *Fasn* by feeding and insulin. USF-1 binds to the *Fasn* promoter constitutively, but its activity is modulated by posttranslational modifications. USF-1 bound to the *Fasn* promoter is phosphorylated by DNA-dependent protein kinase (DNA-PK) during feeding, thereby inducing transcription (Fig 1-1A) [57]. Studies suggest that USF-1 acts synergistically with SREBP-1c on *Fasn* and *Gpam* [58,59]. In contrast, USF-1 has been reported to be deacetylated by histone deacetylase 9 (HDAC9) during fasting, which prevents the recruitment of activating factors [57].

Carbohydrate-responsive element-binding protein (ChREBP) is a transcription factor that induces hepatic lipogenesis in response to glucose signals. ChREBP heterodimerizes with Max-like protein X (MLX) and binds to carbohydrate response elements (ChoREs) in its target genes [60]. Known lipogenic targets for ChREBP include *Acly, Fasn, Acc1* and *Scd1* [61]. ChREBP has been shown to physically interact with hepatocyte nuclear factor 4-alpha (HNF-4α) on the *Fasn* promoter, facilitating its binding during feeding [62]. Hepatic ChREBP deficiency reduces lipogenic gene expression along with SREBP-1c expression, suggesting that both ChREBP and SREBP-1c must to be activated by glucose and insulin respectively to enable the full lipogenic response to feeding [63].

Similar to SREBP-1c, ChREBP can induce its own gene expression in a feed-forward loop (reviewed in Iizuka 2013). The *Chrebpa* gene is also an LXR target and LXRα is necessary for induction of ChREBPα expression and activity [65]. Additionally, post-transcriptional modifications, especially phosphorylation by PKA and 5'-AMP-activated protein kinase (AMPK) during fasting, have been shown to decrease ChREBP DNA binding (Fig 1-1A) [66,67]. In the setting of high glucose availability, xylulose-5-phosphate (Xu5P) ,an intermediate of the pentose-phosphate shunt, leads to the dephosphorylation of ChREBP through Xu5P activated protein phosphatase (PP2a) [68]. ChREBP is also *O*-GlcNAcylated under high glucose conditions, thus stabilizing the protein [69,70,70].

Cholesterol biosynthesis controlled by SREBP-2 is also is upregulated in the fed state. Forkhead box protein O3 (FOXO3) was reported to cause downregulation of the SREBP-2 pathway during fasting by recruiting SIRT6 to the promoter of *Srebf2* (gene for SREBP-2)(Fig 1-1A)[71]. Using liver-specific glucose transporter 2 (GLUT2)-knockout mice, Seyer et al. (2013) showed that the upregulation of cholesterol biosynthesis genes in the fed condition was influenced by hepatic glucose uptake. Interestingly, a recent paper by Lu et al. (2020) indicates that feeding also induces cholesterol synthesis by stabilizing the SREBP-2 target 3-hydroxy-3-methylglutaryl-coenzyme A reductase (HMGCR), which catalyzes the rate limiting enzyme in cholesterol synthesis. They show that feeding-activated mTORC

phosphorylates ubiquitin carboxyl-terminal hydrolase 20 (USP20), which in turn is recruited to the HMGCR complex to prevent its degradation.

There is conflicting evidence as to the role of inositol-requiring, endoplasmic reticulum-to-nucleus signaling protein 1a (IRE1a) and X-box-binding protein-1 (XBP1) signaling in fasting and refeeding. Zhang et al. showed that hepatic growth differentiation factor 15 (GDF15) is activated by IRE1a-XBP1 during fasting-induced hepatic β-oxidation and ketogenesis [74]. However, Pfaffenbach et al. (2010) reported that mTORC1 activates IRE1a-XBP1 in the postprandial period in the context of lipogenesis.

Glucose metabolism

Transcriptional regulators of glucose metabolism during fasting

CREB

Cyclic AMP (cAMP) response element-binding protein (CREB) plays a dominant role in driving hepatic glucose production during fasting. CREB controls the expression of enzymes catalyzing key steps for hepatic glucose production such as glucose 6-phosphatase (G6Pase; encoded by *G6pc*) which is necessary for both glycogenolysis and gluconeogenesis and phosphoenolpyruvate carboxykinase (PEPCK; encoded by *Pck1*) needed for gluconeogenesis from TCA cycle intermediates [76,77]. Inhibition of CREB reduces fasting hepatic glucose production [78]. The CREB homolog CREB-H is also induced during fasting and binds to CREB-regulated transcription coactivator 2 (CRTC2, also known as TORC-2) to promote the expression of gluconeogenic genes [79]. In addition to its direct targets, CREB induces the expression of other transcription factors that promote gluconeogenesis such as yin yang 1 (YY1) and nuclear hormone receptor NUR/77 (NUR77) and ketogenesis such as transcription factor EB (TFEB) [80–82]. CREB is activated during acute fasting through phosphorylation and dephosphorylation events. A cascade involving glucagon receptor-cAMP-PKA leads to the formation of an active CREB-CREB

binding protein (CBP)-CRTC2 complex (Fig 1-2B)(reviewed in Altarejos and Montminy 2011). By contrast, in long-term fasting, SIRT1 deacetylates and AMPK phosphorylates CRTC2. These modifications reduce CREB activity and facilitate a switch to FOXO1/PGC-1α-driven gluconeogenesis [84,85]. In feeding, insulin signaling causes phosphorylation of CBP and CRTC2 via PKCλ/ι and salt inducible kinase 2 (SIK2) respectively, triggering the dissociation of the CREB-CBP-CRTC2 complex and cessation of CREB activity [86,87]. Additionally, during refeeding after fasting, ER stress activates activating transcription factor 6 (ATF6) as part of the unfolded protein response pathway. ATF6 binds to CRTC2 and sequesters it from CREB, thereby inhibiting gluconeogenic gene expression [88].

FOXO1

A member of the FOXO family of transcription factors, FOXO1 regulates hepatic gluconeogenesis in both fasting and feeding. FOXO1 binds to insulin response elements in the promoters of genes involved in gluconeogenesis [89]. During fasting, Mitogen-activated protein kinase (MAPK) phosphatase 3 (MPK3) dephosphorylates FOXO1, increasing its nuclear localization and activation (Fig 1-2B)[90]. In the fed state, insulin suppresses gluconeogenesis by inhibiting FOXO1. Insulin signaling leads to AKT-dependent phosphorylation of FOXO1, which drives its cytosolic localization and proteosome-mediated degradation [91]. Interestingly, the absence of hepatic insulin signaling is sufficient to induce inappropriate gluconeogenesis that can be ameliorated by FOXO1 knockout [92]. FOXO1 is regulated negatively by acetylation, such as by p300/CBP [93]. In response to fasting, FOXO1 is deacetylated and thus activated by zinc finger and BTB domain containing 7c (ZBTB7C) and SIRT1, as well as by histone deacetylases (HDACs) that are phosphorylated by AMPK [94–96].

Similar to CREB, FOXO1 regulates rate limiting steps in gluconeogenesis [97]. The importance of FOXO1 in hepatic glucose homeostasis has been extensively documented by constitutive-active mutant and knockout studies. Liver-specific FOXO1 knockout reduces hepatic gluconeogenesis and glycogenolysis, leading to a 30% decrease in fasting blood glucose [98]. Constitutively active FOXO1

prevents the inhibitory effect of insulin on gluconeogenic genes [99]. There may be some redundancy between FOXO1 and other FOXO family members in regulating gluconeogenesis [100].

Interactions with other proteins can affect FOXO1 activity. PGC-1α and β-catenin bind to FOXO1 and increase its transcriptional activity, while transcription factor 7-like 2 (TCF7L2) competes with FOXO1 on the promoters of gluconeogenic genes, thereby inhibiting their transcription [99,101,102]. The nuclear receptor subfamily 0 group b member 2(Nr0b2 also known as SHP), which is a FOXO1 target, inhibits gluconeogenic FOXO1 activity in a negative feedback loop [103]. Interestingly, the promoter context determines how FOXO1 interacts with HNF4α. In fasting, FOXO1 cooperates with HNF4α on *G6Pase*, but antagonizes HNF4α on the *Gck* promoter [104].

PGC-1α

PGC-1α is a transcriptional coactivator induced by glucagon and glucocorticoid signaling that facilitates gluconeogenesis [105]. CREB induces the gene encoding PGC-1α in the setting of long-term fasting to sustain gluconeogenesis (Fig 1-2B)[78]. FGF21 promotes the expression of PGC-1α as well [12], but PGC-1α in return negatively regulates the expression of FGF21 [106]. PGC-1α is also regulated by post-transcriptional modifications. The gluconeogenic functions of PGC-1α are inhibited in fed state as a result of phosphorylation by S6 Kinase, an effector of mTOR and AKT signaling downstream insulin [107,108]. Moreover, lysine acetyltransferase 2A (KAT2A, also known as GCN5) acetylates and inhibits PGC-1α in the fed state, while SIRT1 deacetylates PGC-1α during fasting, thereby increasing its activity [109,110].

During fasting, PGC-1α interacts with several hepatic transcription factors, including FOXO1 and the nuclear receptors HNF4α, PPARα, and GR [99,105]. Livers of PGC-1α knockout mice show decreased gluconeogenesis along with decreased fatty acid oxidation and increased hepatic steatosis [111,112]. Conversely, PGC-1α overexpression increases hepatic glucose output and fatty acid oxidation [113,114]. Recently, PGC-1α was reported to impact insulin signaling during fasting by altering the ratio of insulin receptor substrates 1 and 2 (IRS1 and IRS2) [115]. While PGC-1α deficiency increases insulin sensitivity, PGC-1α overexpression causes insulin resistance [114,116,117]. Additionally, insulin signaling inhibits

gluconeogenic PGC-1α activity by inducing the expression of SHP–interacting leucine zipper protein (SMILE). SMILE directly competes with PGC-1α and consequently inhibits HNF4α [118].

Other transcriptional regulators in glucose metabolism fasting

GR is activated by binding to stress-related glucocorticoid hormone ligands during fasting [119,120]. GR induces the expression of gluconeogenic genes such as *Pck1* [121]. Hepatocyte-specific GR knockout mice have a survival rate of about 50% in the first 2 days of life due to hypoglycemia. If they survive to adulthood, the knockout mice exhibit fasting hypoglycemia [119]. The nuclear transcription factor Y (NF-Y) and nuclear factor kappa b subunit 2 (NF-κB2) have also been suggested respond to glucagon in fasting and induce gluconeogenesis [122]. NF-Y was shown to promote the expression of gluconeogenic genes through interacting with CREB [123]. Bile acid receptor (FXR), induced by PKA and FOXA1, has also been reported to promote gluconeogenic genes (Ploton et al. 2018; reviewed in Massafra and van Mil 2018)

In addition to its role in fasting-induced fatty acid oxidation, PPARα also affects the expression of genes linked to gluconeogenesis, glycerol metabolism and glycogen synthesis (reviewed in Kersten 2014). Loss of PPARα causes severe hypoglycemia in fasted mice, and reduces hepatic glycogen levels in refed mice. Loss of PPARα also prevents hepatic glycogen breakdown during short-term fasting [127].

.

Transcriptional regulators of glucose metabolism in the fed state

Consistent with its regulation by dietary glucose, ChREBP induces genes linked to glycolysis. ChREBP is necessary for the glucose-dependent induction of pyruvate kinase (PKLR), which catalyzes the last step of glycolysis (Fig 1-2A)[128]. Loss of ChREBP in mice decreases glycolysis at the pyruvate kinase and glucose-6-phosphatase steps and consequently increases liver glycogen content [61]. ChREBPβ expression is upregulated by carbohydrate feeding, while ChREBPα expression is downregulated [129].

A number mechanisms inhibit gluconeogenesis in the fed state. XBP1 can bind to FOXO1 and direct it to degradation (Fig 1-2B)[130]. During feeding both interleukin 6 and 13 (IL6 and IL13)activate

signal transducer and activator of transcription 3 (STAT3) (Fig 1-2A)[131,132] which represses gluconeogenic genes such as *Pck1* and *G6pase* [133]. In the fasted state, SIRT1 deacetylates STAT3, thus inactivating it to negate its repression of gluconeogenesis [134]. Additionally, hypoxia-inducible factor 2-alpha (HIF2a) is activated by hypoxia in postprandial liver where it attenuates glucagon signaling and gluconeogenesis together with its partner ARNT [135,136].

Nuclear receptor subfamily 5 group A member 2 (Nr5a2 also known as LRH-1) plays a role in postprandial glycolysis and glycogen synthesis by stimulating glucokinase (*Gck*) expression [137]. The postprandial uptake of bile acids activates FXR to support glycogen synthesis, while during fasting FXR induced by PKA and FOXA1 promotes gluconeogenic genes (Fig 1-2A, B)(Ploton et al. 2018; reviewed in Massafra and van Mil 2018).

Other fasting/feeding responsive pathways

Several metabolic and non-metabolic processes other than glucose and lipid metabolism are affected by fasting and feeding responses in liver. We highlight some of these, emphasizing how their regulation may contribute to the adaptation to the nutritional state.

Amino acid metabolism

Amino acid catabolism appears to play an important role in providing fuel for gluconeogenesis during fasting. Resulting ammonia from amino acid catabolism is detoxified through urea cycle in periportal hepatocytes and through glutamine synthesis pericentrally [138]. Enzymes involved in both processes such as first rate-limiting enzyme in the urea cycle carbamoyl phosphate synthetase-1 (*Cps1*), argininosuccinate synthetase 1 (*Ass1*) and argininosuccinate lyase (*Asl*) for urea cycle and ornithine-aminotransferase (*Oat*) and proline dehydrogenase (*Prodh*) for glutamine synthesis are upregulated in fasting [139]. However, upregulation of the amino acid catabolism enzymes were limited to the first 24 hours of fasting and to enzymes involved in the degradation of branched-chain keto-acids such as acetyl-

coenzyme A dehydrogenase (Acaddm) and hydratase/3-hydroxyacyl-coenzyme (Ehhadh). This indicates fasting induced amino acid degradation happens primarily outside of liver and liver detoxifies the resulting ammonia. In contrast, protein biosynthesis is rapidly induced during refeeding via mammalian target of rapamycin (mTOR) [140,141].

Hepatic C/EBPα expression is induced by glucagon in fasting. It regulates of the expression of *Cps1,* and amino acid catabolism [142,143]. Through these targets, it has been suggested to promote expression of gluconeogenic genes such as *Pck1*. Furthermore, the tumor suppressor P53 is stabilized by prolonged fasting through an AMPK-dependent mechanism. P53 along with kruppel like factor 15 (KLF15) facilitates amino acid catabolism thus promoting gluconeogenesis [144–146].

Bile acid metabolism

Bile acids are inherently tied to the fasting and feeding cycle. Bile acids are synthesized in liver from cholesterol and stored in the gallbladder. They are secreted into the lumen of small intestine to allow solubilization and absorption of dietary fats and fat-soluble vitamins. Bile acids reabsorbed in the gut are transported to liver where they activate FXR. In the fed state, FXR downregulates bile acid synthesis enzymes via SHP, FGF15 and MAF BZIP transcription factor G (MAFG), in a negative feedback loop [147,148]. Agonist and knockout studies have revealed that FXR also plays a role in keeping post-absorptive pathways in check, including inhibiting SREBP-1c-driven fatty acid and triglyceride synthesis, and promoting triglyceride lipolysis by inhibiting apolipoprotein C3 (APOCIII) and angiopoietin like 3 (ANGPTL3) [149–151].

Iron metabolism

The fasting and feeding processes alter iron metabolism in liver and plasma. Fasting-induced PGC-1α directly induces the expression of 5'-aminolevulinate synthase 1 (ALAS1) (the rate limiting enzyme of hepatic heme biosynthesis) and HEPCIDIN (which inhibits the iron transporter ferroportin) thereby limiting iron efflux [152,153]. These two strategies increase iron

retention in liver during prolonged fasting. SREBP-1c activated in the refed state was shown to induce heme oxygenase 1 (HMOX1), the rate limiting enzyme in heme catabolism. This regulation is postulated to protect cells from oxidative stress [154].

Stress Responses

Endoplasmic reticulum (ER) and mitochondria are sites of high metabolic activity during fasting and feeding cycles. In the 24-hour fasted liver the capacity for ATP synthesis is increased. There is increased tricarboxylic acid (TCA) cycle activity and oxidative phosphorylation from amino acid and fatty acid oxidation [139]. Increased oxidative phosphorylation may lead to oxidative stress due to the accumulation of reactive oxygen species (ROS). Dietary restriction and high-fat feeding–both of which increase fatty acid oxidation–increase the expression of oxidative stress defense genes such as glutathione-S transferases and those involved in glutathione synthesis [155]. ER stress pathways are also upregulated in 24-hour fasted liver [139]. ATF4 activated by ER stress induces the expression of FGF21 [156] which acts to reduce ER stress [157]. The DNA repair enzyme 8-oxoguanine DNA glycosylase (Ogg1) protects mitochondrial DNA from damage from metabolic reactions. Ogg1 has been shown to facilitate the channeling of glucose into the glycolytic pathway, TCA cycle and mitochondrial electron transport chain specifically in the fed liver [158].

Autophagy

Autophagy is a critical adaptation to low nutrient states. In fasting and starvation, autophagy is activated by multiple pathways. FOXOs, activated by AMPK in fasting and starvation, directly induce critical parts of the autophagy machinery [159]. In addition, FOXO3 and FOXO1 can activate autophagy by inhibiting mTOR and interacting with autophagy related 7 (ATG7), a key regulator of the autophagosome [160]. Additional mechanisms for regulation of autophagy are discussed below in the epigenetics section.

High throughput sequencing and -omics studies

Next generation sequencing has become an essential tool for probing the transcriptome. RNA sequencing (RNA-seq) has been very effective at identifying new genes, revealing pathways that respond to specific stimuli, and characterizing global transcriptomic profiles in various contexts. As transcriptomic methods have continued to evolve, studies have combined RNA-seq with other methods in the -omics toolkit, such as DNase I hypersensitive sites sequencing (DNAse-seq) and assay for transposase-accessible chromatin using sequencing (ATAC-seq), both of which profile accessible chromatin regions), chromatin immunoprecipitation followed by sequencing (ChIP-seq), which defines sites of transcription factor binding or histone modification, or metabolomics and proteomics, which profile the metabolome and the proteome respectively. From a bird's eye view, studies comparing the fasted and fed states, or different time points within in a fasting regimen, have found hundreds to thousands of differentially expressed genes–or up to 10% of the hepatic transcriptome [161]. The extent of these change underscores the complexity of the physiological response.

Pathway analysis

Pathway analysis tools aid in describing patterns in large data sets and highlighting unexpected associations. Not surprisingly, the top changing pathways in fasting versus fed liver involve lipid, carbohydrate, and amino acid metabolism [139]. Mitochondrial LCFA uptake, fatty acid β-oxidation, ketogenesis and PPARα signaling are among the most prominent responses peaking at 24 hours of fasting [139,162,163]. Conversely, fatty acid and sterol biosynthesis pathways are downregulated in fasting liver samples, reflecting suppression of SREBP-1c and SREBP-2 activity [162–164]. Gluconeogenesis is upregulated in fasting, relying on enhanced TCA and malate-aspartate cycling enzymes and increased expression of *Pck1* [139]. Liver glycogen is depleted by 12 hours of fasting in mice [165] and 17 hours in rats [162]. Accordingly, at 12 to 24 hours, glycolysis and glycogenolysis genes are downregulated. Enrichment of amino acid metabolism degradation pathways and genes in the urea cycle is observed in 24 hour-fasted

liver, consistent with amino acid oxidation [139,163]. These changes continue at 72 hours of fasting, even though other fasting-related transcriptomic changes are largely resolved. Hellerstein et al. (1997) observed persistence of gluconeogenic flux into glycogen and glycogen turnover humans even during prolonged fasting. Liver glycogen was shown to accumulate in mouse liver after 72 hours of fasting suggesting that amino acid oxidation is the predominant source of fuel for glucose and glycogen synthesis during prolonged fasting. TCA cycle, electron transport and oxidative phosphorylation pathways are induced in 24 hour-fasted liver [139,163]. As these processes can cause oxidative stress, it is not surprising that pathways for unfolded protein response/ER stress are upregulated concurrently. Lastly, fasting is also associated with a downregulation of immune and inflammation-related pathways [163].

Since feeding is used as the comparison state to fasting in most profiling studies, the reverse of what is reported in the fasted is generally observed for fed and refed conditions. When comparing refed to fasted mice, fatty acid oxidation pathways dependent on PPARα and gluconeogenesis through PEPCK are downregulated, while fatty acid biosynthesis is upregulated [167]. Compared to the ad libitum fed state, refed samples show increased enrichment of pathways for the biosynthesis of macromolecules. Zhang et al. (2011) observed that the majority of fasting-induced changes are in fact reversed by refeeding. Cholesterol biosynthesis is upregulated in fed state compared to fasting, and is further upregulated in refed state. Notably, genes that do not change in the fasting and refeeding response are enriched for housekeeping functions including nucleic acid metabolism, RNA processing, and cell organization pathways (Zhang et al. (2011).

Multi-omics and network analysis

Combining -omics technologies allows for integrative analysis. Such analyses may incorporate different profiling techniques (lipidomics, DNAse-seq, ChIP-seq) and computational methods and/or correlate changes in different tissues (adipose, muscle, liver). For example, studies that integrated transcriptomic analyses across multiple organs during fasting found that the previously accepted sequence of using carbohydrate, then lipids, and finally proteins as the source of fuel was not well supported by

their data. In fact, pathways for utilization of these fuels were activated in parallel across different organs [139,164,168]. The fatty acid oxidation pathway and genes involved in ketone body synthesis were upregulated in a number of metabolic organs during fasting, such as liver, kidney, intestine and muscle to preserve glucose for brain [161,164]. Accordingly, the transcriptome of the brain changes minimally in fasting. Network and text mining analyses have further shown that a number of transcription factors are shared in the fasting and feeding process between metabolically active organs, including PPARα, HNF4A, GR, SREBP-1/2, p53, FOXO, early growth response protein 1 (EGR1), activator protein 1 (AP-1, also known as c-JUN), Myc proto-oncogene protein (c-MYC), transcription factor Sp1 (SP1), YY1, and protein C-ets-1 (ETS1) [164,168].

Combining metabolomics and metabolic flux studies with transcription has provided insight into the coordination of metabolic responses. Robertson et al. (2011) showed that changes in the serum and urine metabolome in response to fasting are small in magnitude but broad in scope. The same study found that a reduction in serum glucose coincides with downregulation of the hepatic glycolytic genes *Gck* and *Pklr*. Serum glucose levels partially recovers in between 12 -16 hr of fasting as Pck1 expression goes up. Pck1 expression, thus gluconeogenesis, is upregulated when glycogen stores are depleted [165].As serum FFAs derived from adipose lipolysis increase, the expression of genes for acyl-CoA synthesis, genes facilitating fatty acid import into mitochondria, and genes involved in fatty acid oxidation increase in parallel [161]. Since β-oxidation and TCA cycle requires NAD+, expression of genes to produce NAD+ are upregulated: uncoupling protein 2 (UCP2) which is an PPARα target, and 3-Hydroxybutyrate Dehydrogenase 1 (BDH1), which converts acetoacetate to the ketone β-hyroxybutyrate (β-OH butyrate) [165].In contrast to fasting, responses to refeeding are quick and robust. Within 1-2 hours of refeeding, G6pc and Pck1 are downregulated along with increases in liver glycogen. Serum β-OH butyrate levels are decreased as well as expression of PPARα, CPT1, and Hmgcs2 [165]. Moreover, combining transcriptomics and lipidomics, Régnier et al. (2018) observed increased abundance of many phospholipid species in response to fasting in a PPARα-dependent fashion, along with differential expression of genes involved in

phospholipid homeostasis such as *Chka*, *Chkb*, *Agpat9*, and *Mogat1*. Using metabolic flux and quantitative modelling, Hui et al. (2017) suggests that during fasting glycolysis and TCA cycle are uncoupled and circulating lactate becomes the major substrate for TCA cycle for most tissues. These findings highlight that integrating transcription and metabolome provides a more complete picture of the physiological responses.

Network analysis and motif enrichment analysis can provide insight into specific transcriptional regulators associated with global changes in the transcriptome [27,163,170]. Using advanced computational analyses of DNAse-Seq and histone 3 lysine 27 acetylation (H3K27Ac) ChIP-Seq data (transcription factor footprint depth and motif-flanking accessibility), Goldstein et al. identified two roles for GR during fasting. For gluconeogenic genes, GR rapidly enhanced CREB activity. However, with respect to ketogenesis-related genes, GR action increased the expression of PPARα gradually, leading to slower ramp up of ketogenic genes [24]. Additionally, using self-organizing maps to compare multiple conditions collectively, Rennert et al. (2018) revealed that 24 hour fasting initiated in the morning stimulated glucose consumption and gluconeogenesis, while fasting initiated in the evening was associated with comparatively less gluconeogenesis and more fatty acid and cholesterol synthesis. Sano et al. (2016) used mathematical modeling and transcriptomics to determine that genes upregulated by insulin respond faster than those downregulated, but need a higher dose of insulin to respond.

Epigenetics and transcription factor relationships

Chromatin structure, chromatin remodelers, and histone modifiers all have regulatory roles in the fasting and feeding response. Fasting and feeding dynamically change the genomic accessibility landscape, opening up thousands of new enhancers, rearranging transcription factor binding, and altering cofactor interactions [24]. Several histone and DNA modifiers have been found to influence the response to fasting and feeding, including the well-characterized SWI/SNF chromatin remodeling complexes. A subunit of this complex, SWI/SNF complex 60 kDa subunit (BAF60a) responds to glucagon to activate

fatty acid oxidation genes in fasting by interacting with PGC-1α and engaging in crosstalk with PPARα [173]. Conversely, in the fed state a different subunit, BAF60c, forms a lipoBAF complex that interacts with USF-1 specifically on lipogenic genes and thus promotes their expression [174].

The deacetylase SIRT1, which largely targets transcription factors, is involved in the induction of gluconeogenesis and β-oxidation genes in fasting. SIRT1 is activated in response to an increase in the NAD+/NADH ratio during fasting [175]. CREB induces SIRT1 expression in fasting [176], and the cAMP/PKA pathway has also been implicated in activating SIRT1 through phosphorylation [177]. PKA signaling has been reported to induce an interaction between SIRT1, PPARα, and lysine-specific demethylase 6B(KDM6B, also known as JMJD3) [178], leading to the activation of β-oxidation genes. In fed state, SIRT1 expression and activity are repressed by ChREBP and glycosylation, respectively [176,179]. By contrast, SIRT1 overexpression reduces hepatic steatosis and improves glucose tolerance in obese mice [180]. PPARα signaling and fatty acid beta oxidation are also impaired in hepatocyte SIRT1 knockout mice [22]. SIRT1 deacetylates PGC-1α during fasting (thereby increasing its coactivator activity) [110], and upregulates FGF21 in a PPARα- and PGC-1α-dependent manner. Other studies have shown that SIRT1 affects gluconeogenesis in long-term fasting. SIRT1 deacetylates TORC2 and FOXO1, thereby reducing CREB activity and facilitating a switch to FOXO1/PGC-1α-driven gluconeogenesis [84,94]. SIRT1 has been shown to induce gluconeogenesis by repressing anti-gluconeogenic STAT3 [134]. At the same time, studies suggest that SIRT1 helps to keeps FOXO1-driven gluconeogenesis in check by providing negative feedback through SHP [103].

GCN5/KAT2A, an epigenetic modifier, can wear different hats based on nutritional status. It can function as a histone acetyltransferase (HAT) in fasting when PKA phosphorylates GCN5 in a CITED2-dependent manner [181]. GCN5 is recruited to and acetylates histone H3 at gluconeogenic gene promoters, thus driving fasting gluconeogenesis. But in the fed state, GCN5 can function as an acetyltransferase for PGC-1α. Insulin inhibits the interaction between GCN5 and CBP/P300-interacting transactivator 2

(CITED2) [182]. GCN5 directly acetylates PGC-1α (countering PGC-1α deacetylation by SIRT1), repressing its transcriptional activity [109].

Other epigenetic factors have also been identified as modulators of glucose and lipid metabolism in fasting. For instance methylcytosine dioxygenase TET3, a DNA demethylation enzyme, is recruited to the *Hnf4a* promoter by FOXA2 during fasting [183]. It demethylates the promoter, leading to increased expression of *Hnf4a* and its gluconeogenic target genes. Additionally, glucocorticoids induce histone-lysine N-methyltransferase SETDB2 to regulate *Insig2* transcription during fasting, negatively regulating SREBP-driven lipid synthesis [184]. These examples highlight how DNA and histone modifications contribute to executing responses to nutritional demands.

Noncoding RNAs are an exciting new class of regulators that brings another layer of fine tuning to transcriptional and translational responses in fasting/feeding. MicroRNAs have been noted to be involved in the dynamic transition from fasted to fed state [185]. MicroRNAs abundant in the fed state, such as let-7i, miR-221, and miR-222, target fasting-induced SIRT1, PGC-1α and their target genes *Cpt1*, medium-chain specific acyl-CoA dehydrogenase (*Acadm*), *Sirt3*, and transcription factor a, mitochondrial (*Tfam)*. In the absence of these fed-state microRNAs, gluconeogenesis is disinhibited and cells are unable to switch from catabolism to anabolism, as evidenced by activated AMPK and reduced phosphorylation of AKT [185]. Batista et al. (2019) found that more than 150 non-coding RNAs respond to insulin or fasting and refeeding. Among these, long non-coding RNA (lncRNA) Gm15441 was shown to regulate fatty acid oxidation in hepatocytes [186]. Zhang et al. (2018) showed that lncRNA H19 is induced by fasting and regulates hepatic glucose output by altering the promoter methylation and expression of *Hnf4a*. Another recent study found that 5-methylcytosine is enriched on enhancer RNAs with fasting [188]. Additional research is needed to determine how this RNA modification fine tunes transcriptional regulation.

Transcription factor interactions

Multi-omics methods have highlighted cooperation and antagonism between transcription factors during fasting and feeding. For example, Everett et al. (2013) used transcriptomics and ChIP-seq to reveal

that, although CREB is constitutively bound to its target genes, it engages in cooperative interactions with other factors such as C/EBPβ, GR, PPARα, and FOXA2 during fasting. In addition, TORC2, P300, ATF5 and NF-Y are all activated by fasting and promote gluconeogenic gene expression by enhancing CREB activity [85,123,190,191]. Glucagon stimulates gluconeogenesis by dephosphorylating TORC2, which then travels to nucleus and complexes with CREB [85]. TORC2 also associates with P300 upon glucagon signaling and this enhances its activity [84]. Interestingly, Liu et al. (2008) observed that SIRT1 deacetylates TORC2 in the late stages of fasting, thereby downregulating it.

Transcription factor interactions also impact regulation of hepatic glucose metabolism in the fed state. Insulin phosphorylates CBP, destroying the CREB-CBP complex [86]. However, the closely related coactivator P300 lacks a similar phosphorylation site and therefore does not get inactivated by insulin. P300 continues to bind to CREB on the *Ppargc1* gene, encoding for PGC-1α to maintain basal hepatic glucose production for in glycogen synthesis even in the post-prandial state [190,192]. FXR also influences glucose metabolism in the fed state by interacting with ChREBP. FXR binds to the same site as the ChREBP-HNFα complex on the *Pklr* promoter and triggers the release of ChREBP, leading to repression in the fed state [193]. FXR knockout mice show an increased *Pklr* response to refeeding along with reduced plasma glucose and hepatic glycogen levels [149].

The activity of transcription factors important in post-prandial lipid metabolism is also modulated by cooperative interactions. For instance, HNF-4α physically interacts with ChREBP on the *Fasn* promoter to fully upregulate its expression in response to glucose feeding [62]. Furthermore, SREBP-1c was shown to cooperate with NY-F and LXR at the promoters of lipogenic genes such as *Fasn* and *Acc1* to induce their expression in response to insulin [194–196]. Recently b-cell lymphoma 6 protein (BCL6) was shown to colocalize with and represses PPARα activity at genes involved in lipid catabolism in the fed state [197].

Autophagy can provide a source of macromolecules in the absence of dietary nutrients. Transcriptional regulation of autophagy during fasting also involves transcription factor interactions and

epigenetic modifiers. Fasting-induced FGF21 phosphorylates JMJD3 increasing its nuclear transport and interaction with PPARα [198]. This interaction induces a number of PPARα autophagy target genes including *Tfeb*, *Atg7*, and *Pnpla2 (also known as Atgl)*. In addition, the CREB-TORC2 complex promotes expression of genes involved in autophagy and lipophagy under nutrient-deprived conditions [81]. By contrast, during feeding FXR disrupts the CREB-TORC2 complex and competes with PPARα to trans-repress these genes [81,199]. In later stages of feeding, FGF19 induces SHP which recruits the lysine-specific histone demethylase 1A(KDM1A, also known as LSD1) to CREB-bound autophagy genes and promotes the disassociation of TORC2, leading to inhibition of autophagy [200].

Insulin signaling and insulin resistance

Insulin signaling and the mechanisms by which it is altered in insulin resistance have been the focus of intense study. Insulin is secreted by glucose-sensing pancreatic β cells in the postprandial state. In the liver, insulin induces lipogenesis and lipoprotein synthesis, allowing conversion of dietary carbohydrates to triglycerides and their export to adipose tissue for storage. Insulin also suppresses gluconeogenesis and glycogenolysis and promotes glycogen synthesis. Insulin-induced hepatic lipogenesis is dependent on cell autonomous signaling. Insulin reaches the liver through the periportal vein and binds to the insulin receptor (IR) on hepatocytes. IRS1 and IRS2 are direct targets of insulin receptor and their expression is dynamically regulated in fasting/feeding [201]. Upon insulin binding, they recruit phosphoinositide 3-kinase (PI3K) which generates phosphatidylinositol (3,4,5)-trisphosphate (PIP3). PIP3 promotes recruitment of pyruvate dehydrogenase kinase 1 (PDK1) which activates AKT by phosphorylation (reviewed in Titchenell et al. 2017). Activation of mTOR and suppression of FOXO1 by AKT are necessary for insulin induction of lipogenesis through SREBP-1c [203]. Insulin also suppresses expression of INSIG1 and INSIG2, which inhibits SREBP-1c processing and activation [204].

Studies point to hepatic and extra-hepatic insulin effects on liver glucose output in the postprandial state. Liver IR knockout (LIRKO) mice show hyperglycemia, confirming that FOXO1 is

derepressed without hepatic insulin signaling [205]. However, in the absence of both AKT and FOXO1, hepatic glucose production remains responsive to insulin, indicating that additional modes of regulation exist [206]. Insulin has widespread effects on the hepatic transcriptome. Batista et al. (2019) profiled the transcriptomic effects of insulin in the absence of changing glucose levels. They reported that hepatic insulin alters not only glucose and lipid metabolic pathways, mitochondrial function and autophagy, but also non-metabolic pathways such as Toll-like receptors (TLRs) and Notch signaling. Using proteomics, Capuani et al. (2015) showed that loss of IR induces oxidative stress pathways, suggesting that insulin signaling in liver is protective against oxidative stress. Insulin has also been shown to repress the expression of adiponectin receptors (AdipoR1 and AdipoR2) reducing sensitivity to adiponectin, which mediates fatty acid oxidation through AMPK and PPARα [208].

Diet-induced obesity can lead to selective hepatic insulin resistance, in which suppression of glucose production in the post-prandial state is impaired but insulin-stimulated lipogenesis and very low-density protein (VLDL) secretion remain intact. Diet-induced obesity and insulin resistance alter the expression of number of genes involved in fasting and feeding. IRS1 and IRS2 expression is altered in insulin resistance. Kubota et al. (2016) described that in obese mice, insulin signaling is impaired in the periportal zone, the primary site for gluconeogenesis, as *Irs2* expression is reduced there. At the same time insulin signaling is enhanced in the primary site for lipogenesis (the perivenous zone) as the predominant *Irs1* in this zone, remains unaffected. This phenomenon may shed light on how differential regulation of insulin signaling can lead to selective insulin resistance. Additionally, PGC-1α induced in fasting was shown to increase the IRS2 to IRS1 ratio in hepatocytes, increasing the sensitivity for insulin induced suppression of glucose production [115]. This phenomenon may help explain how continuous feeding could reduce the IRS2 to IRS1 ratio and impair glucose suppression. Further supporting this point, FGF21 secreted in fasting has been suggested to sensitize insulin signaling at the beginning of feeding [210].

Effect of time on fasting and feeding response

Circadian Rhythm

Light input to the suprachiasmatic nucleus (SCN) of the hypothalamus creates oscillations in circadian clock proteins to set the body's daily sleep-wake cycle. The sleep-wake cycle establishes an intrinsic fasting-feeding rhythm. In peripheral tissues such as the liver, up to 12% of the total transcriptome has been shown to vary with the circadian cycle, with many of these transcripts encoding metabolic proteins [211–213]. The circadian cycle is driven by the actions of a complex consisting of the proteins clock circadian regulator (CLOCK) and brain and muscle ARNT-like 1 (BMAL1). This complex promotes transcription of the *Per* and *Cry* families ofgenes. The period circadian regulator (PER) and cryptochrome (CRY) proteins subsequently form a heterodimeric complex which represses the transcription of *Clock* and *Bmal1*, creating the characteristic back-and-forth 24-hour rhythm of the circadian cycle (Fig 1-3). In mice, which are nocturnal, BMAL1 and CLOCK protein expression increases during the light phase while PER and CRY increase during the dark. However, in humans, this cycle is reversed, with BMAL1 and CLOCK increasing during the night and PER and CRY increasing during the day.

In the liver, the CLOCK:BMAL1 complex functions as a pioneer factor, opening chromatin to allow binding of other transcription factors such as HNF6 [214]. CLOCK:BMAL1 also regulates daily fluctuations in blood cholesterol through its activation of low density lipoprotein (LDL) receptor transcription [215], and regulates hepatic glycogen content by activating transcription of glycogen synthase 2 [216]. As feeding occurs, insulin suppresses BMAL1:CLOCK by causing AKT to phosphorylate BMAL1 at Ser42, leading to its nuclear exclusion [217]. During fasting, glucagon causes recruitment of the CREB:CRTC2 complex to the *Bmal1* promoter to enhance its expression [218]. Recent studies have shown, however, that this fasting-induced

increase in expression is accompanied by a loss in BMAL1 phosphorylation and acetylation and a decrease in expression of its target genes [219].

During feeding and acute fasting, PER2 promotes glycogenesis by binding E-boxes in the promoters of genes encoding the protein phosphatase 1 subunits PP1R3A and PP1R3B, which activate glycogen synthase. [220]. Accordingly, whole-body loss of *Per2* lowers fasting hepatic glycogen and glycogen synthase levels [221]. Degradation of CRY1 by the DNA damage-binding protein 1-Cullin 4A (DDB1-CUL4A) E3 ligase enhances FOXO1-mediated gluconeogenesis in the liver [222]. Small molecule activators of CRY have been shown to inhibit glucagon-mediated gluconeogenesis in primary hepatocytes [223]. In humans, polymorphisms causing increased CRY2 levels have been correlated with increased hepatic triglyceride content and fasting hyperglycemia [224]. *Cry1*-/-*Cry2*-/- mice show elevated blood glucose upon refeeding following an overnight fast and severely impaired glucose clearance [225].

In the accessory circadian loop, the BMAL1:CLOCK transcriptional targets ROR (receptor tyrosine kinase-like orphan receptor) and REV-ERB compete for the ROR/REV-ERB Response Element (RRE) in the BMAL1 promoter [226]. REV-ERB levels rise during the dark phase to repress *Bmal1* expression, while ROR levels rise during the light phase to increase expression [227]. REV-ERB controls diurnal recruitment of HDAC3 and the nuclear receptor co-repressor complex to the *Bmal1* promoter to repress transcription [228,229]. In the liver, REV-ERBα and β are required for circadian oscillations of core clock genes such as *Bmal1* and *Cry1*. Whole-body REV-ERBα/β deficient mice have disrupted daily wheel-running patterns, as well as elevated fasting glucose and triglycerides [230]. RORα and RORγ both regulate circadian variations in *Insig2* expression to provide a check on SREBP-1c-mediated lipogenesis during feeding [231].

Liver-specific RORα deletion in mice leads to hepatic steatosis, obesity and insulin resistance on high-fat diet (HFD) [232].

Outside of the canonical clock genes, a host of other transcription factors have been shown to exhibit circadian variations in expression and activity. Of the 49 nuclear receptors expressed in mice, 20 exhibit rhythmic circadian oscillations, including the PPAR family, retinoic acid receptor RARα, retinoid X receptor RXRα, the estrogen receptors, and thyroid receptor α. Many of these receptors peak shortly after the light-dark transition when mice begin to feed [233].

Time restricted feeding and intermittent fasting

As circadian proteins exert control over metabolism, food intake conversely regulates circadian cycles. Mice fed a high-fat diet have altered diurnal feeding behavior, consuming more food in the day and less in the night, as well as locomotor activity [234]. Restricting the food availability of nocturnal mice to daytime hours inverts the circadian rhythm of peripheral tissues, such as the liver, while having no effect on the SCN [235]. Furthermore, subjecting wild-type mice to a 24-hour fast results in loss of rhythmicity of greater than 80% of liver transcripts that normally display circadian variation [236]. Further evidence of the influence of food timing on metabolism comes from studies of time-restricted feeding (TRF), in which food is limited to a certain interval each day. TRF protects against the development of metabolic disease in a number of mouse models. This effect is believed to stem from the alignment of food intake with circadian timing in the body's peripheral tissues, particularly liver, which allows for more efficient clearing and processing of ingested nutrients [237].

Mice subject to a daily regimen of 8 hours feeding/16 hours fasting on HFD take in the same number of total calories as their ad libitum fed counterparts, but do not develop metabolic

syndrome [238]. A key mediator of this effect is the liver, where TRF rescues the blunted rhythmicity of circadian genes and the function of nutrient-responsive pathways like mTOR, CREB and AMPK that are altered by HFD [239]. This protective effect has been shown to extend to mice subjected to high-fructose and high fructose/high-fat dysmetabolic diets as well, as long as food availability was limited to less than 12 hours a day. Feeding in TRF HFD mice is accompanied by a concomitant increase in GCK expression; however, in ad libitum HFD mice, GCK levels remain persistently elevated throughout the day. Thus, modulation of the fasting-refeeding interval restores glucose homeostasis in HFD-fed mice. In the livers of TRF HFD-fed mice, PPARγ displays mild oscillations in amplitude throughout the circadian cycle with a peak in during the active phase. In ad libitum HFD-fed mice, however, these oscillations dramatically increase in amplitude and instead peak in the day/inactive phase [240].

TRF has also been shown to prevent the development of metabolic abnormalities in mice with clock gene mutations. Whole-body *Cry1*-/-*Cry2*-/- KO mice have near complete loss of rhythmic gene expression in the liver, an effect partially rescued by TRF [236]. In addition, genetically modified mice that lack a regular feeding rhythm consume the same number of calories as their ad libitum counterparts, but resist weight gain and hyperleptinemia [241]. Recently, these findings have been extended to humans. In a study of 19 patients with metabolic syndrome on statins or antihypertensives, limiting food intake to a 10-hour window each day over 12 weeks led to reductions in body weight, visceral fat, blood pressure, total cholesterol, LDL, and HbA1c [242].

Fasting and refeeding protocols

Although it is unsurprising that the hepatic transcriptome differs dramatically between ad libitum feeding and 24 hour fasting conditions, it has also been found that significant differences exist even between ad libitum feeding and 24 hours refed livers, with expression differences in key pathways controlling lipid metabolism and small molecule biochemistry (Zhang 2011). A study of both BALB/cJ and C57BL/6j mice fasted for 24 hours and refed found that differential gene expression peaks at 6 hours post refeeding with significant upregulation of lipogenic pathways in comparison to amino acid and carbohydrate metabolism (Chi 2020). Moreover, fasting-refeeding regimens are themselves highly heterogeneous. As stated in the Pathway analysis section, a time course comparing the hepatic transcriptome after 0, 12, 24 and 72 hours of fasting found that strong induction of the urea cycle was apparent at every time point. In contrast, pathways controlling amino acid, carbohydrate, and lipid metabolism peak at 24 hours and return to baseline by 72 hours, at which point beta oxidation and ketogenesis pathway expression increases (Sokolovic 2008). Another time course study in 48 hour fasted mice revealed upregulation of hepatic gluconeogenesis and ketogenesis at 3 hours; additionally these mice have marked upregulation of PPARa targets such as *Pck1*, *G6pc*, and *Fgf21* (Schupp 2013). Another more recent study comparing 24 hour fasted mice refed for either 12 or 21 hours found that even after 12 hrs of refeeding, mice have continued dysregulation of liver lipid metabolism and autophagy, but this effect which is largely abrogated in the 21 hr refed group (Rennert 2018). By building a better understanding of the dynamics of fasting and refeeding in mice, these experiments can be standardized across different labs based on the desired pathways of study (ie ketogenesis, gluconeogenesis).

Effect of diet, exercise and sex on fasting and feeding response

Diet

The contents of the diet play a modifying role in transcriptional responses to both fasting and feeding. Studies have compared diets rich in fat versus carbohydrates, glucose versus fructose, high versus low protein, as well the effects of calorie restriction. HFD has been found to increase hepatic de novo lipogenesis (e.g. expression of *Fas* and *Scd1*) to a lesser degree than carbohydrate feeding [243]. Furthermore, cholesterol biosynthesis genes controlled by SREBP-2 are downregulated by increased dietary cholesterol [155]. In contrast to fatty acid biosynthesis genes, mitochondrial and peroxisomal β-oxidation genes (such as *Cpt1a* and *Acox1*, respectively) are induced in HFD-fed mice [155]. PPARα, the master regulator of fatty acid oxidation, is induced by fat feeding, drawing a similarity to the extended fasted state, as both contexts use fat as a primary energy source [243]. Consistent with this idea, AMPK activity is increased in livers fed with PUFAs or high-fat diet [244,245]. In contrast to fasting, HFD also increases some aspects the immune response, such as *Nfkb1* and its target genes tumor necrosis factor *Tnfa*, *Il1b*, prostaglandin-endoperoxide synthase 2 *(Ptgs2),* and nitric oxide synthase 2 *Nos2* (Lee at al 2013).

Fatty acid synthesis genes are more robustly upregulated by high-fructose diets compared to complex carbohydrate diets [246]. Also, the dynamics of the fructose and glucose transcriptional responses are different. Glucose refeeding causes a more acute SREBP-1c induction [247]. Furthermore, in the absence of insulin signaling, lipogenic genes such as *Fasn* are more induced by fructose than glucose feeding. Recent studies suggest that ChREBP may be playing an important role in this process. Fan et al. (2017) documented increased expression of the ChREBP target *Pklr* in fructose-fed mice compared to glucose fed mice. They also reported that while LXRα facilitates the increase in ChREBP activity in glucose-fed mice, the ChREBP response to fructose feeding was independent of LXRα. Additionally, while excess dietary fructose can increase stress signaling via c-Jun N-terminal kinase (JNK) signaling, glucose feeding has been reported to promote hepatic inflammatory responses more than fructose feeding, as

evidence by increased expression of TLR2 and inflammatory genes such as C-X-C motif chemokine ligand 2 (*Cxcl2)*, *Cxcl10*, *Cxcl1*, *Nfkb1*, and *Nfkb2* [248,249].

Dietary protein content is also a modifier of hepatic transcription. Unlike food restriction, where proportionality of nutrients is preserved, modified protein diets affect many aspects of whole body homeostasis. Refeeding with high-protein diet after a prolonged fast can cause acute liver damage [250]. Conversely, feeding with low-protein diet affects growth through downregulation of insulin-like growth factor I (*Igf1)* and induces inflammatory genes such as *Il6* [250]. Dietary protein induces PPARγ-dependent hepatic IGF-1 secretion and promotes mTOR phosphorylation and the interaction between PPARγ and mTOR [251]. Leucine deficiency was shown to upregulate transcription of tribbles homolog 3 (*Trib3)*, a factor known to inhibit insulin signaling by binding to AKT [252]. TRB3, encoded by *Trib3*, also interacts with ATF4, inhibiting it from inducing FGF21[156].

Calorie restriction

Calorie restriction (CR) has been associated with health benefits and longevity. CR is a less extreme version of fasting that can be continued for extended periods, at least in laboratory settings. CR decreases the expression of lipogenic genes such as *Fasn* and *Elovl3* and genes involved in formation of lipid droplets such as perilipin-2 *(Plin2)* and fat storage-inducing transmembrane protein 1 (*Fitm1)* [155]. On the other hand, genes involved in lipid droplet breakdown and fatty acid oxidation are increased by CR. Drawing parallels to a fasting-like state, CR animals also respond to fasting with increased expression of PPARα [253]. Decreased lipid formation and increased lipid breakdown leads to a decrease in fat mass [155,254,255]. However, refeeding chow or HFD upregulates lipogenesis more robustly in CR compared to ad libitum fed mice [256]. This is reminiscent of the observation that humans often gain more weight back than they have lost after stopping restrictive dieting. CR feeding also leads to increased expression of genes involved in oxidative stress response such glutathione synthesis genes and glutathione-S transferases [155]. Some benefits of CR have been proposed to be mediated by SIRT1. Although SIRT1 activity is increased by CR in many tissues, SIRT1 activity is actually decreased in liver by CR [257].

Exercise

Exercise can change the energy demands of the body and reprogram metabolism in many tissues. Exercise has been reported to blunt the upregulation of lipogenesis in liver in response to carbohydrate feeding. However, exercise was less effective in reducing the lipogenic response in fructose feeding [246]. Exercise is also known to increase insulin sensitivity in adipose and muscle but not in liver [258]. On the other hand, exercise can increase expression of genes involved in fatty acid oxidation and transport into mitochondria [259]. Additionally, exercise has been suggested to decrease hepatic oxidative stress [260] and to decrease HFD-induced NF-κB activation and proinflammatory cytokine production [261]. These beneficial effects of exercise on lipid metabolism appear to be independent of the mTOR pathway [262] and potentially mediated by increased PPARα-stimulated fat oxidation [263].

Sex Differences

Premenopausal women are more resistant to diet-induced insulin resistance than men. Sex differences are also seen in responses to fasting and feeding. Bazhan et al. (2019) showed that changes in expression of genes involved in the fasting response, such as *Fgf21, Ppara,* and *Cpt1a,* were more pronounced in female mice than in males. By contrast, they reported that hepatic expression of *Fasn* was higher in male mice than females, possibly due to male-specific hyperinsulinemia. Male mice also have higher insulin to glucagon ratios, leading to increased glucose metabolism [265]. According to this study, male mice exhibit increased hepatic glucose output and expression of gluconeogenic genes such as *G6Pase* and *Pck1* compared to females. Males also have higher glycogen synthesis, which is commonly observed with high gluconeogenic capacity.

Growth hormone secretion and signaling is also sexually dimorphic. While adult males secrete growth hormone in episodic bursts, females display a continuous pattern of growth hormone section [266]. Growth hormone may exert its impact on sex-specific hepatic metabolic gene expression through STAT5

and its male-biased transcriptional repressor BCL6. BCL6 binds preferentially to STAT5 target genes involved in lipid metabolism that have a female-biased expression [267].

Limitations

Rodent models provide many benefits to the researchers, however they have limitations when translating the findings to the clinic. Humans have both physiological and psychological difference in relation to feeding and fasting behavior in comparison to mice. While mice eat small portions frequently during the dark, humans eat few larger meals during the day [268]. Humans may choose to eat or not eat for social reasons, which are not captured by most experimental designs in rodent models. Many clinical tests are run on overnight fasted patients. Overnight fasting in mice is not an equivalent for this state because of their nocturnal feeding and higher rate of metabolism. While mice glucose levels are significantly lower after an overnight fast, humans are able to maintain their basal glucose levels for more than 18 hours [165,269]. It is suggested that fasting mice 5-6 hr during the day better resembles the human overnight fasting when comparing glucose and insulin levels. Additionally, its been observed that while mice respond to prolonged fasting with enhanced insulin stimulated glucose utilization, humans experience an impairment of insulin stimulated glucose utilization [270]. These differences need to be taken into account when comparing to patients.

Conclusions

Changes in nutrients, hormones, and post-translational modifications regulate a broad hepatocyte transcriptional network. During fasting, liver switches to using lipids and amino acids as its primary energy source to make ketones and glucose, respectively. PPARα, FOXO1, PGC-1α and CREB are among the key players enacting this shift. In the fed state, liver takes up glucose and increases glycolysis

and lipogenesis in response to carbohydrates via ChREBP and Srebp1c. The fasting/feeding response is also shaped by a network of additional transcriptional regulators. High-throughput -omics methods have just started investigating these complex relationships and their effects in a systematic way. Many other pathways, including those involving bile acids, iron metabolism, immune responses, circadian rhythms and stress responses are affected by nutritional status. Proper control of hepatic transcription by diet is crucial for physiology, and perturbation of these pathways are a hallmark of metabolic diseases. With the continued development of new methods and new genetic models, future research is likely to reveal additional connections and expand our understanding of this central physiologic response.

Figures

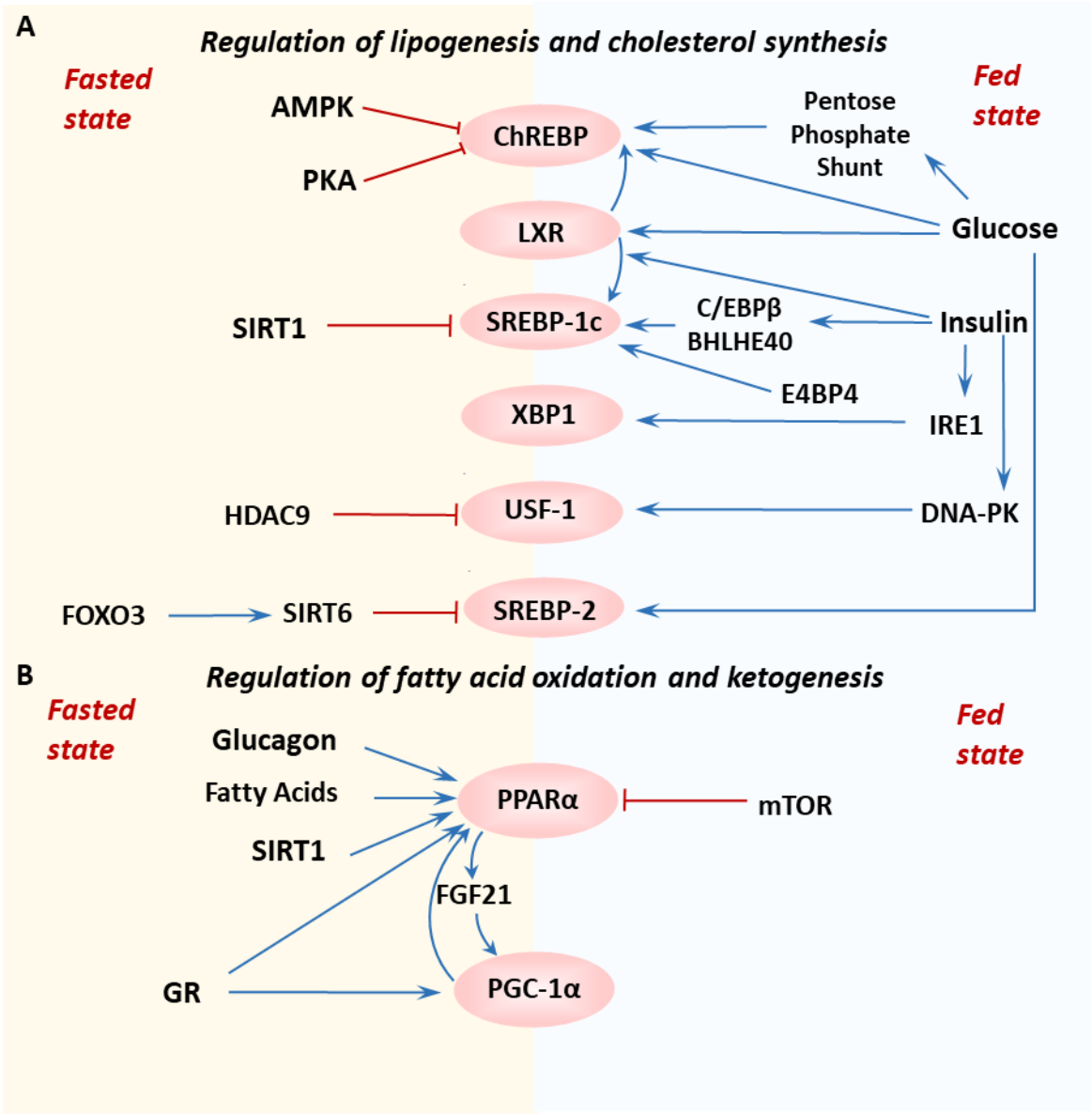

Figure 1-1-1: Transcription factors that regulate lipid metabolism in fasted and fed state

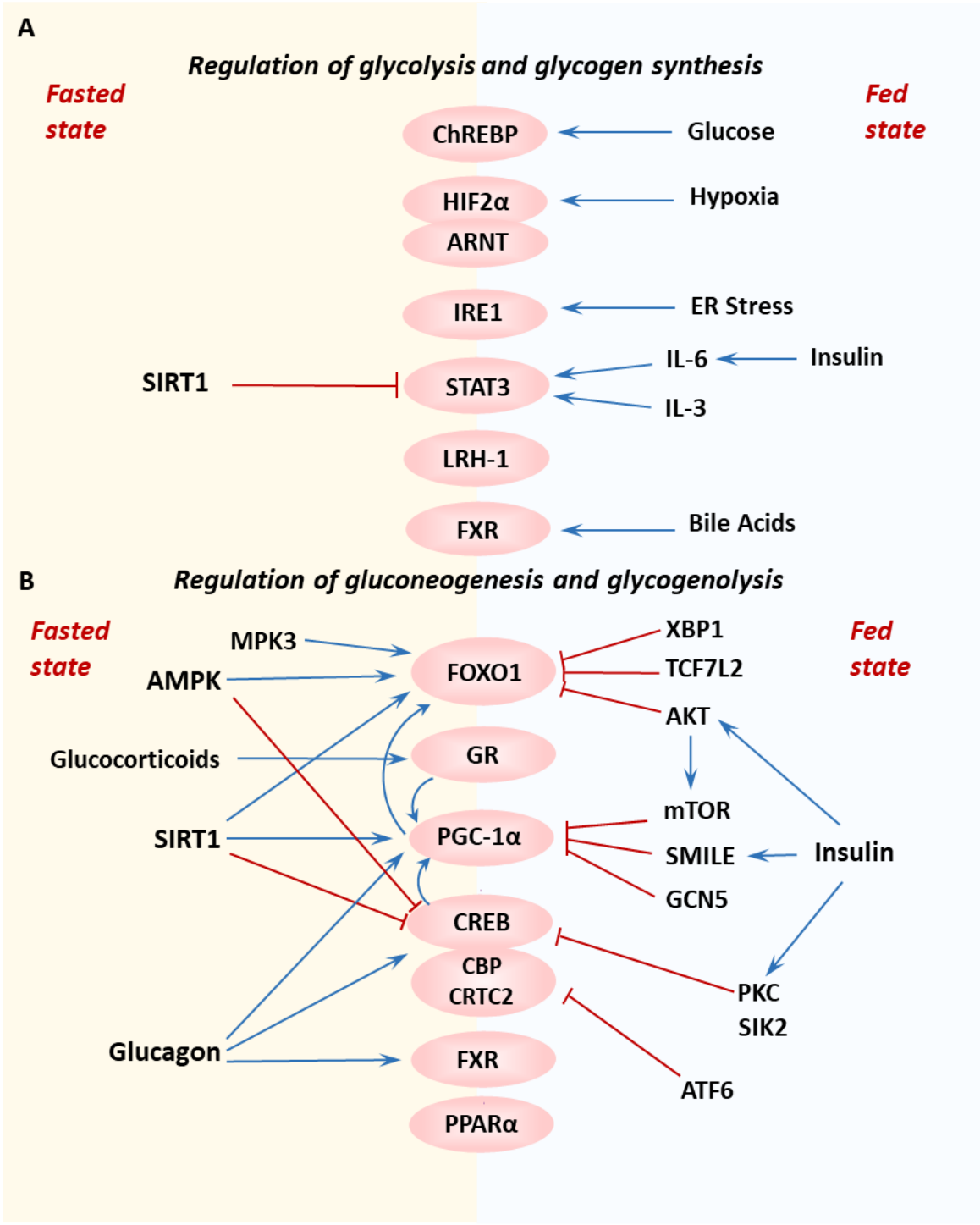

Figure 1-1-2: Transcription factors that regulate glucose metabolism in fasted and fed states

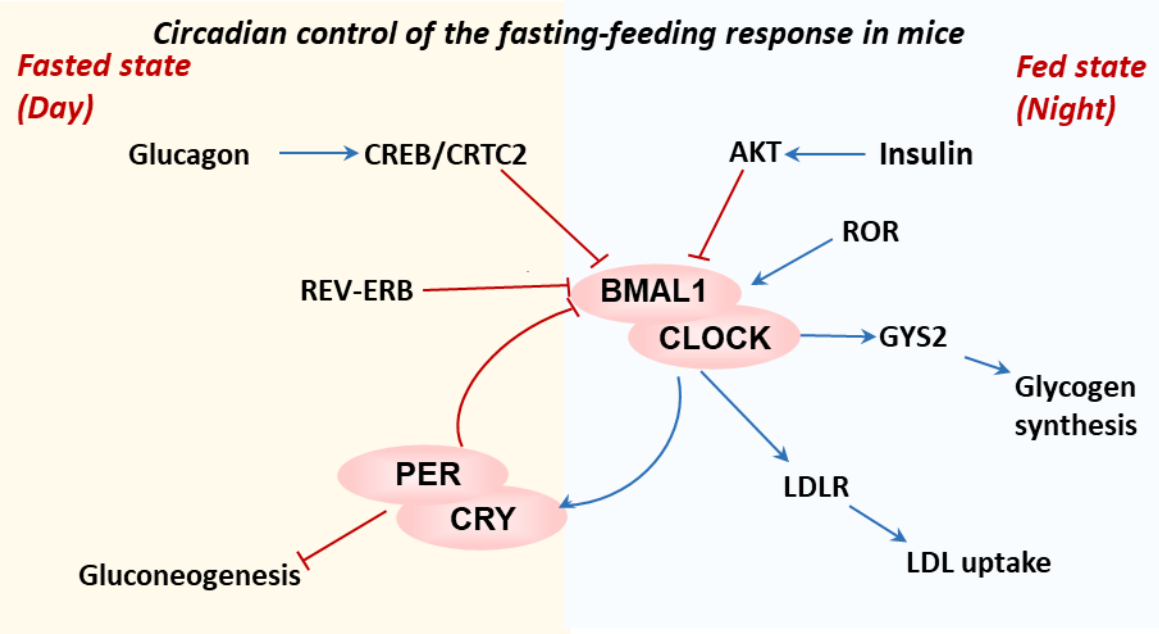

Figure 1-1-3:Interplay of circadian rhythm and hepatic gene regulation in mice

Figure legends

Figure 1-1: Transcription factors that regulate lipid metabolism in fasted and fed states. A: Transcription factors such as ChREBP, LXR, SREBP1c, XBP, USF-1 and SREBP2 are activated by various factors in response to feeding signals such as glucose and insulin. These transcription factors induce the expression of genes that promote lipogenesis and cholesterol biosynthesis. Some of these transcription factors are also known to be actively inhibited during fasting. B: Transcription factors such as PPARα and PGC-1α are activated by glucagon, SIRT1 and glucocorticoid receptor during fasting. These transcription factors induce the expression of genes that promote fatty acid oxidation and ketogenesis during fasting. Ketone bodies can be used as energy source for many other tissues.

Figure 1-2: Transcription factors that regulate glucose metabolism in fasted and fed states. A: Transcription factors such as ChREBP, HIF2α-ARNT, IRE1, STAT3, LRH-1 and FXR are activated by various factors in response to feeding such as glucose and insulin. These factors induce the transcription of genes that promote glycolysis and glycogen synthesis. In response to an increase in available glucose and insulin, energy metabolism switches to using glucose as fuel and replenishes glycogen stores.B: Transcription factors such as FOXO1, GR, PGC-1α, CREB, PPARα, FXR, are activated by glucagon, AMPK, SIRT1 and glucocorticoids during fasting. These transcription factors induce the expression of genes that promote gluconeogenesis and glycogenolysis. This switch is crucial in maintaining blood glucose levels during fasting. There is evidence for crosstalk between these transcription factors, one inducing the expression of another. Some of these transcription factors are also known to be actively inhibited by insulin signaling in response to feeding.

Figure 1-3: Interplay of circadian rhythm and hepatic gene regulation in mice. Left: PER/CRY is the major effector of the circadian clock in the liver during the day while mice are asleep. Effects of PER/CRY include inhibition of gluconeogenesis and suppression of BMAL1/CLOCK. BMAL/CLOCK activity is also repressed by REV-ERB transcription factors and glucagon via CREB/CRTC2. Right: at night, when mice are active and feeding, the BMAL1/CLOCK complex is the main circadian regulator of the liver transcriptome. Its effects include increasing LDL uptake and glycogenesis while also increasing levels of the PER/CRY complex. Among the factors that increase BMAL1/CLOCK expression is the daytime accumulation of ROR. As feeding occurs throughout the night, rising insulin levels cause Akt to suppress BMAL1/CLOCK activity.

Chapter 2 : Hepatic GATA4 regulates cholesterol and triglyceride homeostasis in collaboration with LXRs

Lara Bideyan[1], Maykel López Rodríguez[1], Christina Priest[1], John P. Kennelly[1], Alessandra Ferrari[1], Prashant Rajbhandari[1], An-Chieh Feng[2], Sergei G. Tevosian[3], Stephen T. Smale[2], Peter Tontonoz[1,#]

[1]Department of Pathology and Laboratory Medicine, Department of Biological Chemistry, University of California, Los Angeles, Los Angeles, United States.

[2]Department of Microbiology, Immunology, and Molecular Genetics, University of California, Los Angeles, Los Angeles, United States

[3]University of Florida, Department of Physiological Sciences Box 100144, 1333 Center Drive, Gainesville, FL 32610, USA

Corresponding author

ptontonoz@mednet.ucla.edu

Version of an manuscript under review in Genes and Development

Abstract

GATA4 is a transcription factor known for its crucial role in the development of many tissues, including liver; however, its role in adult liver metabolism is unknown. Here, using high-throughput sequencing technologies, we identified GATA4 as a transcriptional regulator of metabolism in liver. GATA4 expression is elevated in response to refeeding, and its occupancy is increased at enhancers of genes linked to fatty acid and lipoprotein metabolism. Knocking out GATA4 in adult liver (Gata4LKO) decreased transcriptional activity at GATA4 binding sites especially during feeding. Gata4LKO mice have reduced plasma HDL cholesterol and increased liver triglyceride levels. The expression of a panel of GATA4-binding genes involved in hepatic cholesterol export and triglyceride hydrolysis was downregulated in Gata4LKO mice. We further demonstrate that GATA4 collaborates with LXR nuclear receptors in liver. GATA4 and LXRs share a number of binding sites, and GATA4 was required for the full transcriptional response to LXR activation. Collectively, these results show that hepatic GATA4 contributes to the transcriptional control of hepatic and systemic lipid homeostasis.

Introduction

Liver plays a vital role in systemic lipid and glucose metabolism [5]. Liver is the major site for synthesis of lipids and lipoproteins. It converts excess dietary carbohydrates and proteins into lipids during feeding, and maintains glucose homeostasis through gluconeogenesis during fasting. Dysregulation of hepatic metabolism is central to the development of non-alcoholic fatty liver diseases (NAFLD), insulin resistance, and atherosclerosis [271,272]. Dissection of the transcriptional landscape in physiological responses such as fasting and feeding is needed to expand our understanding of metabolic regulatory networks and their vulnerabilities in pathologies.

GATA4 is a zinc finger protein belonging to GATA family of transcription factors. While GATA1 - 3 are expressed in the hematopoietic and central nervous system, GATA4 - 6 are expressed in endoderm- and mesoderm-derived tissues such as heart, liver, pancreas and gonads [273]. GATA4 is known to play an essential role in the development of many of these tissues and in cardiac hypertrophy [274,275]. Global knockout of GATA4 is embryonic lethal due to heart and liver agenesis [274,276], making studies of adult tissues challenging. In liver, GATA4 has been reported to be involved in hepatocyte differentiation and to serve as a tumor suppressor gene [277]. GATA4 activity in stellate cells has been tied to quiescence and the prevention of liver fibrosis [278]. The action of GATA4 in liver sinusoidal epithelial cells (LSECs), but not in hepatocytes, appears to be important for liver regeneration [279,280]. However, the role of GATA4 in transcriptional regulation in adult hepatocytes is poorly understood.

GATA4 is a pioneer factor that binds predominantly to enhancer regions and is capable of opening closed chromatin [281]. GATA4 binding to its target genes is tissue-specific, in part due to its interactions with other transcription factors. While it is capable of both activating and

repressing gene expression, prior studies suggest that in liver GATA4 functions primarily as an activator [279]. GATA4 is known to recruit the transcriptional activator p300 to chromatin, where it increases the acetylation of histone H3 on lysine 27 (H3K27Ac) and enhancer activity [282].

In addition to its roles in differentiation and identity maintenance, GATA4 has been associated with metabolism. Genetic studies in humans have found association of GATA4 with plasma triglycerides (TG) and with type 2 diabetes (T2D) [283–286]. Other reports have suggested that GATA4 regulates steroidogenesis and glycolysis in Leydig cells [287,288] and that loss of intestinal GATA4 prevented diet-induced obesity [289]. However, the metabolic consequence of hepatocyte specific loss of GATA4 in adult mice are unknown.

In this study, we used integrated transcriptional and epigenetic analyses to characterize GATA4 as a regulator of the feeding response in adult liver. We show that loss of GATA4 alters the hepatic transcriptional landscape during feeding, reduces plasma HDL cholesterol levels, and increases liver triglyceride accumulation. Finally, we demonstrate that GATA4 cooperates with LXR in the regulation of genes linked to cholesterol homeostasis.

Results

GATA4 activity and expression is upregulated in response to feeding.

To investigate changes in the hepatic transcriptional landscape during feeding, we conducted ATAC-Seq and RNA-Seq on livers of mice fasted for 12 hours, and mice fasted and then refed with 12 hours with high sucrose diet. We adapted the time points and diet from previously published protocols to maximize the insulin and lipogenic response [33]. Based on the chromatin accessibility profiled via ATAC-Seq, we inferred genomic regions that were changing in activity during feeding. We identified 3314 differentially accessible peaks, with 1231 gaining accessibility in fasted and 2083 gaining accessibility refed conditions (Fig. 1A). The differentially accessible peaks in fasted and refed states were primarily located in intergenic and intronic regions, followed by promoter regions (Fig. 1B). Annotating peaks to the closest promoter led to the observations that peaks more accessible in fasting were associated with genes involved in the PPAR signaling pathway (Fig. S1A), and that peaks more accessible in refeeding were associated with fatty acid biosynthesis, ChREBP activation, and other pathways (Fig. S1B). These associations strongly suggested that the dynamic changes in the chromatin we observed in response to fasting and refeeding were linked to transcriptional changes known to regulate these metabolic processes [290].

We next sought to identify transcription factors that might have differential activity in these two states. We analyzed how the prevalence of different transcription factor binding motifs changed across all peaks in relation to the change in accessibility in those peaks between fasting and refeeding. The peaks were ranked by fold change and grouped into bins. We then ran motif enrichment analysis for each of these motifs on each bin and plotted the p-values (Fig. 1C). Motifs for transcription factors known to be involved in fasting, such as those for PPARα,

glucocorticoid receptor (GR), and FOXO1, were enriched in bins more accessible in fasting livers. Similarly, motifs for factors known to be involved in feeding, such as those for SREBP1, C/EBP and JUN, were enriched in peaks more accessible in refed livers. Interestingly, GATA family motif was enriched in peaks more accessible during refeeding, compared to peaks similarly or more accessible during fasting (Fig. 1C, S1C). In the refed condition, the average accessibility of peaks with GATA4 motif within the top 10 bins was more than 50% higher in refed than in fasted mice (Fig. 1D). This finding was unexpected, as GATA family proteins were not previously known to be involved in the feeding response. The peaks with higher accessibility in refeeding that also had GATA family motifs clustered separately from those with motifs for other transcription factors, defining a unique signal and activity pattern for the GATA family in the refeeding response (Fig. S1D). Peaks with increased GATA family motif accessibility in refed livers were associated with genes linked to lipid, lipoprotein, and fatty acid metabolism, including *Srebf1*, *Insig1*, *Apoa1*, *Gpam*, *Pnpla3*, *Acsl5*, *Acaca*, *Fabp1*, *Elovl5* and others (Fig 1E). Further analysis showed enrichment of the C/EBPα motif among refed peaks with GATA motifs (p-value = 1e-205), suggesting possible collaboration between C/EBPα and GATA proteins in the feeding response (Fig. S1E).

RNA-Seq showed that, among the GATA family, only transcripts for *Gata4* and *Gata6* were expressed in liver (Fig. 1F). *Gata4* was more abundant than *Gata6* and its levels increased approximately 2-fold in response to refeeding. In contrast, *Gata6* decreased in refeeding, making GATA4 the most likely mediator of the increased GATA family activity seen in our ATAC-Seq analysis. Additionally, we validated the upregulation of *Gata4* transcript and protein levels by qPCR (Fig. S1F-G) and by western blotting (Fig. 1G). Analysis of publicly available RNA-Seq data comparing ad libitum fed mice to 24 hour-fasted mice [170], showed that circadian regulation

of *Gata4* is dependent of feeding (Fig. S1H). We further determined that insulin was the likely cause of the *Gata4* upregulation during feeding. In Hepa1-6 cells, treatment with insulin resulted in similar upregulation of *Gata4* expression (Fig. 1H). Based on these observations, we hypothesized that GATA4 plays a role in the hepatic metabolic response to feeding.

Loss of GATA4 alters the hepatic feeding response

Since GATA4 is essential for liver development[276], we knocked out GATA4 in liver of *Gata4*-floxed mice by administration of a hepatocyte-specific AAV8-Cre vector (Gata4LKO mice). QPCR analysis of fasted and refed mice one week after injection showed up to an 83% reduction in *Gata4* expression in mice receiving AAV8-Cre compared to vector control (Fig. 2A). Since liver endothelial and stellate cells are also known to express *Gata4* [280], residual *Gata4* expression was expected. This remaining *Gata4* expression was not responsive to feeding.

Metabolic phenotyping revealed that Gata4LKO mice had lower plasma cholesterol levels in both fasted and in refed conditions (Fig. 2B), implying GATA4 might have a role in cholesterol homeostasis independent of the feeding response. Fast protein liquid chromatography (FPLC) fractionation of plasma from refed mice showed decreased HDL cholesterol levels in Gata4LKO samples compared to controls (Fig. 2C). Plasma triglycerides (TG) and non-esterified fatty acids (NEFA) were not different between groups (Fig. S2A, B). Liver cholesterol was increased in Gata4LKO mice in the fasted state (Fig. 2D), suggesting a possible defect in cholesterol transport from liver to plasma. Fasted liver TGs trended higher in Gata4LKO samples compared to controls (Fig. 2E), while liver glycogen was reduced in refed Gata4LKO mice (Fig. 2F).

Lipidomic analysis revealed feeding-specific effects of loss of hepatic GATA4 on glycerophospholipids and ceramides. Total and many individual ceramide species were increased in refed Gata4LKO mice, and there was a statistically significant interaction between genotype and feeding status (Fig. 2G, H). Among phospholipids , phosphatidylglycerol (PG) and phosphatidylcholine (PC) species trended higher in refed Gata4LKO mice, while phosphatidylethanolamines were unchanged (Fig. S2C - E). Lastly, liver FA and sphingomyelin levels were increased in Gata4LKO mice across nutritional states (Fig. S2F, G, H). Overall, our phenotypic analysis demonstrated that loss of hepatic GATA4 altered phospholipid and ceramide metabolism during feeding, and cholesterol metabolism in both fasted and fed states.

GATA4 transcriptional targets in fasted and refed liver

We next conducted RNA-Seq and H3K27Ac ChIP-Seq on control and Gata4LKO livers from mice fasted or refed with high sucrose diet. Principal component analysis and hierarchical clustering showed clustering of replicates, and separation of knockout from control samples, in each condition for both RNA-Seq and H3K27Ac ChIP-Seq (Fig. S3A, B, C). Both methods showed greater separation between knockout and control samples in the refed condition.

The RNA-Seq data revealed genes differentially expressed between Gata4LKO and control liver during fasting or feeding (Fig. S3D). Downregulated genes in Gata4LKO mice were enriched for those linked to “lipid and lipoprotein metabolism”, “lipid mobilization” and “HDL-mediated lipid transport” (Fig. 3A). These included genes involved with cholesterol efflux, such as *Apoa1*, *Apoa2*, *Abcg5*, *Abcg8*, *Abca1*, *Alb*, and *Soat2*, and genes with lipid binding and lipid hydrolase functions, such as *Fabp2*, *Ces2a*, *Ces3b*, *Ces2g*, *Lipc*, and *Lipa* (Fig. 3B). Many of these genes were downregulated in both fasted and refed conditions (Fig. 3C). We also performed gene set enrichment analysis (GSEA) by ranking all genes based on their fold change

and p-value in refed Gata4LKOs and controls. GSEA independently showed downregulation of the cholesterol efflux pathway in Gata4LKO mice (Fig. 3D). The finding of reduced plasma HDL cholesterol in Gata4LKO mice is consistent with reduced cholesterol efflux from liver (Fig. 2B, C).

Genes relating to FA and glycerophospholipid metabolism were downregulated in Gata4LKO compared to control mice, specifically in the refed condition (Fig. 3B). Integrated pathway analysis (IPA) determined the "SREBP1 pathway" to be downregulated in refed Gata4LKO mice based on the downregulation of the *Srebf1* gene and SREBP1c target genes such as *Gpam Pnpla3* and *Acyl* in refed Gata4LKO mice (Fig. S3E). Moreover, genes that were only downregulated in refed Gata4LKO mice were enriched for the "glycerophospholipid metabolism pathway", and included *Pcyt2, Pgs1, Pisd,* and *Pla2g12b* (Fig. 3B, C). The refed-specific changes in this pathway were consistent with increases observed in glycerophospholipids in Gata4LKO mice (Fig. S2C-E). Genes relating to ceramide metabolism were downregulated in refed Gata4LKO mice, especially *Sgpl1*, which encodes the protein that performs the last step in ceramide degradation (Fig. 3B). Reduction of *Sgpl1* expression was consistent with the increased ceramide levels seen in refed Gata4LKO livers (Fig. 2G, H). Using publicly available GATA4 liver ChIP-Seq data (GSE49131), we determined that many of these downregulated genes involved in cholesterol and sphingomyelin metabolism and SREBP signaling had GATA4 binding sites within or proximal to the gene body, making them likely to be direct targets of GATA4 (Fig. S3F).

In fasting mice, we observed that SREBP2 and its targets in the cholesterol biosynthesis pathway were strongly downregulated in Gata4LKO livers compared to controls (Fig. 3B, C). Cholesterol inhibits its own biosynthesis by downregulating the SREBP2 targets [291]. The

increased cholesterol levels in fasted Gata4LKO livers were therefore in line with the downregulation of cholesterol synthesis genes (Fig. 2D).

In contrast to the downregulation of many genes linked to lipid metabolism genes, genes relating to glucose metabolism and gluconeogenesis pathways were upregulated in Gata4LKO livers compared to controls (Fig. 3E). In particular, qPCR analysis confirmed that the gene for rate limiting enzyme for gluconeogenesis, PEPCK (*Pck1*), had higher expression in refed Gata4LKO mice (Fig. S3G). Increased gluconeogenesis would be consistent with the reduced glycogen levels observed in Gata4LKO liver (Fig. 2F). Overall, these results indicate complementary shifts in both lipid metabolism and glucose metabolism in the absence of GATA4.

Loss of GATA4 reduces transcriptional activity at GATA4 binding sites

H3K27Ac is a marker of active enhancer sites [292]. By performing H3K27Ac ChIP-Seq on the same livers used for RNA-Seq, we assessed activity in regulatory regions in relation to transcriptional changes in Gata4LKO mice in both fasted and refed conditions. We analyzed the H3K27Ac changes near GATA4 binding sites from GATA4 liver ChIP-Seq (GSE49131) and observed an average decrease in enhancer activity at GATA4 binding regions in both fasted and refed Gata4LKO livers (Fig. S4A). We identified GATA4 binding regions with differential enhancer activity in Gata4LKO and control livers unique to each nutritional condition (Fig. 4A). A majority of the differentially regulated GATA4 binding regions lost enhancer activity in Gata4LKO liver and the magnitude of loss was greater in the refed state (Fig. 4B, top). To further address whether GATA4 was required for changes in transcriptional activity during feeding, we analyzed H3K27Ac signal in the regions of ATAC peaks with increased GATA family motif accessibility in refed livers. The average level of H3K27Ac near these peaks was

greater in refed controls than in fasted controls. Moreover, the increase in activity during feeding was blunted in Gata4LKO liver (Fig. 4B, bottom). For instance, candidate Gata4 sites associated with the feeding-induced genes *Pnpla3, Acsl5, Srebf1*and others lost enhancer activity in refed Gata4LKO liver, while the GATA4 binding site at its canonical target gene *Zfpm1* lost activity in Gata4LKO liver in both conditions (Fig. 4C, S4B). We validated the differential binding of GATA4 at some of these sites by conducting ChIP-qPCR at on the same liver samples (Fig. 4D). GATA-binding sequences from *Ces2a, Fabp5, Gpam, Pnpla3, Ralgps1* were enriched in GATA4-ChIP samples from refed compared to fasted liver, indicating increased binding of GATA4 with feeding at these regions.

Integrating H3K27Ac activity with the Gata4LKO RNA-Seq and GATA4 ChIP-Seq data, we sought to understand the factors that correlated with changes in gene expression. We asked if GATA4 binding or H3K27Ac at a GATA4 binding site was predictive of its differential expression of the cognate gene between WT and Gata4LKO mice. Indeed, the strength and change in H3K27Ac signal, and GATA4 binding were strongly associated with downregulated genes (Fig. 4E, F, and S4C).

To assess how other transcription factors were responding to the loss of hepatic GATA4, we analyzed transcription factor motif enrichment at sites of changing H3K27 acetylation. As expected, the GATA motif was enriched in regions with decreased H3K27 acetylation in refed Gata4LKO liver (Fig. S4D). Interestingly, binding motifs for two key transcription factors involved in the fasting response, PPARα and FOXO1, were enriched in regions with increased H3K27 acetylation in refed Gata4LKO liver (Fig. S4E). This suggests inadequate suppression of fasting responses in refed Gata4LKO liver. We further conducted pathway analysis on the genes associated with regions of differential H3K27 acetylation in refed Gata4LKO liver. Regions with

decreased H3K27 acetylation were enriched for genes associated with the AKT and insulin signaling pathways (Fig. S4F). Regions with increased H3K27 acetylation were enriched for genes associated with AMPK signaling (Fig. 4G). For some of these genes, including *Srebf1* and *Pck1*, changes in H3K27 acetylation mirrored changes in gene expression (Fig. 3B, S3F), providing further evidence for disruption of the feeding response in Gata4LKO liver.

Loss of hepatic GATA4 leads to TG accumulation in liver

Based on the observation that loss of GATA4 altered the expression of some hepatic genes regardless of feeding status, we explored potential metabolic functions for GATA4 beyond our fasting and refeeding paradigm. We hypothesized that increasing the TG and cholesterol content in their diet might provoke additional phenotypes in Gata4LKO mice. We fed mice chow or western diet (WD) for 3 - 4 weeks after AAV injection, and sacrificed them after 6 hours of fasting. Plasma cholesterol levels were lower in Gata4LKO mice compared to controls on both chow and WD (Fig. 5A). Liver cholesterol levels were modestly increased in Gata4LKO mice only in the chow-fed condition (Fig. 5B). Both on chow and WD, liver TGs more than doubled in Gata4LKO mice (Fig. 5C). Hematoxylin and eosin (H&E) and Oil Red O staining of liver sections from WD-fed mice confirmed hepatic lipid accumulation in Gata4LKO mice (Fig. 5D, S5A). Lipidomic analysis of chow-fed liver samples showed that liver TGs with diverse fatty acid content were broadly increased (Fig. 5E). On both chow and WD, liver fatty acids were also elevated in Gata4LKO mice compared to controls (Fig. S5B). Liver glycogens were reduced in Gata4LKO, especially on WD (Fig. S5C). There was no difference in VLDL secretion (Fig. S5D)

We analyzed gene expression to further characterize the phenotype of Gata4LKO mice on WD. Data from RNA-Seq of Gata4LKO and control mice after 3 weeks on WD clustered by

genotype (Fig. S6A) and revealed 716 genes downregulated and 1029 upregulated in Gata4LKO liver (Fig. S6B). Expression of genes linked to cholesterol metabolism, including transport genes such as *ApoA1*, *Apoc1*, *Abcg5*, *Abcg8,* were reduced in WD-fed Gata4LKO mice (Fig. 5F). Many of these genes were also differentially expressed in chow-fed control and Gata4LKO livers (Fig. S6C). Moreover, fatty acid biosynthesis genes such as *Srebf1*, *Acly*, *Acaca*, and *Acsl3* showed reduced expression in WD-fed Gata4LKO mice (Fig. 5F). Given the reduction in gene expression linked to FA biosynthesis, increased lipid synthesis was unlikely to be the cause of the TG accumulation in Gata4LKO liver. We therefore assessed the expression of genes involved in FA oxidation. PPARα targets such as *Acox1*, *Ehhadh* and others were upregulated in Gata4LKO mice (Fig. 5G, S6D). This pattern suggested that PPARα was activated in Gata4LKO liver secondary to hepatic TG accumulation. Interestingly, the expression of genes relating to TG hydrolysis, including *LipC*, *Ces2a*, *Aadac*, and *Ces1g* were reduced in Gata4LKO mice, suggesting a possible mechanism for the hepatic TG accumulation (Fig. 5H). Additionally, genes linked to lipid and lipoprotein uptake, such as *Lpl*, *Cd36*, and *Vldlr*, were upregulated in Gata4LKO mice, suggesting that increased lipid uptake may also contribute to hepatic lipid accumulation (Fig. 5G).

GATA4 collaborates with LXR to induce their joint transcriptional targets

Many of the genes downregulated in Gata4LKO mice, including *Abca1*, *Abcg5*, *Abcg8*, *Srebf1* and *Fasn*, are LXR targets[293–296]. IPA analysis predicted that LXRα transcriptional activity was downregulated in Gata4LKO liver (Fig. 6A). ChIP-X Enrichment Analysis (ChEA) showed that downregulated genes in Gata4LKO mice (fasted, refed or WD-fed) were enriched for LXR ChIP-Seq targets [297] (Fig. 6B). Moreover, LXR ChIP-Seq showed the LXR cistrome was enriched for GATA4 binding sites, especially when mice were treated with the LXR agonist

T0901317, suggesting common binding of the two transcription factors (Fig. 6C). GATA4-LXR co-binding regions were associated with genes involved in lipid and lipoprotein metabolism, and lipid transport (Fig. S7A).

LXR and GATA4 co-binding regions were associated with changes in enhancer and transcriptional activity in Gata4LKO liver. Enhancers with both LXR and GATA4 binding sites on average lost H3K27Ac enrichment in Gata4LKO liver (Fig. 6D). Moreover, a strong LXR binding signal at a GATA4 binding enhancer was predictive of the downregulation of H3K27Ac level of that enhancer and transcript level of the cognate gene in Gata4LKO liver (Fig 6E, F). Examples of LXR and GATA4 co-binding genes include *Abca1*, *Abcg5, Abcg8, Ces2a*, *Fabp5*. Each of these had reduced expression and H3K27 acetylation at the LXR-GATA4 binding regions in Gata4LKO livers compared to controls (Fig. 3B, 6G).

To further assess the role of GATA4 in hepatic LXR signaling, we treated control and Gata4LKO mice with the LXR agonist GW3965. Gene expression analysis revealed a panel of genes whose expression showed a significant interaction between genotype and LXR agonist treatment, including *Abcg5*, *Ces2a*, *Fabp2*, *Fabp5*, and *Soat2* (Fig. 6H). Induction of these genes by LXR agonist was blunted in Gata4LKO livers. We noted other genes whose expression was reduced in Gata4LKO livers at baseline but not after treatment with LXR agonist treatment, including *ApoA5, Insig2, and Scarb1* (Fig. S7A). The expression of certain genes involved in glucose metabolism, such as *G6pc*, *Pck1*, and *Pfkfb1*, also showed interaction between Gata4LKO genotype and LXR agonist treatment, indicating the LXR-GATA4 collaboration was not limited to cholesterol and triglyceride metabolism (Fig. S7B).

GATA4 is associated with human LDL and HDL cholesterol levels

To address whether GATA4 was associated with hepatic metabolism in humans, we probed the T2D Knowledge Portal for associations between GATA4 and human metabolic traits from combined GWAS studies. We found SNPs within a linkage disequilibrium (LD) block containing GATA4 that were associated with LDL and HDL cholesterol (p-value < 5e8) (Table S1). The top SNPs in this LD block for both phenotypes were within intronic regions of the *GATA4* gene (Fig. S8).

Discussion

Here we used ATAC-Seq to profile transcription factor motifs associated with genome-wide changes in chromatin accessibility in response to feeding. This approach led to the identification of GATA4 as a transcriptional regulator of the liver metabolism during feeding. Expression of GATA4 is induced in response to insulin, GATA4 binding to certain targets is increased in response to feeding, and GATA4 binding is associated with transcriptional activity at the enhancers of a battery of genes linked to lipid metabolism. In line with an important role in liver physiology, deletion of GATA4 from adult mouse liver altered plasma and hepatic lipid levels. Our analysis also revealed that GATA4 cooperates with the nuclear receptor LXR in the regulation of cholesterol metabolic genes in liver. These results identify GATA4 as an important transcriptional modulator of hepatic lipid homeostasis.

By deleting GATA4 via Cre-mediated recombination in adult liver, we assessed the impact of loss of GATA4 on global hepatic gene expression. Taking a broad view, we noted that some but not all GATA4 binding sites lost enhancer activity (as reflected by H3K27Ac) in Gata4LKO mice. Moreover, as seen in other studies [282], GATA4 target regions that lost acetylation upon GATA4 deletion were more likely to be associated with reduced gene expression. Additionally, the strength of GATA4 binding and H3K27Ac level were predictive of whether or not a given GATA4 binding site was functional. This suggests that the local epigenetic context influences the impact of GATA4 binding on transcriptional activity.

Our integrated genome-wide analyses revealed at least two discreet functions for GATA4 in hepatic gene expression. One is to promote the expression of genes linked to fatty acid, phospholipid, and ceramide metabolism during feeding. A cadre of genes in these pathways had GATA4 binding motifs with increased ATAC accessibility during feeding in our analysis.

Deletion of GATA4 compromised the expression of these genes specifically in refed liver. In particular, the SREBP1c pathway–a key mediator of insulin signaling–was downregulated in refed Gata4LKO liver. GATA4's collaboration with LXR may contribute to its effects on SREBP1 pathway, since LXR is necessary for maximum expression of SREBP1c and several of its target genes in response to feeding [293,296].

A second function for GATA4 in liver is to regulate a different set of genes independent of feeding status. Most prominent in this group of targets are those linked to cholesterol metabolism. Accordingly, mice lacking GATA4 in liver had reduced plasma HDL cholesterol and increased liver cholesterol levels. A number of key genes in cholesterol efflux, including *Apoa1*, *Abca1*, *Abcg5*, and *Abcg8* were downregulated in Gata4LKO livers; these may contribute to HDL phenotype. ABCA1 mediates cholesterol transport from cells to Apo-AI, which is the major protein component of HDL [298]. LXR induces cholesterol efflux by upregulating some of these same genes [299]. It is likely that the disruption of the GATA4 -LXR collaboration causes a reduction in cholesterol efflux from Gata4LKO liver. A previous study suggested that the loss of GATA4 in jejunum reduced dietary cholesterol absorption, supporting GATA4's ability to impact cholesterol transport [300].

Liver triglycerides accumulated over time in Gata4LKO mice, and the high fat content of a WD exacerbated this accumulation. This finding is consistent with a prior study showing that GATA4 knockdown caused TG accumulation in HepG2 cells treated with oleic acid [285]. Evidence from gene expression and functional assays argue against possible defects in VLDL secretion or fatty acid oxidation, or an increase in fatty acid biosynthesis, as the causes of hepatic lipid accumulation in Gata4LKO mice. Rather, a number of triglyceride hydrolysis genes (including *Lipc*) were downregulated, and genes involved in FA and TG uptake (such as *Lpl*)

were upregulated in Gata4LKO mice. Many members of the *Ces* family, including *Ces1g* and *Ces2a* which are known to have triglyceride hydrolase functions, were also downregulated in response to loss of *Gata4* [301]. Future studies are needed to confirm the mechanisms underlying the phenotypes of Gata4LKO mice.

Previous GWAS studies have associated the *GATA4* gene and GATA4 binding with hyperlipidemia in humans [285,286]. Using GWAS databases, we found SNPs with associations to HDL and LDL cholesterol levels in humans map within the GATA4 gene. However, functional studies are needed to validate the role of these variants in human metabolism.

Our study identified LXR as an important transcriptional partner for GATA4 in liver. GATA4, HNF4A and LXR were also shown to participate in the regulation of *ABCG5* and *ABCG8* in HepG2 cells [302,303]. Our data reveal that GATA4 and LXR collaborate at many loci across the genome, and that the overlap in their binding increases when LXR is activated. LXR appears to require the presence of GATA4 to fully activate its shared targets. Genes with enhancers that bound both GATA4 and LXR were more likely to be downregulated in Gata4LKO livers, indicating the functional importance of this cooperation. Moreover, loss of GATA4 interfered with the upregulation of some LXR target genes in response to LXR agonist treatment. In summary, hepatic GATA4 plays a central role in the transcriptional regulation of hepatic lipid metabolism in collaboration with LXR.

Methods

Mice

C57BL/6J mice from Jax Laboratories (Strain #:000664) were used as wildtype mice in initial ATAC-Seq and RNA-Seq screen. Gata4 floxed/floxed mice were previously described[304] and were obtained from Jax Laboratories (Strain: 008194) and maintained on a mixed 129/C57BL/6 background. Gata4LKO were created by injecting AAV.TBG.PI.Cre.rBG (Catalog #:107787-AAV8, Addgene) or AAV.TBG.PI.Null.bGH (Catalog #:105536-AAV8, Addgene) for control at 5 x 10^11 genome copies per mouse concentration at 8 – 10 weeks of age. High sucrose (HS) diet (69% sucrose 10% fat, D07042201) and RD Western Diet (40% calories from fat, 0.2% cholesterol, D12079B) were obtained from Research Diets. In fasting and refeeding experiments, the refed group was fasted for 12 h starting at 9 am and refed for 12 h with HS diet starting at 9 pm. The fasted group was fasted for 12 h starting at 9 PM. Both groups had access to water throughout and were sacrificed 9 – 10 AM the following day. In other experiments, mice started fasting at 8 – 9 AM and were sacrificed at 2 – 3 PM. Mice had ad libitum access to chow, unless another diet is specified and were housed in pathogen-free, facilities maintained at 22 °C on 12-h light/dark cycles. The mouse studies were approved by the University of California Los Angeles (UCLA) Chancellor's Animal Research Committee.

ATAC-Seq sample preparation and sequencing

ATAC-Seq from tissue was conducted as previously published[305]. In summary, fresh tissue was homogenized in nuclear isolation buffer (20 mM Tris-HCl, 50 mM EDTA, 5 mM Spermidine, 0.15 mM Spermine, 0.1% mercaptoethanol, 40% glycerol, 1mM EGTA, 60 mM KCl, 1% IGEPAL pH 7.5) and filtered (40 μM). Samples were centrifuged and resuspended with cold resuspension buffer (RSB) (10 mM Tris-HCl, 10 mM NaCl, 3 mM MgCl2, pH 7.4).

Transposase reaction was performed on approximately 50,000 nuclei from these samples, DNA was purified using Qiagen MinElute Kit and libraries were prepared as described[306]. Size selection was done with AMPure XP magnetic beads. Libraries were quantified using NEBNext Library Quant Kit for Illumina and were sequenced on Illumina HiSeq 4000 as single-end 50 bp.

RNA-Seq sample preparation and sequencing

RNA was extracted from frozen tissue using TRIzol (Invitrogen) and Qiagen RNeasy Mini Kit. The libraries were made with KAPA Stranded kit with mRNA capture. Libraries for were sequenced on Illumina HiSeq 3000 as single-end 50 bp or paired-end (50 bp) on Novaseq SP 100 cycles.

Chromatin Immunoprecipitation

Chromatin was prepared from frozen tissue using truChIP Chromatin Shearing Tissue Kit (Covaris). Chromatin was sheared using Diagenode Bioruptor Pico for 30 s ON/ 30 s OFF 10 cycles in SDS lysis buffer (1% SDS, 10 mM EDTA pH 8.1; 50 mM Tris-HCl, pH 8.1) supplemented with protease inhibitor cocktail. Input were de-crosslinked overnight at 65C in elution buffer (0.1M NaHCO3; 0.1% SDS; 200mM NaCl) followed by treatment with RNAseA (0.125ug/ml, Thermo Scientific) and Proteinase K (0.1mg/ml). Chromatin was purified using QIAQuick PCR Purification Kit and quantified using Qubit (dsDNA HS). Dynabeads Protein A (Invitrogen) were preincubated with 4 μg of H3K27Ac (ab4729, Abcam) or Rabbit anti-GATA4 Antibody (A303-503A, Fortis Life Sciences) in ChIP dilution buffer (0.01% SDS; 1.1% Triton X-100; 1mM EDTA, pH 8.1; 16.7 mM Tris-HCl, pH 8.1; 167 mM NaCl + proteinase inhibitor) for 1.5 h at room temperature. 7 – 10 μg of chromatin was incubated overnight with the corresponding antibody-bound beads with rotation for immunoprecipitation (IP). IP samples

were washed with low salt wash buffer (0.1% SDS; 1% Triton X-100; 2 mM EDTA pH 8.1; 20mM Tris-HCl pH 8.1; 150 mM NaCl), followed by high salt wash buffer (0.1% SDS; 1% Triton X-100; 2 mM EDTA pH 8.1; 20mM Tris-HCl pH 8.1; 500 mM NaCl), LiCl wash buffer (250 mM LiCl; 1% deoxycholic acid; 1mM EDTA pH 8.1, 10 mM Tris-HCl pH 8.1; 1% Igepal) and finally 2 washes with TE Buffer (1 mM EDTA pH 8.1; 10 mM Tris-HCl pH 8.1)[307]. IP samples were de-crosslinked and purified as described for the input above. GATA4 ChIP samples and inputs were assessed using qPCR. Previously defined Gata4 negative genomic regions [Fx-neg and Alb-neg][279] were used to normalize across all samples in the qPCR calculation. Values represent the average fold-change over the negative regions. Primer sequences for targets and controls are presented in SI Appendix, Table S2. H3K27Ac ChIP samples and inputs were assessed by single-end 50 bp sequencing in HiSeq 3000.

High-throughput sequencing data processing

For RNA-Seq, reads were aligned to the mm9 or m10 genome using STAR[308]. DESeq2 and Seqmonk were used to generate normalized counts or reads per kilobase of transcript, per million mapped reads (RPKM). DESeq2 was used to identify differentially expressed genes with FDR < 0.05 cutoff. For ATAC-Seq and ChIP-Seq, trimmed sequences were aligned to the mm9 using bowtie2[309]. Reads were filtered using samtools[310]. Peaks were called using MACS2 and consensus peaks were created using bedtools[311]. For ATAC-Seq, peaks were quantitated across samples, normalized to million reads per sample and peak length (RPKM), using Seqmonk. Differentially accessible peaks were determined using EdgeR[312]. For ChIP-Seq, peaks were quantitated and differentially expressed peaks were selected using Diffbind[313]. FDR < 0.05 was used to identify differentially accessible or enriched peaks.

Peaks were annotated to genes with nearest promoter via Homer[314]. Replicates were merged using samtools. Bedgraphs were created using Homer and visualized using IGV[315]. Peaks with minimum 10 counts were ranked based on the fold difference between the conditions. Ranked peaks were divided into bins each containing ~1000 peaks and known motif analysis was run for each bin using Homer. The p-value for each motif across all bins were calculated. Highly similar motifs (> 0.9 similarity score) are summarized by one motif and motifs that are not differentially enriched are omitted from the heatmap for simplicity. Homer was used to identify the genomic regions the motifs were present.

High-throughput Sequencing Data Analysis and Visualization

Heatmaps were created using ClustVis web tool[316]. Unit variance scaling was used except for Fig. S1C, D. Bioplanet, Wikipathways, and KEGG from Enrichr, Gene Set Enrichment Analysis (GSEA), and Integrated Pathway Analysis (IPA) software were used for pathway enrichment analysis [317,318]. FDR <0.05 was used for identifying differentially expressed genes. The genes were ranked based on fold change and p-value (-log2FC*-log10p-value) for GSEA analysis. DeepTools2 was used to quantify and profile the signal intensity in the ATAC-Seq and ChIP-Seq samples across defined peaksets [319]. Bedtools window function with 500 bp range was used to identify H3K27Ac peaks near GATA4 and LXR ChIP-Seq sites.

Plasma and liver metabolic assays

Lipids were extracted from liver using the Bligh and Dyer method [320]. Total cholesterol, and NEFAs were measured using commercially available TC and NEFA kits from WAKO and triglycerides were measured using TG kit from Sekisui Diagnostics both for plasma and liver lipid extract. To resolve lipoprotein classes by fast protein liquid chromatography, plasma was

injected into a Superose 6 10/300 (GE Healthcare Life Sciences) chromatography column and sequential fractions (1-80) were collected for measurement of cholesterol by colorimetric assay (WAKO, NC9138103).

Lipidomics

Our lipidomics experiments use direct infusion-tandem mass spectrometry and were performed on SCIEX 5500 triple-quadrupole (QQQ) with a Shimadzu auto-sampler, SelexION ion mobility device, and Shimadzu LC. Species are quantified using Sciex Lipidyzer Platform and Sciex and Avanti Polar Lipid standards.

Liver glycogen assay

Frozen liver samples were prepared as described previously by precipitating proteins [321]. Glycogen Assay kit (Sigma-Aldrich) was used according to manufacturer's instructions and the measurements were normalized to protein content.

RT-qPCR

TRIzol was used to isolate RNA from frozen tissue and concentrations and quality were measured using Nanodrop. cDNA was made and Real-time RT-qPCR (Bio-Rad) and Applied Biosystems Quant Studio 6 Flex was used for RT-qPCR. Primers are in SI Appendix,Table S3. Counts were normalized to the 36B4 expression from the same samples.

Western Blotting

Proteins were isolated with radioimmunoprecipitation assay buffer buffer (Boston BioProducts) as previously described[321]. Samples were loaded to Bis-Tris gels and proteins were separates by electrophoresis prior. They were transferred to polyvinylidene difluoride

membranes. The membranes were blocked in 5% nonfat milk in phosphate-buffered saline (PBS). Rabbit anti-GATA4 Antibody (Cat # A303-503A-M, Fortis Life Sciences) anti-actin antibody (A2066, Sigma-Aldrich) were used as the primary and horseradish peroxidase–conjugated anti–rabbit IgG (Jackson Laboratory) was used as the secondary antibody. Signal was produced using Immobilon Forte Western HRP Substrate (EMD Millipore).

Histology

Tissues were fixed in 4% paraformaldehyde. Tissues were mounted in paraffin and 10-μm sections were cut. Sections were stained with hematoxylin and eosin (H&E). Oil Red O staining was done as previously described[322]. Tissues were fixed in Tissue-Tek O.C.T. compound (cat No. 4583) on dry ice. 5-μm sections were cut using Microm HM 505 E cryostat and placed on glass slides. Oil Red O solution (Sigma, cat. No. 00625, ~0.4%) was used for staining. Zeiss Axioskop 2 plus bright-field light microscope was used to capture the images.

VLDL secretion assay

6 h fasted mice were injected with 1.0 g/kg of body weight poloxamer-407 (10% (w/v) in saline, Catalog #:16758, Sigma-Aldrich) [323]. Blood samples were collected at 0, 1, 2, 3 and 4 h time points via retroorbital bleeding and cardiac puncture for the final time point. Plasma was obtained by centrifuging blood by 2,000g for 15 min. Plasma was assayed for lipids as described above.

LXR Agonist treatment

Nine-week-old mice on Gata4LKO and control mice, 1 week after AAV injection, were gavaged with 40 mg/kg GW3965 prepared in canola oil [324] at 17 h, and then 8 h before before

sacrifice. Mice were 4 h fasted at the time of killing. Dimethylsulfoxide in canola oil was used as vehicle control. Gene expression was determined via RT-PCR as described above.

Cell culture studies

Hepa1-6 cells were deprived of FBS, glucose, and glutamine in base Dulbecco's Modified Eagle Medium (DMEM) which was supplemented with or without 100 nM insulin for 8 h RNA was extracted and RT-PCR was used in assessing *Gata4* expression.

GWAS data

The SNPs and the Manhattan plot for the GATA4 loci for HDL and LDL trait were obtained from Type2Diabetes Knowledge Portal on August 1st, 2022. GATA4 loci was defined as the default LD block spanning chr8:11,484,468-11,667,511 in hg19 genome build.

Additional datasets

Gata4 expression throughout 24 h with and without fasting (GSE107787), GATA4 ChIP-Seq (GSE49132) and LXR liver ChIP-Seq data with and without agonist treatment (GSE35262)[33] were obtained from Gene Expression Omnibus (GEO).

Data availability

RNA-Seq (GSE212485) and ATAC-Seq (GSE212483) of fasted and refed wildtype liver, RNA-Seq (GSE212486) and H3K27Ac ChIP-Seq (GSE212484) of fasted and refed Gata4LKO and control liver and RNA-Seq (GSE212486) of livers of Gata4LKO and control mice on western diet were deposited to the NCBI Gene Expression Omnibus under the SuperSeries accession number GSE212488.

Competing Interest Statement

The authors declare no competing interests.

Acknowledgements

Funding for this project was provided by grants from the NIH (HL136618, DK126779, and DK063491) to P.T. We thank all members of the Tontonoz laboratory for technical support and valuable discussions. We thank the staff at the UCLA Technology Center for Genomics and Bioinformatics, UCLA Broad Stem Cell Research Center, UCLA Lipidomics Core and Translational Pathology Core Laboratory for their services and assistance.

Author Contributions

L.B. and P.T. designed the study and wrote the manuscript. L.B., M.L.R., C.P., J.P.K., and A.F. conducted the experiments. L.B., M.L.R., J.P.K., A.C.F, and P.R. analyzed the data. S.G.T. and S.T.S. provided critical reagents and analysis methodology.

Figures and Tables

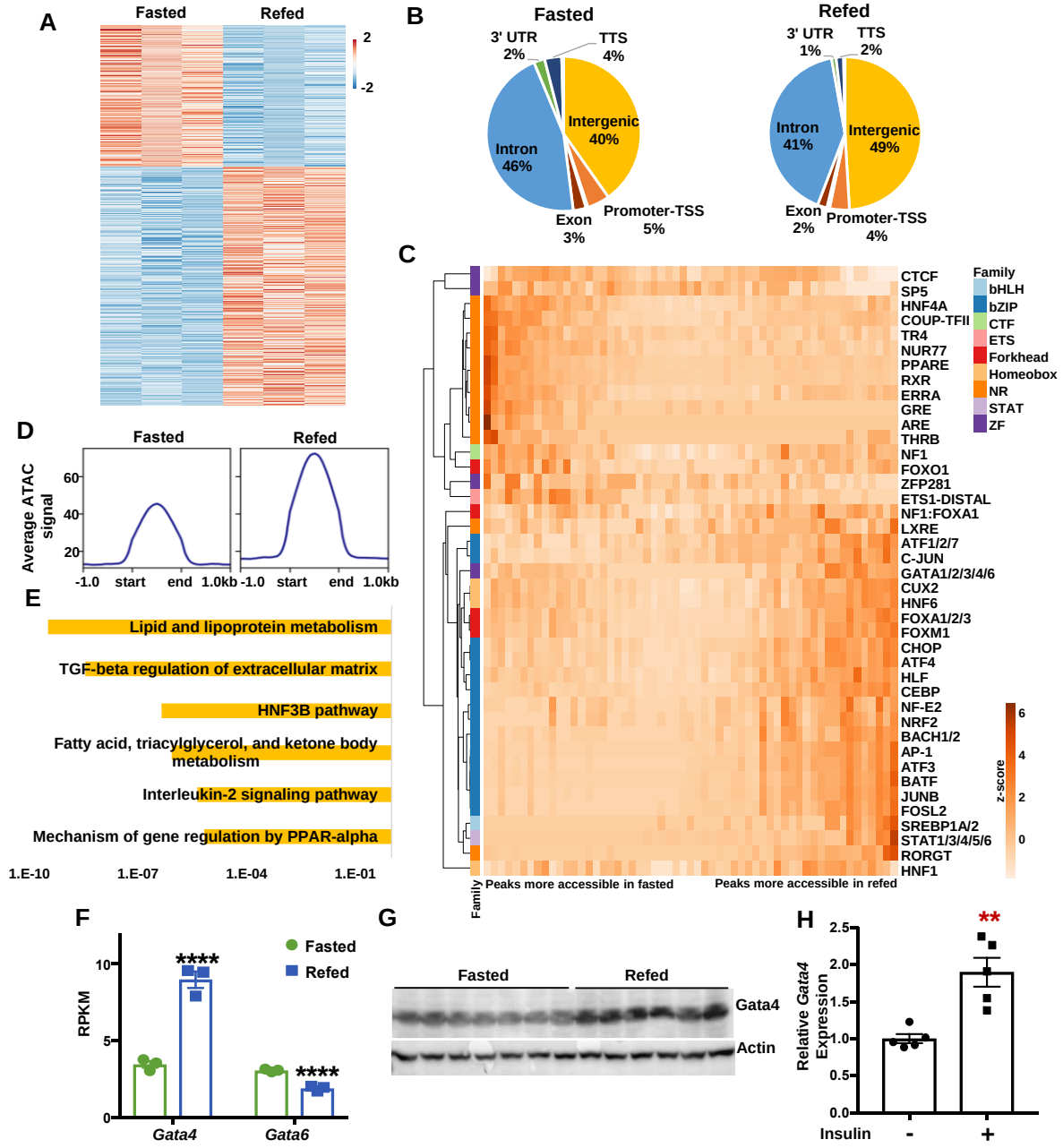

Figure 2-1: GATA4 motif accessibility and expression is upregulated in liver by feeding.

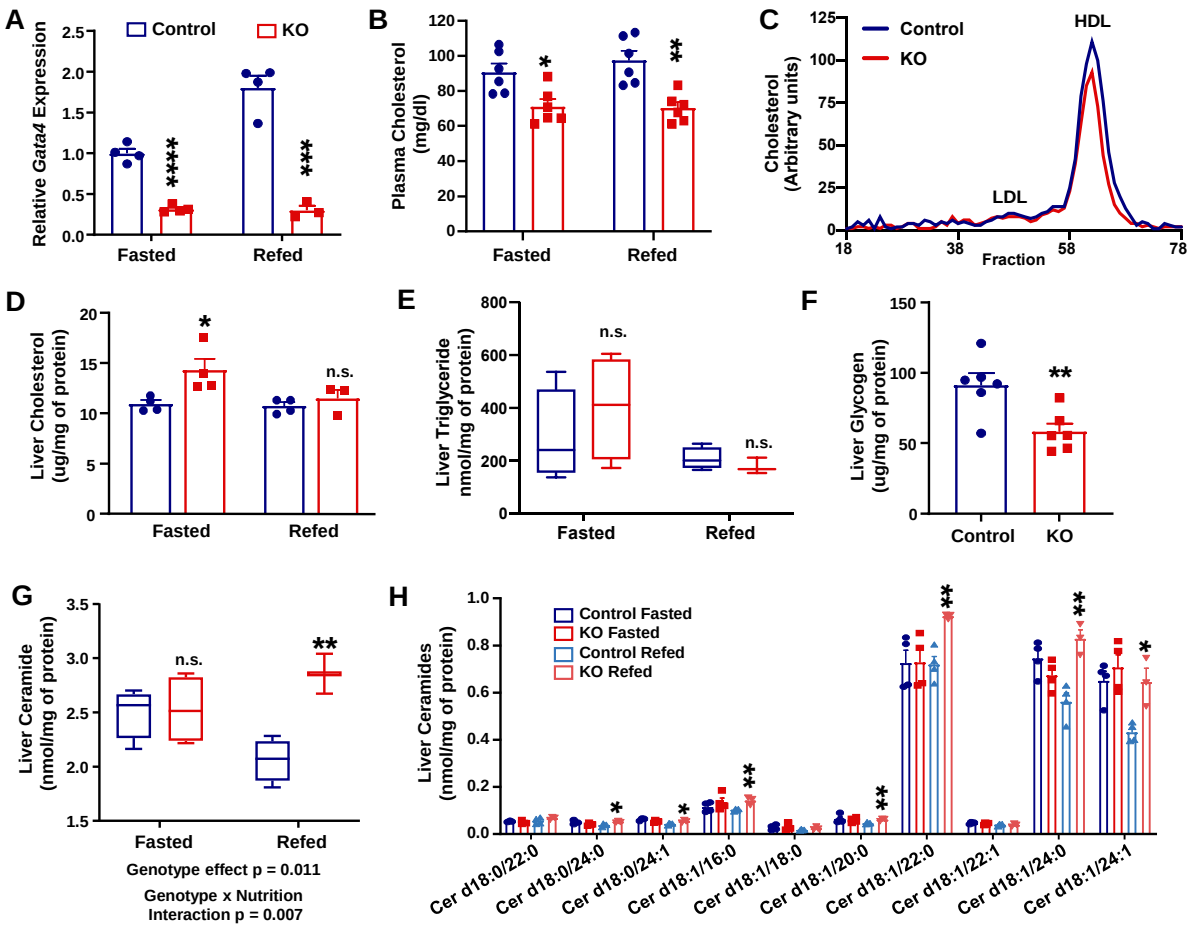

Figure 2-2: Loss of Gata4 in liver alters the hepatic and systemic lipid profile in fasting and in feeding.

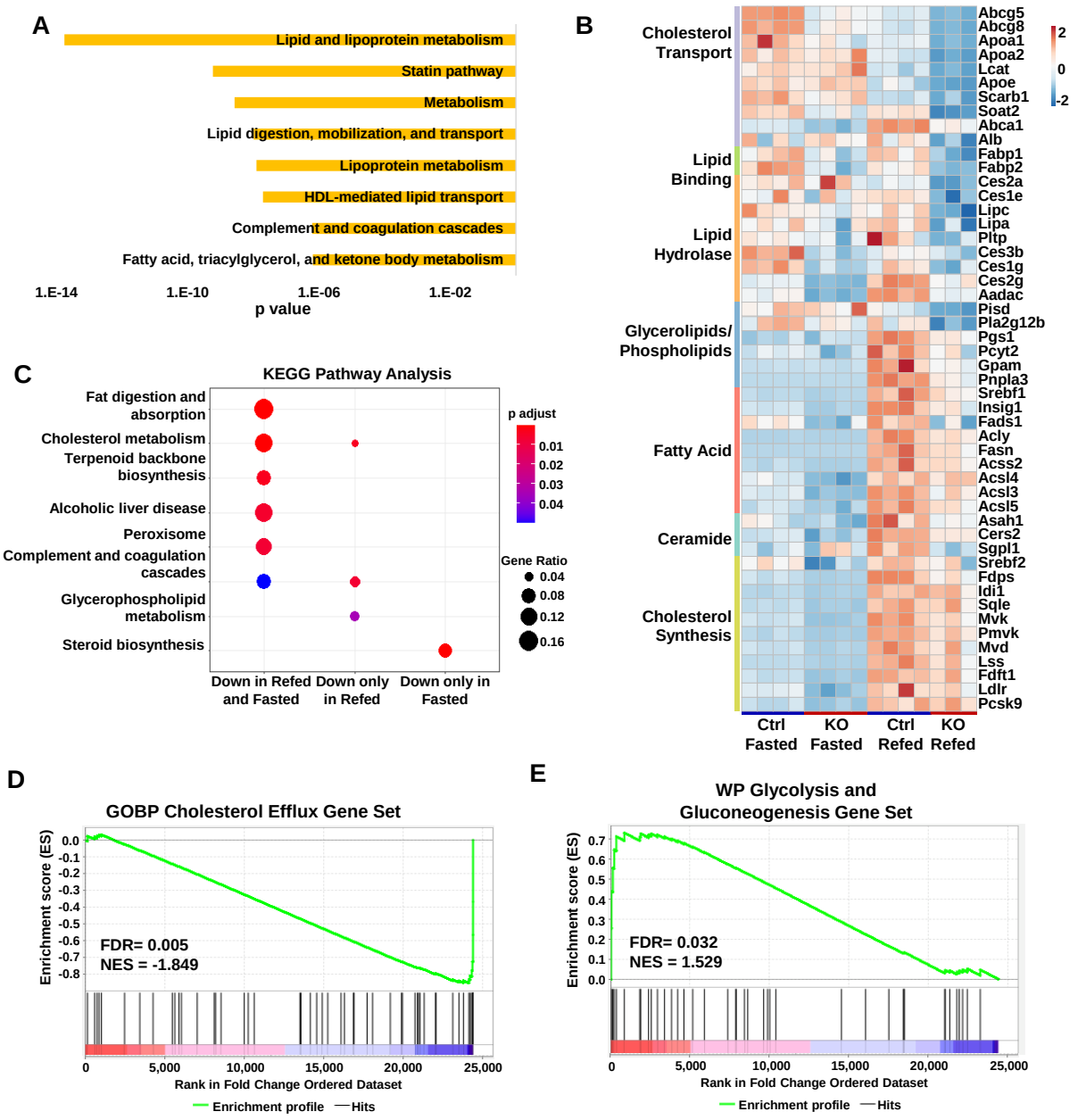

Figure 2-3: Loss of Gata4 downregulates lipid metabolism pathways in fasting and in feeding.

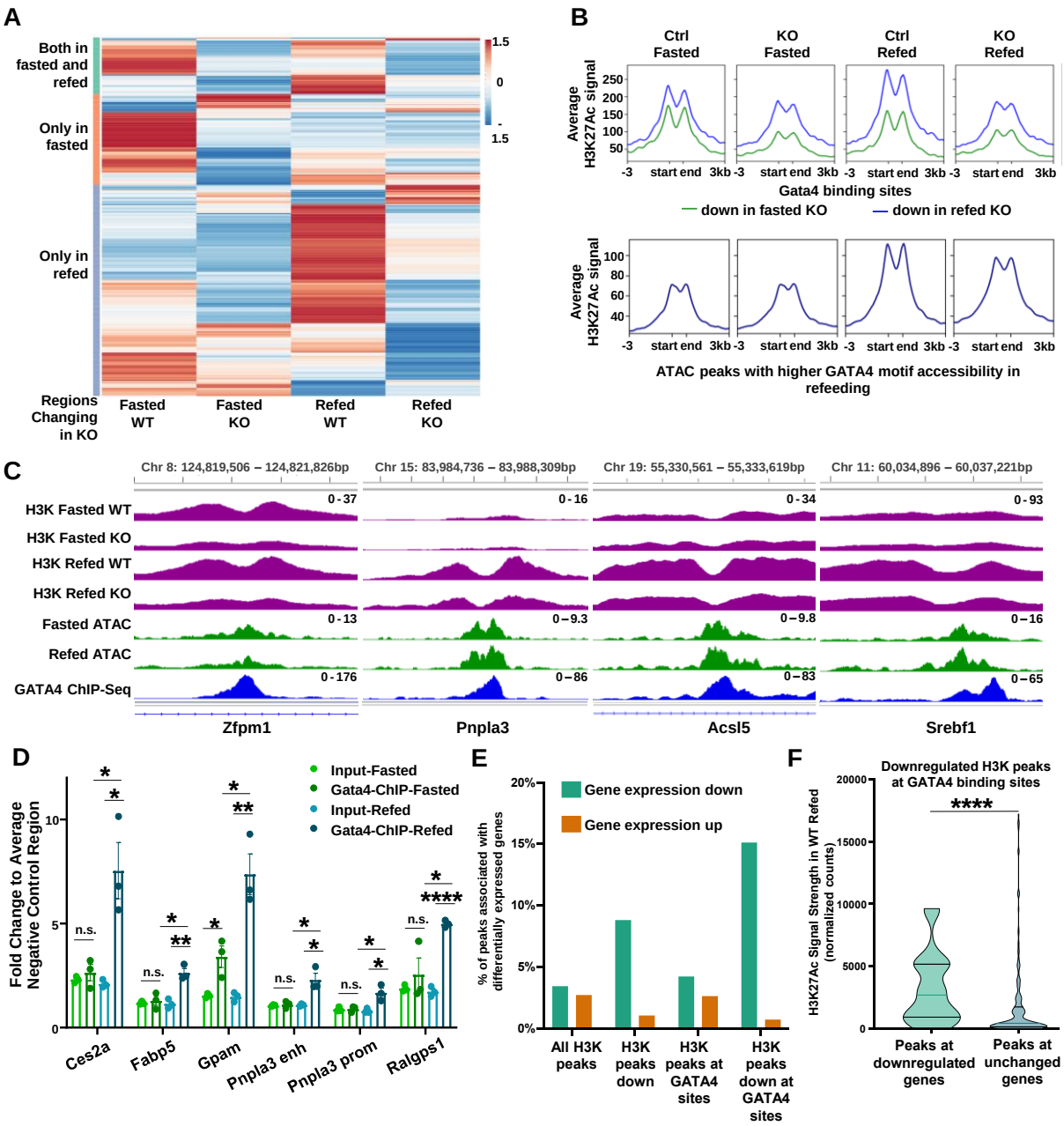

Figure 2-4: GATA4 has common and differential targets in fasted versus refed liver.

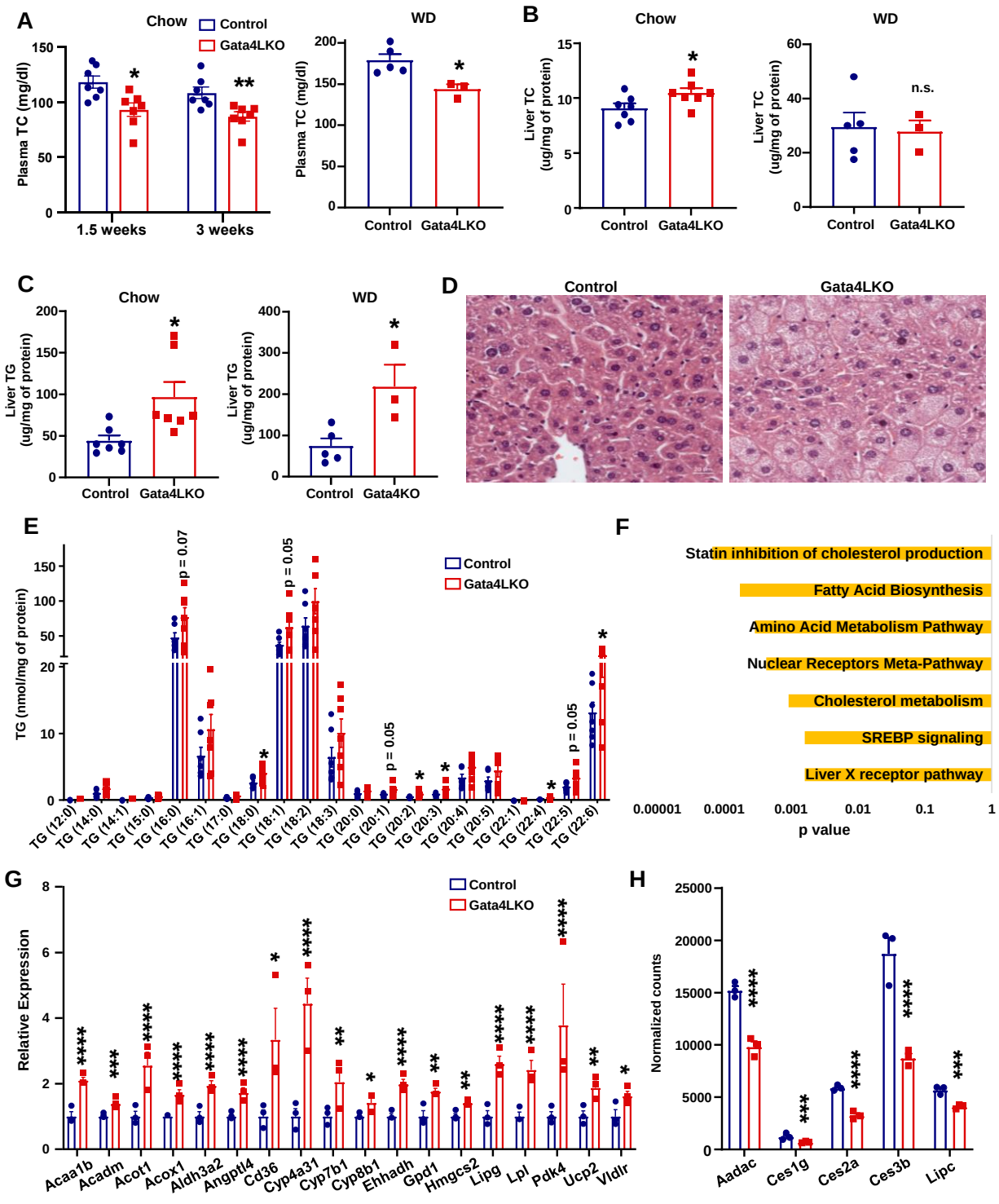

Figure 2-5: Loss of Gata4 results in reduction in plasma cholesterol and accumulation of liver triglycerides.

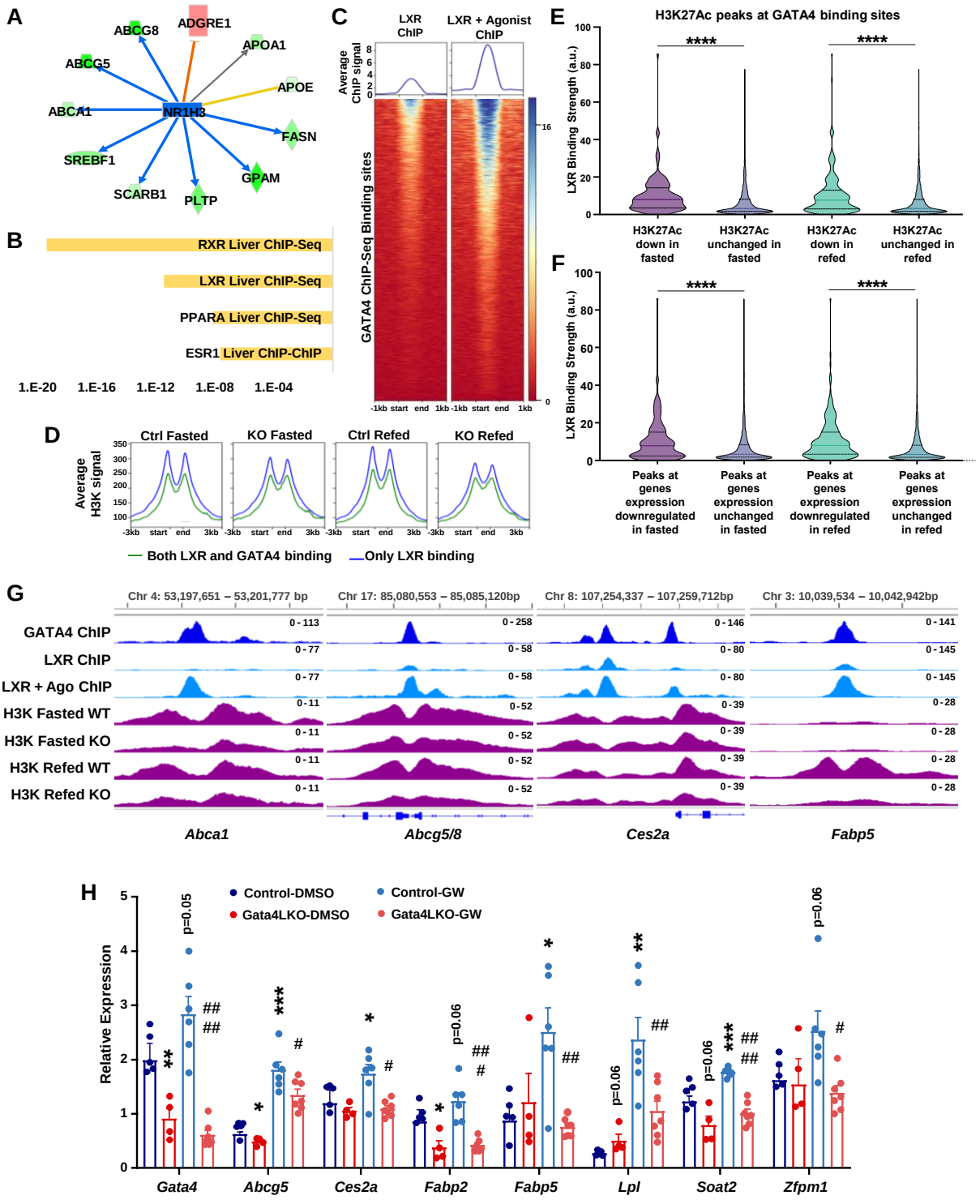

Figure 2-6: GATA4 collaborates with LXR to induce shared transcriptional targets.

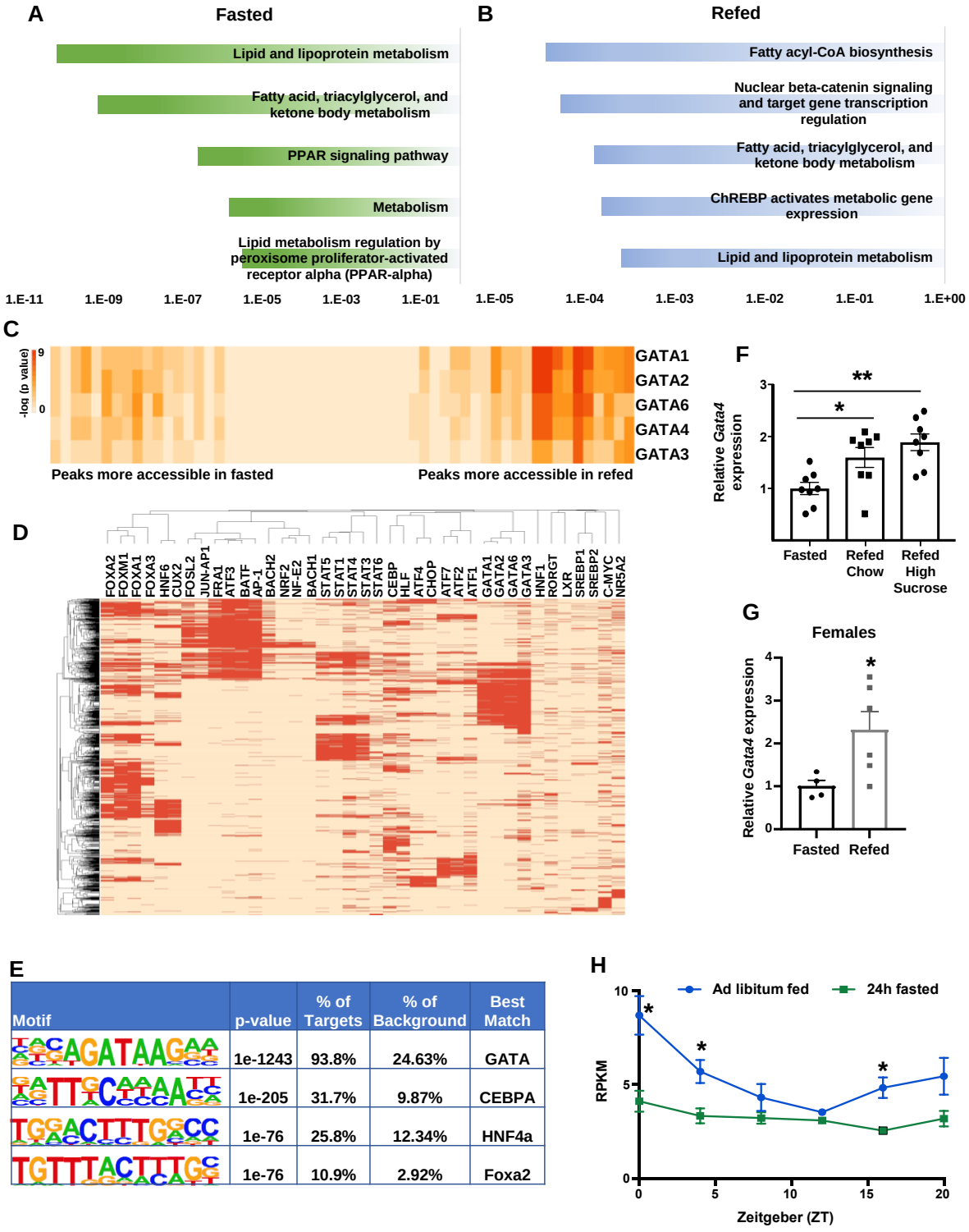

Figure 2-S1: ATAC-Seq reveals changes in transcriptional regulatory landscape..

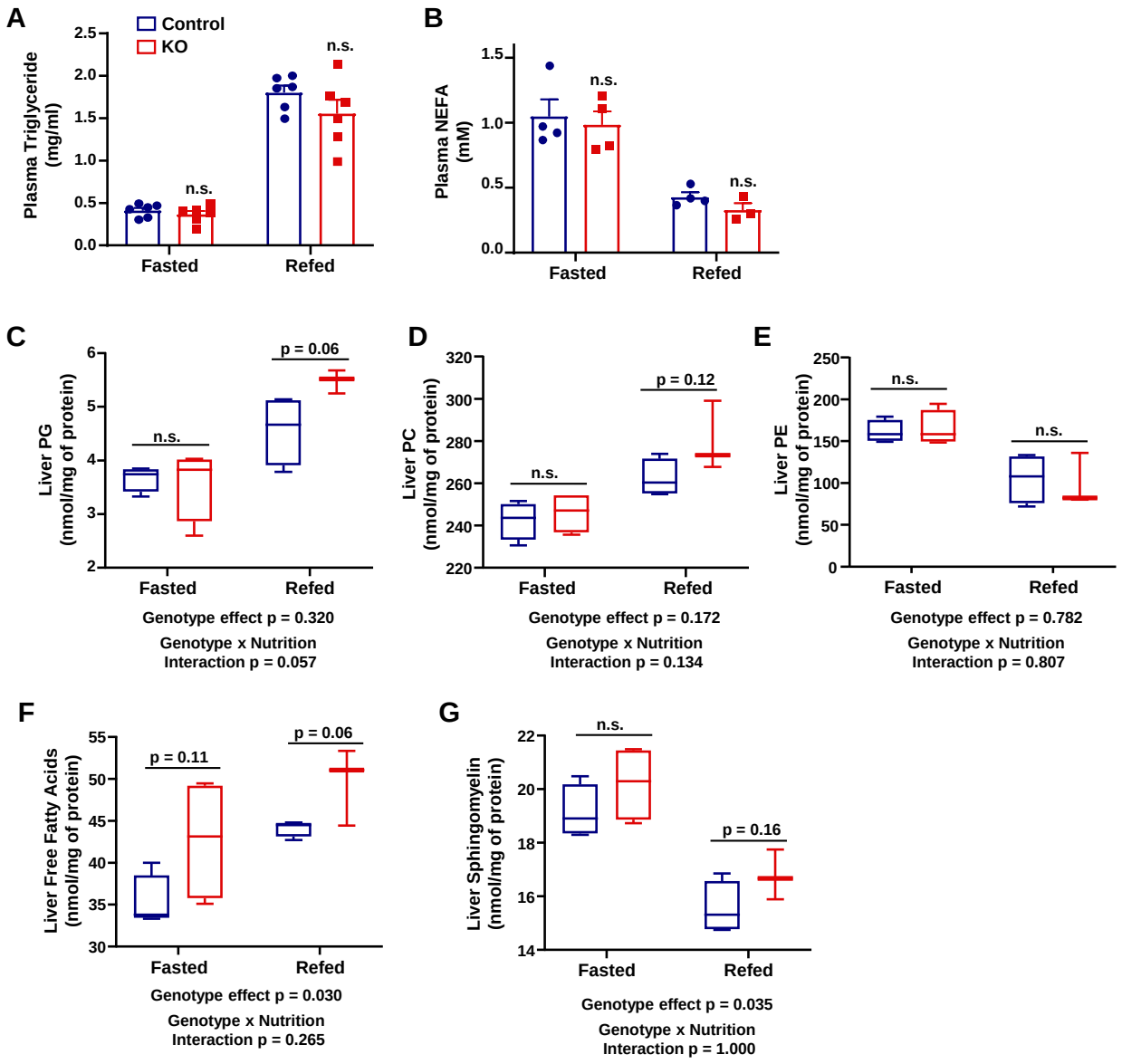

Figure 2-S2: Loss of hepatic GATA4 changes the lipidome in fed state.

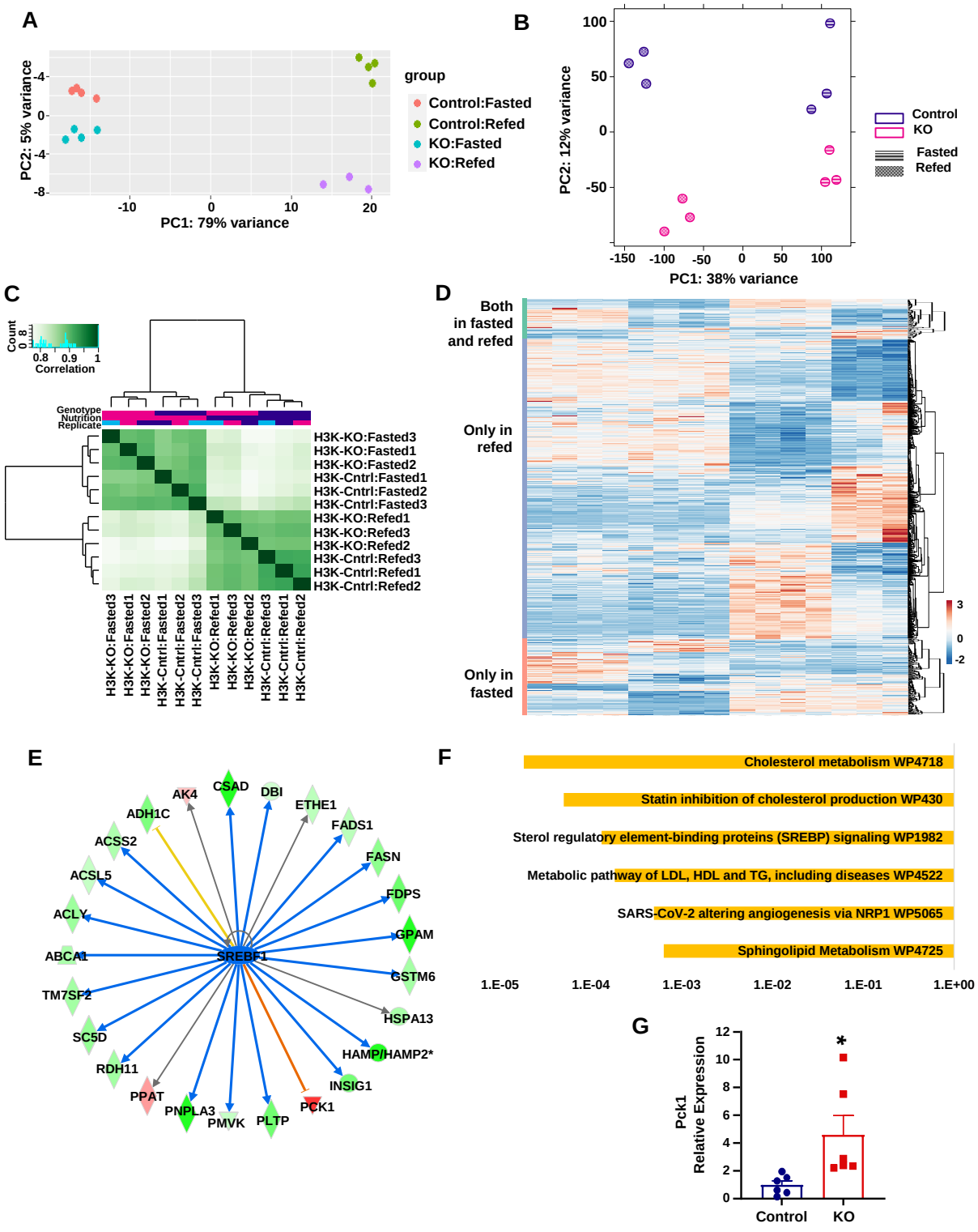

Figure 2-S3: Loss of GATA4 impairs the transcriptional response to feeding.

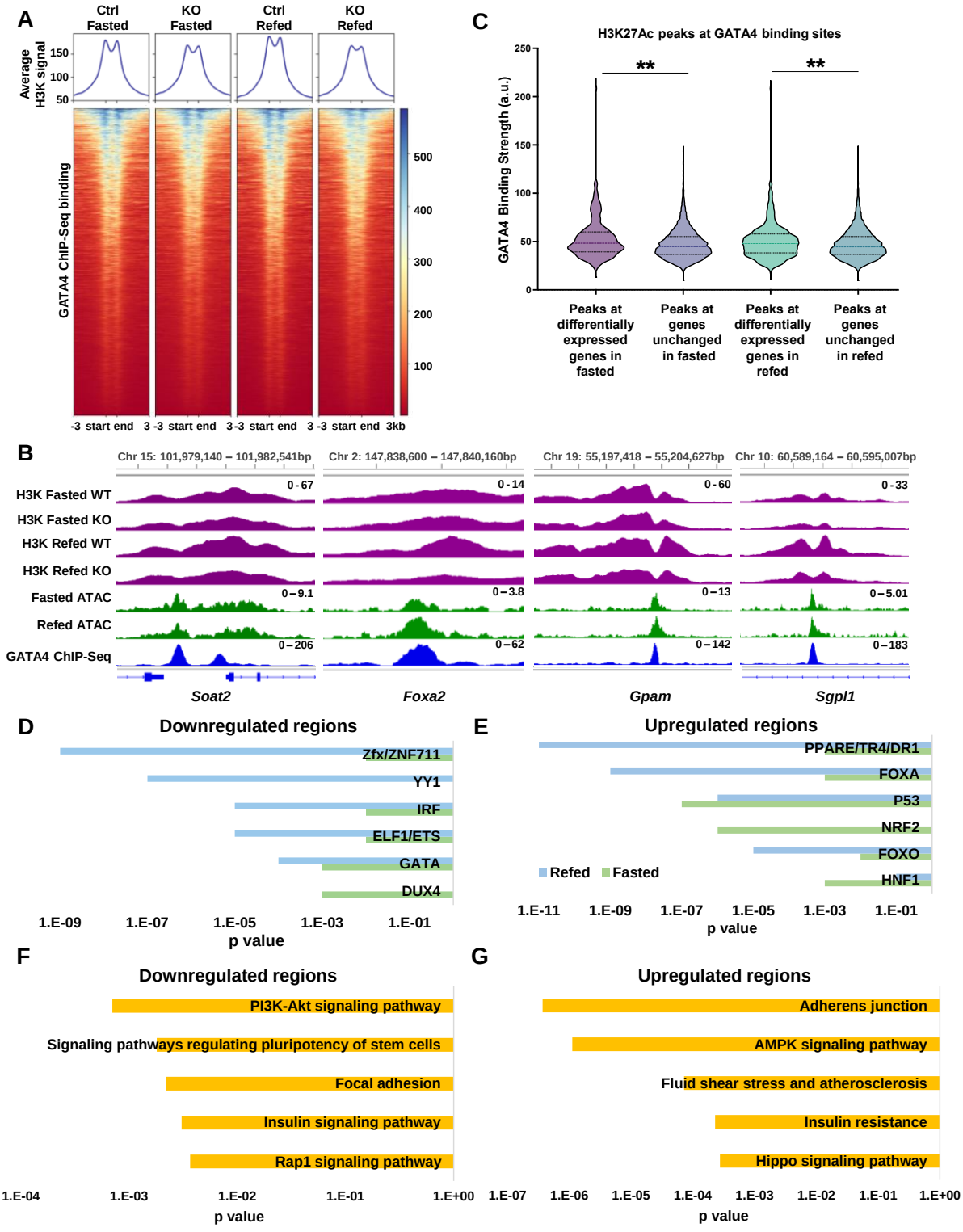

Figure 2-S4: Loss of GATA4 changes the epigenetic landscape.

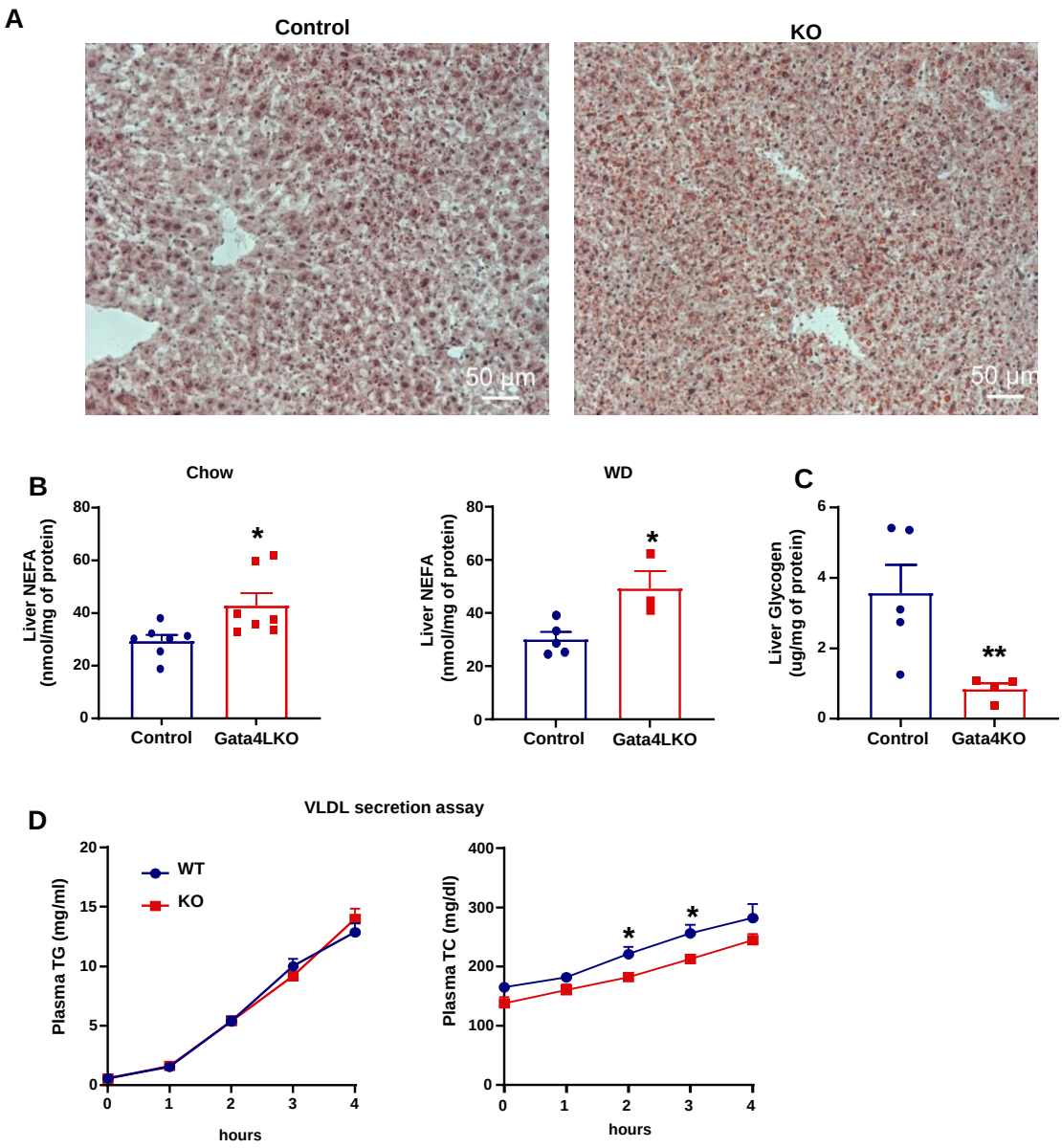

Figure 2-S5: Loss of GATA4 leads to hepatic lipid accumulation.

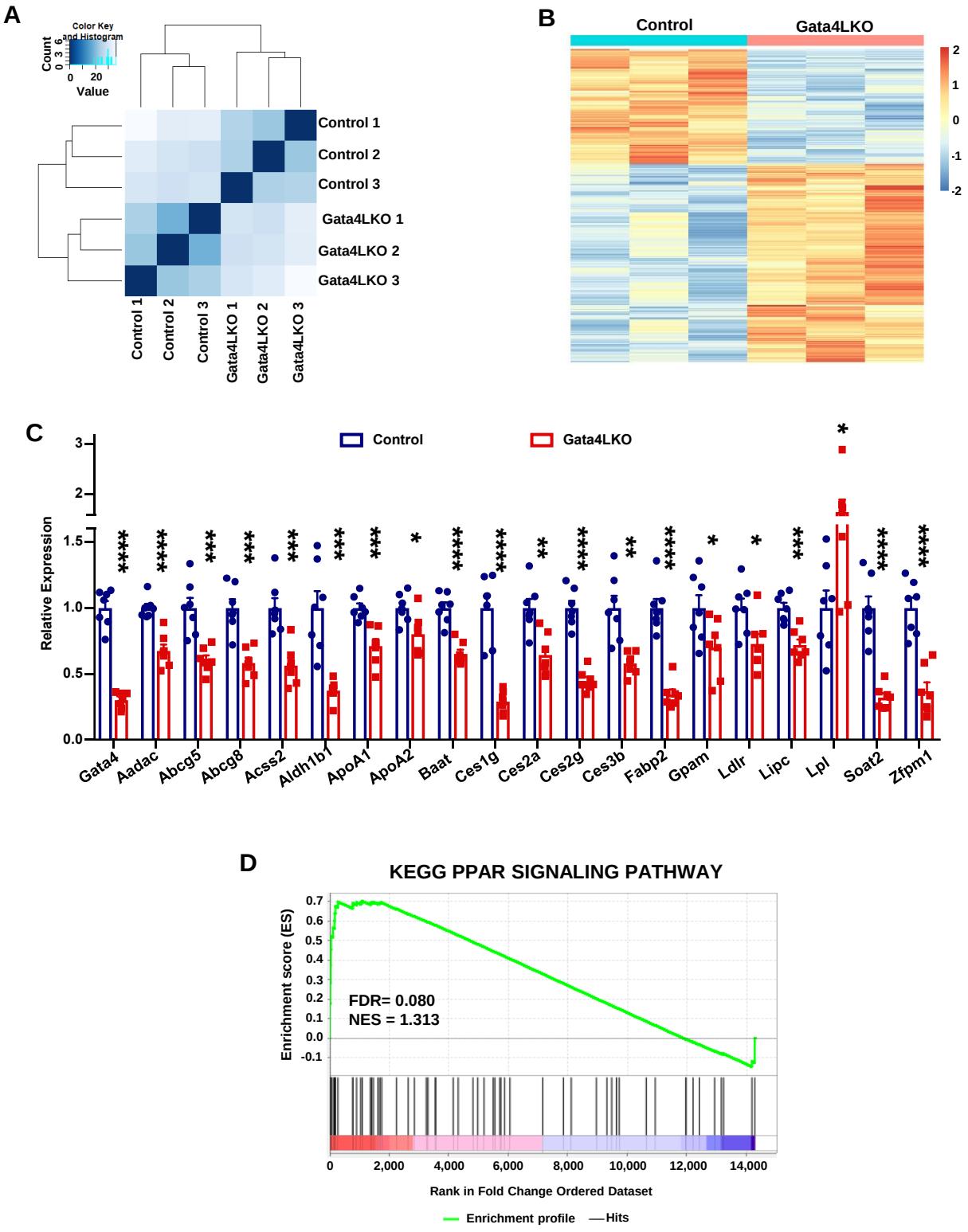

Figure 2-S6: Gata4LKO mice altered expression of triglyceride hydrolysis and lipid uptake genes.

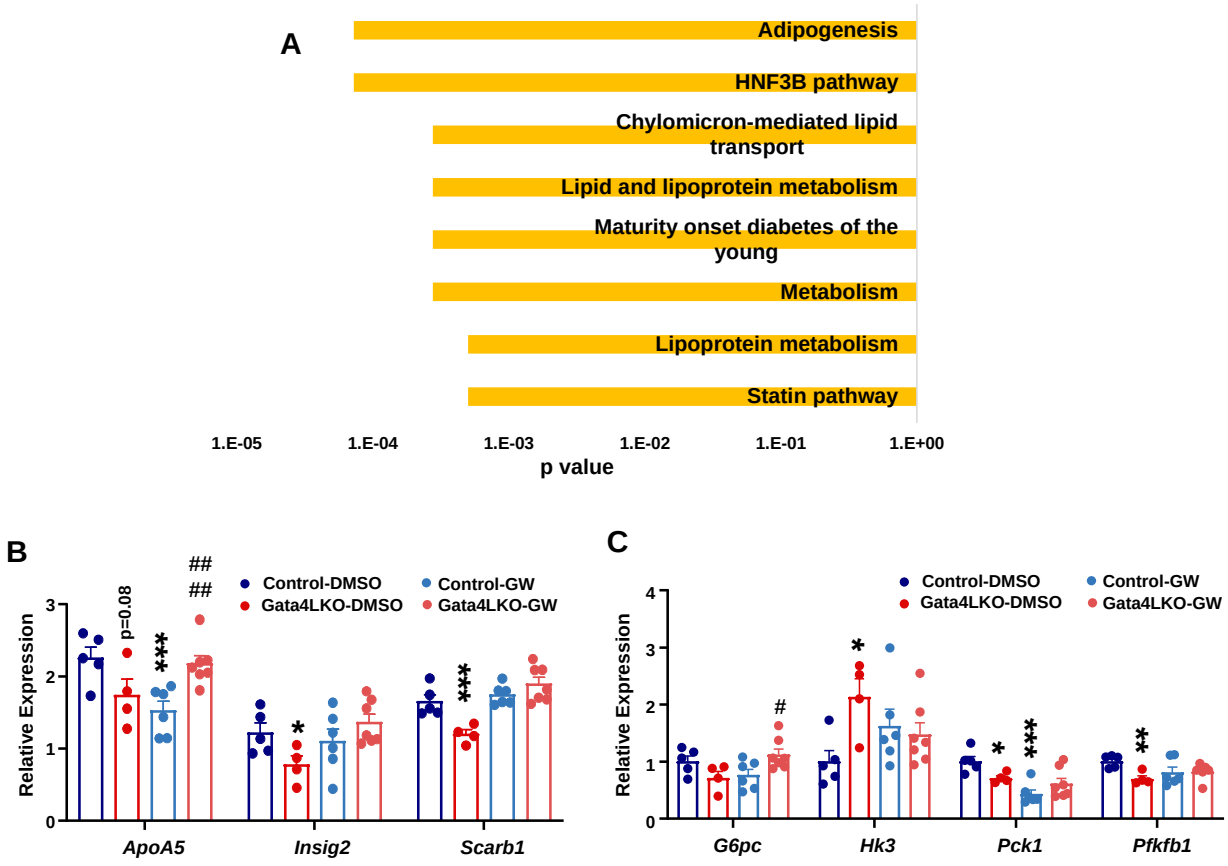

Figure 2-S7: Loss of GATA4 affects response to LXR agonist

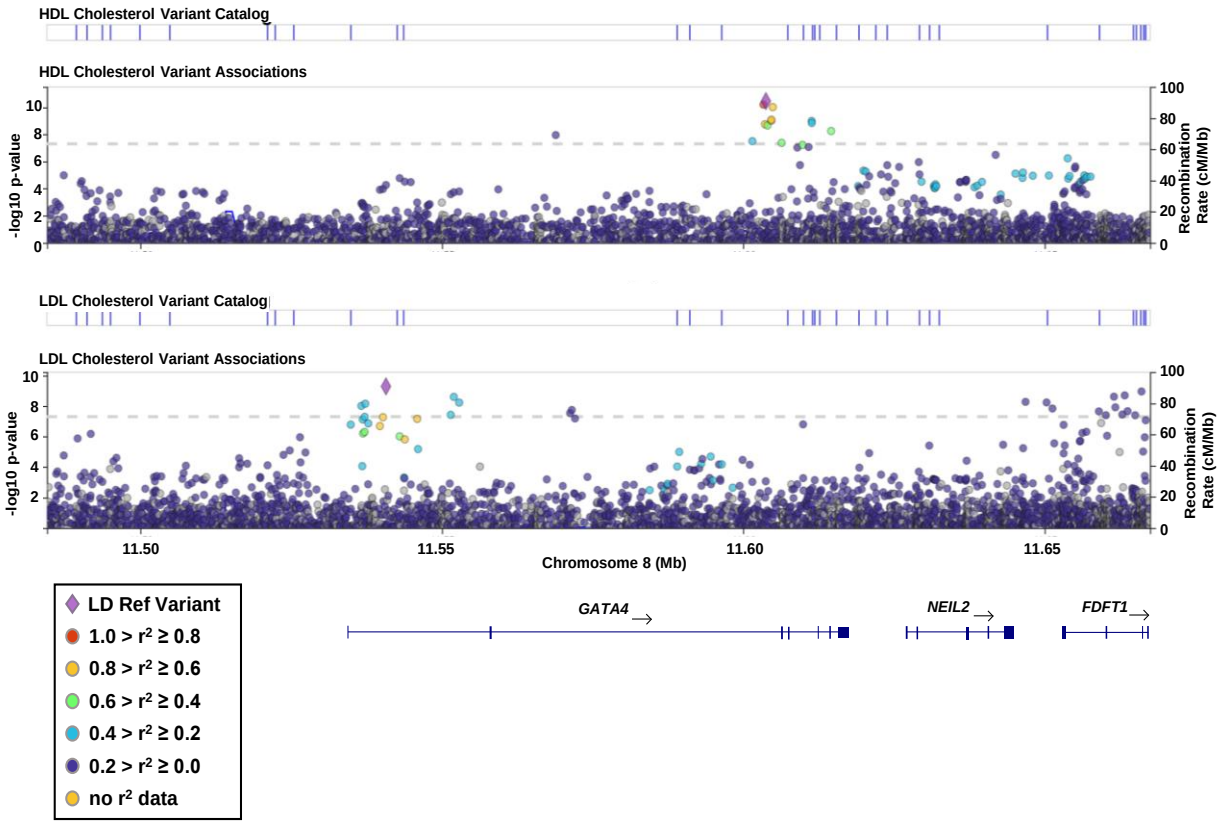

Figure 2-S8: SNPs at GATA4 locus are associated with LDL and HDL cholesterol in humans.

Table 2-S1:Summary of SNPs associated with LDL and HDL at GATA4 locus

SNP ID	reference	Minor Allele	consequence	Closest gene	LDL p value	LDL beta	HDL p value	HDL beta
rs11784455	T	A	intron variant	GATA4	5.15E-10	-0.008	0.000055	0.0053
rs181750463	G	C	non coding transcript exon variant	FDFT1	1.11E-09	0.0504	0.9186	-0.0008
rs55756391	C	T	intron variant	FDFT1	2.00E-09	-0.01	0.04831	-0.0036
rs184974686	T	A	intron variant	FDFT1	2.43E-09	0.049	0.8683	-0.0014
rs13262332	G	A	intron variant	GATA4	2.51E-09	0.0086	0.000189	-0.0055
rs883034	C	T	upstream gene variant	FDFT1	5.31E-09	-0.0104	0.104	-0.0037
rs113567822	C	T	upstream gene variant	FDFT1	5.83E-09	-0.0103	0.05702	-0.0042
rs12676469	T	A	intron variant	GATA4	5.94E-09	0.0083	0.000165	-0.0055
rs4368939	A	A	intron variant	GATA4	7.07E-09	-0.0076	0.01061	0.0037
rs4840575	G	T	intron variant	GATA4	9.76E-09	0.0077	0.001289	-0.0045
rs76030580	C	G	intron variant	FDFT1	1.22E-08	-0.01	0.07105	-0.0036
rs75224198	C	T	upstream gene variant	FDFT1	1.45E-08	-0.0103	0.02692	-0.0044
rs10112464	C	G	intron variant	GATA4	1.81E-08	-0.037	0.493	0.0044
rs80051943	C	T	intron variant	FDFT1	2.18E-08	-0.01	0.06999	-0.0036
rs112056952	T	C	intron variant	FDFT1	2.25E-08	-0.0097	0.0538	-0.0038
rs61265429	T	A	intron variant	GATA4	2.95E-08	-0.0367	0.4807	0.0046
rs10098874	G	A	intron variant	FDFT1	3.60E-08	-0.0091	0.07952	-0.0029
rs34838488	A	G	intron variant	GATA4	3.81E-08	0.0077	0.00026	-0.0053
rs113207154	G	C	5 prime UTR variant	FDFT1	4.01E-08	-0.0099	0.08363	-0.0037
rs7843716	T	G	intron variant	FDFT1	4.05E-08	-0.0101	0.1352	-0.0035
rs4841586	A	G	intron variant	C8orf49	0.6075	-0.001	3.459E-11	0.0132
rs66535756	A	G	intron variant	C8orf49	0.6545	-0.0009	6.284E-11	0.0129
rs28628715	A	G	intron variant	C8orf49	0.2233	-0.0024	9.564E-11	0.0125
rs28709984	C	T	intron variant	C8orf49	0.1296	-0.0031	8.094E-10	0.0124
rs28626371	G	T	intron variant	C8orf49	0.1376	-0.003	9.77E-10	0.0123
rs17153747	T	C	intron variant	C8orf49	0.1102	-0.0032	1.01E-09	0.0124
rs17153752	C	T	intron variant	C8orf49	0.3342	-0.0018	1.42E-09	0.0119
rs4841585	C	T	intron variant	C8orf49	0.4237	-0.0014	1.769E-09	0.0126
rs904006	C	C	intron variant	C8orf49	0.1304	0.003	2.176E-09	-0.0115
rs3729856	A	G	missense variant	C8orf49	0.3008	-0.0019	5.623E-09	0.0118
rs78197677	C	T	intron variant	GATA4	0.0076	-0.0084	1.114E-08	0.0177
rs4841584	A	C	intron variant	C8orf49	0.0009	-0.0092	3.137E-08	0.015
rs10503425	G	C	intron variant	C8orf49	0.5655	-0.0004	4.199E-08	0.0106

Table 2-S2: Primer list for RT-qPCR

RT-qPCR primers	F	R	Notes
36b4	GGCCCTGCACTCTCGCTTTC	TGCCAGGACGCGCTTGT	
Abcg5	TGGATCCAACACCTCTATGCTAAA	GGCAGGTTTTCTCGATGAACT	
Abcg8	TGCCCACCTTCCACATGTC	ATGAAGCCGGCAGTAAGGTAGA	
Acss2	AAACACGCTCAGGGAAAATCA	ACCGTAGATGTATCCCCCAGG	
Aldh1b1	CTCCAGGGCAGGACTACCTC	CATGCCACTCGTTGTTGATGA	
ApoA1	GGCACGTATGGCAGCAAGAT	CCAAGGAGGAGGATTCAAACT	
ApoA2	TGGTCGCACTGCTGGTAAC	TTTGCCATATTCAGTCATGCTCT	
Apoa5	TCCTCGCAGTGTTCGCAAG	CGAAGCTGCCTTTCAGGTTCT	
Baat	GGAAACCTGTTAGTTCTCAGGC	GTGGACCCCCATATAGTCTCC	
Ces2a	GTGGACTGGTTGTAGGATCAGC	TTCTTCTGCACCCAGCGTAAG	
Ces2g	AGGTCCAAGGCAGGCTCAT	GGCCCTCCATATTCATCGTAACA	
Ces3b	AGCTCCTAGCAGACCAGCAAT	AAGGGCCGTGAAATCTCCAAC	
Fabp2	GTGGAAAGTAGACCGGAACGA	CCATCCTGTGTGATTGTCAGTT	
Fabp5	TGAAAGAGCTAGGAGTAGGACTG	CTCTCGGTTTTGACCGTGATG	
G6pc	TGCAAGGGAGAACTCAGCAA	GGACCAAGGAAGCCACAAT	
Gata4	CACGCTGTGGCGTCGTAAT	CTGGTTTGAATCCCCTCCTTC	used in Fig2- 1, S1
Gata4 excised exons	CGAGGGTGAGCCTGTATGTAA	CTGCTGTGCCCATAGTGAGAT	used in Fig2- 2, 6, S6
Gata6	CGAGGAATCAAAAGTCAGG	AGTCAAGGCCATCCACTGTC	
Gpam	ACAGTTGGCACAATAGACGTT	CCTTCCATTTCAGTGTTGCAGA	
Hk3	TGCTGCCCACATACGTGAG	GCCTGTCAGTGTTACCCACAA	
Insig2	GCGGCACAGCCTCAGCT	GCATGACACTGGACCACTCTCTT	
Ldlr	AGGCTGTGGGCTCCATAGG	TGCGGTCCAGGGTCATCT	
Lipc	ATGGGAAATCCCCTCCAAATCT	GTGCTGAGGTCTGAGACGA	
Lpl	GCTGGTGGGAAATGATGTG	TGGACGTTGTCTAGGGGGTA	
Pck1	TTGAACTGACAGACTCGCCCT	TGCCCATCCGAGTCATGA	
Pfkb1	ATGAGCTGCCCTATCTCAAGT	GTCCCGGTGTGTGTTCACAG	
Scarb1	TCCTGGGAGCCCTTTTTACT	GCCCATCATCTGCCAACT	
Soat2	ACAAGACAGACCTCTTCCCTC	ATGGTTCGGAAATGTTGCACC	
Zfpm1	AGGAAACAGAGCAATCCCCG	CAGGTGGGCTCACATCTTCT	

Table 2-S3: Primer list for ChIP-qPCR

ChIP-qPCR primers	F	R
Alb neg	TCCTACTGCAGGGCTCTTGC	TGTAGCCTTGGGCTTGTGCT
Ces2a	CAAGAGGCCAGGGAAGGAAG	AGGGGTGTAGGTGTGGACAT
Fabp5	CCTGAACACTTGGAAACTCCT	TACTGTGGGTAAACAGCAATCA
Fx neg	GCGTCATGGCCTTAGTTTCC	GTGAGATGGATGCCTGCCTAC
Gpam	AACAGTGGAGGAGGAGGAA	CATGCTCTGAAGCTTTCGATTG
Pnpla3 enhancer	TGGTTGGCCTTTTGGAACCT	CAGCTGACCTCACTTAGCCC
Pnpla3 promoter	AGTTCCACTCTCTCCTGTCTTC	GGTGCATGGGCAAATGTTTAAT
Ralgps1	GCAAAGGTGCCCAGAGATAA	TGAGGTGGTGTGCTGATTG

Figure Legends

Figure 2-1: GATA4 motif accessibility and expression is upregulated in refed liver in comparison to fasted

A) Heatmap of top 1000 ATAC-Seq peaks with highest and lowest fold change in fasted versus refed livers. B) Genomic features of those top 1000 regions gaining accessibility in fasted liver (left) and refed liver (right). C) Heatmap of GATA family motif enrichment across all ATAC-Seq peaks, ranked and binned based on the accessibility fold change between fasted and refed liver. Shown are 60 bins each containing approximately 1000 peaks. The motif enrichment p-value is plotted. D) Hierarchical clustering heatmap for transcription factor motif co-occurrence among the top 1000 regions gaining accessibility in refed livers. Each row represents a peak and red indicates presence of the corresponding motif in that peak. E) Pathway enrichment analysis of genes associated with peaks that have a GATA4 motif and are in the top 10 bins that gain accessibility in refed liver. F) Normalized counts of GATA family members that are detected via RNA-Seq. G) Western blot analysis of GATA4 protein expression in fasted and refed liver. H) qPCR analysis of Gata4 expression in Hepa1-6 cells with treated with DMEM without FBS,

glucose or glutamine with or without 100nM insulin for 8 hours. * indicate p value from Student's t-test to their respective control.

Figure 2-2: Loss of Gata4 in liver has common and different effects on lipid metabolism in fasting and refeeding response.

A) qPCR assessment of expression of Gata4 expression in Gata4LKO fasted and refed livers in comparison to their control. B) Plasma total cholesterol measurements at 12 fasting and then 12h HS refeeding of Gata4LKO and control mice. C) Total cholesterol of FPLC fractionated plasma of 12 h HS refed Gata4LKO and control mice. Plasma of 4 – 5 mice were pooled for each group. D) Liver total cholesterol measurement of fasted and refed mice. E) Lipidomics analysis of total species of liver triglycerides (TG) Gata4LKO and control livers in fasted and refed condition. F) Liver glycogen measurement of refed Gata4LKO versus control mice. Total (G) and individual species (H) of liver ceramides from the lipidomics analysis in (E). I) Hierarchical clustering heatmaps of TG species summarized by their fatty acid content from the same lipidomics samples. * indicate p value from Student's t-test to their respective control. 2-way ANOVA analysis is conducted for some and genotype and interaction between genotype and feeding effect is reported.

Figure 2-3 Gata4 has common and differential targets in fasted versus refed liver.

RNA-Seq and H3K27 acetylation ChIP-Seq were conducted on samples for 12 h fasted and 12h refed with high sucrose diet after 12h fasting of Gata4LKO and control liver. A) Bioplanet pathway enrichment analysis of downregulated genes in refed Gata4LKO liver RNA-Seq in comparison to refed Gata4 floxed control liver. B) Heatmap of expression of selected genes involved indicated metabolic processes and are downregulated in fasted or refed Gata4LKO liver

in comparison to their respective controls. FDR <0.05 in pairwise comparison was used to determine differential expression. C) KEGG pathway enrichment analysis of downregulated genes in both fasted and refed Gata4LKO in comparison to their respective controls, genes only downregulated in Gata4LKO versus control in refed liver and genes only downregulated in Gata4LKO Vs control in fasted liver. Gene Set Enrichment Analysis (GSEA) of GO biological pathway cholesterol efflux pathway (D) and Wikipathways glycolysis and gluconeogenesis (E) gene set among all expressed genes ranked for their fold change in Gata4LKO versus control liver in refed condition descending order.

Figure 2-4: Loss of GATA4 reduces transcriptional activity at GATA4 binding sites.

A) Heatmap of H3K27Ac ChIP-Seq peaks that change in Gata4LKO in comparison to control in only in fasted or refed or both conditions. B) Profile of signal from H3K27 acetylation ChIP-Seq of fasted control, fasted Gata4LKO, refed control, and refed Gata4LKO (top) at GATA4 ChIP-Seq sites from GSE49131 and (bottom) at regions identified from ATAC within the top 10 bin of increasing in accessibility and have GATA4 motif. C) % of H3K27Ac peaks filtered based on their overlap with GATA4 ChIP-Seq peaks or change in enrichment in refed Gata4LKO that are associated with differentially expressed genes in refed Gata4LKO in comparison to its control by proximity to their promoter. D) IGV view of H3K27 Acetlation ChIP-Seq of GATA4LKO and control livers both in refed and fasted conditions, ATAC-Seq of wildtype refed and fasted livers and GATA4 ChIP-Seq at example regions for common (Zfpm1) and differential targets (Pnpla3, Acsl5 and Srebf1) of GATA4 between fasted and refed conditions. Tick marks are 500bp apart. E) GATA4 ChIP-qPCR of selected candidate regions for increased GATA4 activity in refed samples. The bar graph shows values for target regions of both the input and ChIP samples that are normalized to the average of two negative control regions within each sample. * reflect the p-

value from Student's t-test between ChIP samples from fasted and refed states or to their respective input controls.

Figure 2-5: Loss of Gata4 results in reduction in plasma cholesterol and accumulation of liver triglycerides

Plasma total cholesterol (A), liver total cholesterol (B) and liver triglycerides (C) of Gata4LKO and control mice after 3 weeks on chow (left) or western diet (right). D) H&E staining of Gata4 and control liver sections at 10c and 40x magnification after 4 weeks of western diet feeding. E) Lipidomics analysis of triglycerides summarized based on their fatty acyl tail content of Gata4LKO and control on chow for 3 weeks. F) Pathway enrichment analysis of downregulated genes in livers of Gata4LKO mice versus control after 3 weeks of western diet feeding using RNA-Seq. G) Normalized counts of downregulated genes in Gata4LKO livers from RNA-Seq in (F) relating to triglyceride degradation pathway. H) qPCR analysis of example target genes from mice in (E). Mice for all of the panels were sacrificed 6h fasted. * indicate p value from Student's t-test to their respective control except for (H), in which it represents adjust p value.

Figure 2-6: GATA4 collaborates with LXR to induce their joint transcriptional targets

A) IPA summary of LXRα pathway in Gata4LKO RNA-Seq. Green indicates downregulated and red indicated upregulated targets in refed Gata4LKO livers in contrast to control. Blue shows predicted downregulation of activity. B) ChIP Enrichment Analysis (ChEA) of the downregulated genes in RNA-Seq of Gata4LKO versus control liver after 3 weeks of western diet treatment as described in Figure 2-4. C) Profile (top) and heatmap (bottom) of signal from LXR ChIP-Seq with vehicle or LXR agonist T0901317 treament at GATA4 ChIP-Seq sites. D) IGV view of GATA4 ChIP-Seq, LXR ChIP-Seq with and without agonist treatment and H3K27

Acetlation ChIP-Seq of GATA4LKO and control livers both in refed and fasted conditions at example regions for common LXR and GATA4 targets. E) Profile (top) and heatmap (bottom) of signal from H3K27Ac ChIP-Seq from fasted and refed control and Gata4LKO samples at LXR ChIP-Seq sites (with T0901317 treatment). F) qPCR assessment of selected genes that showed a significant interaction between genotype and LXR agonist treatment effect using 2-way ANOVA. * indicate p value to Control-DMSO condition and # indicate p value to Control-GW condition using Student's t-test.

Figure 2-S1: ATAC-Seq reveals changes in transcriptional regulatory landscape

A) All ATAC-Seq peaks are sorted, ranked and plotted based on the fold change between accessibility in refed condition in comparison to fasted. Pathway enrichment of top 1000 regions that gain accessibility in fasted (B) or in refed (C). D) Heatmap for transcription factor motif enrichment across all ATAC-Seq peaks, ranked and binned based on the accessibility fold change between fasted and refed liver. Shown are 59 bins each containing approximately 1000 peaks. Some transcription factors with very similar motifs (>0.9 similarity score) are represented by one motif and the remainder are omitted for simplicity. The motif enrichment –log(p-value) is plotted. E) Motif enrichment analysis among the top 10000 regions that gain accessibility in refed liver and have a GATA4 motif. F) qPCR analysis of Gata4 expression in livers of 12h fasted versus 12hour refed with chow or 12 hour refed with high sucrose diet male mice. G) qPCR analysis of Gata4 expression in livers of 12h fasted versus 12 hour refed with high sucrose diet female mice. H) Analysis of data from GSE107787 showing hepatic GATA4 expression during 24 hours in mice that are either ad libitum fed or 24 hour fasted at each time point. * indicate p value from Student's t-test to their respective control

Figure 2-S2: Loss of hepatic GATA4 changes the lipidome in fed state

Plasma triglyceride (A), non-esterified fatty acids (NEFAs) (B) and liver NEFAs (C) of fasted and refed Gata4LKO and control mice. Lipidomics analysis of total species of liver phosphatidylglycerols (D), phosphotidylcholine (E) phosphotidyethanolamines (F) and sphingomyelins (G) in Gata4LKO and control livers. H) Hierarchical clustering heatmaps of free fatty acid species (E) from the lipidomics samples in Figure 2. p value from Student's t-test to their respective control is displayed. 2-way ANOVA analysis is conducted and genotype and interaction between genotype and feeding effect is reported for some.

Figure 2-S3: Loss of GATA4 impairs the transcriptional response to feeding

A) PCA plot of RNA-Seq of Gata4LKO and control in fasted and refed condition. B) PCA plot and hierarchical clustering (C) of H3K27Ac ChIP-Seq of Gata4LKO and control samples in fasted and refed condition. D) Hierarchical clustering heatmap of differentially expressed genes in Gata4LKO versus control in refed or fasted condition combined. E) Integrated Pathway Analysis (IPA) summary of SREBP1 pathway in Gata4LKO livers in refed condition. Green indicates downregulated and red indicated upregulated targets. Blue indicates downregulation of the activity of SREBP1. F) qPCR analysis of Pck1 expression in Gata4LKO versus control livers in fasted and refed condition. * indicate p value from Student's t-test.

Figure 2-S4: Loss of GATA4 changes the epigenetic landscape

A) Profile and heatmap of signal from H3K27 acetylation ChIP-Seq of Gata4LKO versus control livers in fasted and refed conditions at regions that are statistically upregulated or downregulated due to the genotype effect (loss of Gata4) taking both fasting and refeeding condition into account. B) IGV view of H3K27 Acetlation ChIP-Seq of GATA4LKO and control livers both in refed and fasted conditions, ATAC-Seq of wildtype refed and fasted livers and GATA4 ChIP-

Seq at additional example regions for common (Soat2) and differential targets (Foxa2, Gpam and Sgpl1) of GATA4 between fasted and refed conditions. Top enriched motifs in regions in upregulated (C) and downregulated (D) H3K27Ac peaks in Gata4LKO in comparison to control in fasted and refed condition. KEGG pathway enrichment analysis of regions with decreased (E) and increased (F) H3K27 acetylation in refed Gata4LKO livers.

Figure 2-S5: Loss of GATA4 leads to hepatic lipid accumulation

A) Oil Red O staining of livers of Gata4LKO and control mice on western diet for 3 weeks. B) Liver non-esterifies fatty acids of Gata4LKO and control mice after 3 weeks on chow (left) or western diet (right). C) Liver glycogen measurements of Gata4LKO and control mice on western diet for 3 weeks. D) Triglyceride and total cholesterol measurment of plasma of Gata4LKO and control mice on western diet for 3 weeks after poloximer injection during vldl secretion assay.

Figure 2-S6: Gata4LKO mice on western diet have increased expression of lipid uptake genes.

Hierarchical clustering heatmap of samples (A) and heatmap of differentially expressed genes (B) from RNA-Seq of Gata4LKO and control mice on western diet for 3 weeks. C) Relative expression of downregulated PPARa target genes from RNA-Seq. * indicate adjusted p-values. D) GSEA plot of KEGG PPAR signaling pathway from RNA-Seq. E) Correlation plot of relative Lpl expression by qPCR and triglyceride measurements from livers of Gata4LKO and control mice on western diet for 4 weeks.

Figure 2-S7 Loss of GATA4 interacts with LXR agonist treatment

A) Pathway enrichment analysis of genes associated with common GATA4 and LXR binding sites. Blue indicates downregulation of the activity of LXRα. B) qPCR assessment of selected genes that showed a significant interaction between genotype and LXR agonist treatment effect

using 2-way ANOVA from livers described in Figure 5C. These genes are downregulated in response to loss of Gata4LKO in DMSO treatment but either upregulated or no response in GW treatment. C) qPCR assessment of glucose metabolism genes with a significant interaction between genotype and LXR agonist treatment effect using 2-way ANOVA from livers described in Figure 5C. * indicate p value to Control-DMSO condition and # indicate p value to Control-GW condition using Student's t-test.

Figure 2-S8 SNPs are GATA4 are associated with LDL and HDL cholesterol in humans

Manhattan plot for HDL and LDL cholesterol traits at the linkage disequilibrium (LD) block containing human GATA4 gene obtained from Type2Diabetes Knowledge Portal.

Chapter 3 : Integrative analysis reveals multiple modes of LXR transcriptional regulation in liver

Lara Bideyan[1], Wenxin Fan[1], Karolina Kaczor Urbanowicz[2,3], Christina Priest[1], David Casero[1,4], and Peter Tontonoz[1#]

[1]Department of Pathology and Laboratory Medicine, Department of Biological Chemistry, and Molecular Biology Institute, University of California, Los Angeles, CA, 90095, USA

[2]Division of Oral Biology & Medicine, School of Dentistry, UCLA, Los Angeles, CA, United States

[3]Institute for Quantitative and Computational Biosciences, UCLA, Los Angeles, CA, United States

[4]F. Widjaja Foundation Inflammatory Bowel & Immunobiology Research Institute, Cedars-Sinai Medical Center, Los Angeles, CA, USA.

Abstract

The nuclear receptors LXRα and LXRβ play crucial roles in hepatic metabolism. Many genes induced in response to pharmacologic LXR agonism have been defined; however, the transcriptional consequences of loss of LXR binding to its genomic targets are less well characterized. Here we addressed how deletion of both LXRα and LXRβ from mouse liver (LXRDKO) affects the transcriptional regulatory landscape by integrating changes in LXR binding, chromatin accessibility, and gene expression. Many genes involved in fatty acid metabolism showed reduced expression and chromatin accessibility at their intergenic and intronic regions in LXRDKO livers. Genes that were upregulated with LXR deletion had increased chromatin accessibility at their promoter regions and were enriched for functions not linked to lipid metabolism. Loss of LXR binding in liver reduced the activity of a broad set of hepatic transcription factors, inferred through changes in motif accessibility. By contrast, accessibility at promoter NFY motifs was increased in the absence of LXR. Unexpectedly, we also defined a small set of LXR targets for direct ligand-dependent repression. These genes have LXR binding sites but showed increased expression in LXRDKO liver and reduced expression in response to LXR agonist. In summary, the binding of LXRs to the hepatic genome has broad effects on the transcriptional landscape that extend beyond its canonical function as an activator of lipid metabolic genes.

Significance Statement

LXRs are critical regulator of hepatic metabolism and function but their mechanisms of action at the genome level are incompletely understood. We perform integrated analysis of genome-wide chromatin accessibility, gene expression, and transcription factor binding. We reveal distinct mechanisms of LXR transcriptional regulation of both metabolic and non-metabolic genes in liver. We show that LXR can both activate and repress genes and that LXR binding impacts the activity of other transcription factors.

Introduction

Liver X receptors LXRα and LXRβ (encoded by *Nr1h3* and *Nr1h2*) play important roles in hepatic lipid metabolism. LXRs are crucial for the lipogenic response to feeding as regulators of *Srebf1*, *Fasn*, and *Scd1* [33,293,296]. LXRs play a role in phospholipid remodeling via control of *Lpcat3* expression [325,326]. In liver as in other tissues, LXRs are also central to cholesterol homeostasis. Activated LXRs induce genes involved in cholesterol efflux such as those encoding ABCA1, ABCG5 and ABCG8, block LDL uptake through IDOL, and promote cholesterol conversion to bile acids through CYP7A1 [294,327–329]. Beyond metabolism, LXRs have been shown to regulate immune responses in macrophages, including those in the liver [330–332]. LXRα is a lineage determining factor for Kupffer cells and is necessary to maintain gene expression defining their identity [333–335].

LXRs are activated by oxysterols such as 27-hydroxycholesterol and 4β-hydroxycholesterol and intermediates in the cholesterol biosynthetic pathway, such as desmosterol [336–339]. Loss of LXRs leads to pathological cholesterol accumulation in liver when mice are fed high-cholesterol diet [340]. In the absence of excess dietary cholesterol, the primary consequences of LXR deletion in liver are perturbations in fatty acid and phospholipid metabolism [341,342]. Many studies have used synthetic agonists such as GW3965 and T0901317 as tools to investigate the role of LXRs in hepatic gene expression [343]. Activation of LXRs with synthetic agonist improves atherosclerosis and glucose tolerance, but also increases hepatic lipogenesis [344–346]. Chromatin Immunoprecipitation with Sequencing (ChIP-Seq) studies have defined LXR binding sites in the hepatic genome and noted increased LXR binding to lower affinity DNA sites in the presence of synthetic agonist [297].

Given the widespread use of synthetic agonists to identify LXR-responsive genes, it is not surprising that LXRs have been characterized primarily for their roles as ligand-dependent activators. Recent studies using alternative approaches and genome-wide techniques have revealed multiple modes of LXR gene regulation. Ramón-Vázquez et al. defined three modes of LXR action in macrophages. The first is the classical mode of agonist-activated genes; the second is a de-repression mode, in which target genes are upregulated both in response to agonist and in the absence of LXRs; and the third is a pharmacologically non-responsive mode for genes that require LXRs for expression but do not change in response to agonist [347]. Systematic analyses of different modes of LXRs action on gene expression *in vivo* in key metabolic tissues have not yet been performed.

LXRs bind to DNA as obligate heterodimers with RXR. The canonical LXR binding site (LXRE) is a repeated nuclear receptor half-site motif (AGGTCA) separated by 4 nucleotides (DR4)[348]. LXR liver ChIP-Seq studies have suggested broader LXR binding to genomic sites other than DR4 motifs. One notable limitation of genome-wide bioinformatic approaches, however, is the degenerate nature of many LXREs and PPREs, which makes motif identification challenging. Many biologically critical LXREs and PPREs are not perfect DR4 or DR1 elements [349,350]. Studies integrating genomic analyses of multiple nuclear receptors, including LXR and PPARα, have shown greater overlap between receptor targets than expected [297]. Such extensive co-binding has been proposed to lead to functional crosstalk. In support of this idea, loss of LXRs was shown to diminish activation of PPARα targets in response to PPARα agonist [342].

The dynamics of the transcriptional landscape in response to LXR binding to the genome are largely unknown. Tools such as Assay for Transposase Accessible Chromatin (ATAC-Seq) can provide a bridge between transcription factor binding and gene expression by revealing

dynamic changes in chromatin accessibility [351]. In this study, we investigated the transcriptional dynamics of LXR in mouse liver. We performed RNA-Seq and ATAC-Seq on livers of LXRα and LXRβ double-knockout (LXRDKO) mice to characterize the effect of loss of LXRs on the transcriptional landscape. Incorporating available LXR liver ChIP-Seq data, we identified how LXR binding sites changed and how those changes related to differential gene expression. We also profiled the differences in activity of other transcription factors in response to loss of LXRs using the accessibility of their binding motifs. We integrated our results from the LXRDKO model with data from synthetic agonist treatment studies [352] to define distinct modes of LXR action in the liver, including the ability to act as a ligand-dependent repressor. These finding contribute to a more thorough understanding of how LXRs impact the transcriptional landscape and orchestrate hepatic metabolism.

Results

Transcriptional changes in liver of LXRDKO mice.

We performed RNA-Seq on livers of whole-body LXRα/β double knockout (LXRDKO) mice to profile transcriptional changes provoked by the absence of these transcription factors. We identified 246 upregulated and 321 downregulated genes using an adjusted p-value less than 0.05 (SI Appendix Fig. 3-S1A). Many classical LXR targets were downregulated, including *Srebf1* and *Fasn* (SI Appendix Fig. 3-S1B, C)[293,296,353]. Downregulated genes associated with lipid metabolism pathways as expected, and overlapped substantially with the set of direct LXR target genes annotated in publicly available ChIP-Seq data-sets (SI Appendix Fig. 3-S2A, B). In addition, lipid metabolism genes associated with PPARα were downregulated in LXRDKO livers. Macrophage and Kupffer cell marker genes, such as *Cd5l*, *Cd163* and *Clec4f* were also among the most downregulated genes. Reduced expression of these genes likely reflects a change in the immune cell profile in LXRDKO liver, as LXR is known to be important for Kupffer cell identity [330,334,335]. Interestingly, most of the genes upregulated in the absence of LXR expression were not established LXR targets and did not have obvious links to lipid metabolism (SI Appendix Fig. 3-S1B, C). These genes were enriched for pathways including cysteine and methionine metabolism and DNA repair/p53 response (SI Appendix Fig. 3-S2A).

Changes in chromatin accessibility in liver of LXRDKO mice.

We next aimed to further delineate how the absence of LXRs induced the observed changes in gene expression. To understand how changes in transcription in the absence of LXRs related to genome-wide chromatin accessibility, we performed ATAC-Seq to quantify genome-wide chromatin accessibility on the livers of the same mice used in the transcriptomics analysis above. It has been reported that changes in accessibility in response to perturbation in the liver

are less dramatic than in other tissues [335,354,355]. 95,342 peaks were detected across the samples. Correlation between samples is shown in SI Appendix Fig 3-S3A, B. We ranked our ATAC-Seq peaks based on the absolute change in accessibility between LXRDKO and WT livers. After filtering out peaks with very weak signals, 73,597 peaks remained, of which 57.60% had passed an irreproducible discovery rate of 1e-6 [356]. We viewed the top 1000 peaks with increased or decreased accessibility in LXRDKO livers to detect overall patterns in the changes in chromatin accessibility. Genomic sites that lost the most accessibility in the LXRDKO liver largely became inaccessible in LXR liver (Fig. 3-1A). In comparison, sites that gained the most accessibility in the LXRDKO liver were already open in WT samples and became even more accessible in LXRDKO livers.

Top peaks that lost accessibility were enriched in intergenic and intronic regions (Fig. 3-1B). In comparison, top peaks that gained accessibility in the absence of LXRs were more likely to be found in promoter and exonic regions of the genome. Consistent with this observation, top peaks gaining accessibility in the absence of LXRs were more likely to be located within 1kb of transcription start sites (TSSs), while top peaks losing accessibility were enriched in regions >10kb away from TSSs (SI Appendix Fig 3-S3C). These findings broadly suggest reductions in potential enhancer activity and increases in direct promoter activity on a range of genes in LXRDKO livers.

Integrating gene expression and chromatin accessibility

Average accessibility across the gene was decreased in the genes downregulated in the absence of LXR in comparison to upregulated ones (SI Appendix Fig 3-S3D). Genes downregulated in the absence LXR were more likely on average to lose accessibility in their intergenic and intronic peaks, compared to those whose expression increased or did not change

(SI Appendix Fig 3-S3E). On the other hand, promoter peaks in genes upregulated in LXRDKO liver were more likely to gain accessibility, compared to those whose expression decrease or did not change. These results agree with the enrichment of intergenic and intronic regions in the top peaks losing accessibility and the enrichment of promoters for top peaks gaining accessibility. Pathway enrichment analysis revealed that the set of genes proximal to top peaks losing accessibility in LXRDKO liver were enriched in lipid metabolism pathways, in agreement with the types of genes downregulated (SI Appendix Fig. 3-S4). Genes proximal to top peaks gaining accessibility were enriched for pathways other than lipid metabolism (e.g., endocytosis). These observations support a degree of correlation between chromatin accessibility and gene expression in LXRDKO liver.

Correlation of accessibility, LXR binding, and gene expression.

To further examine changes in accessibility occurring at LXR binding sites, we integrated our RNA-Seq and ATAC-Seq results with LXR ChIP-Seq data from liver of mice treated with vehicle (basal) or the LXR agonist T0901317 [297]. Our analysis revealed that 35.8% of the downregulated genes and 20.7% of the upregulated genes in LXRDKO liver were putative LXR ChIP-Seq targets (compared to 7.8% of the non-differentially expressed genes; Fig. 3-2A). When we included genomic LXR binding sites observed only with T0901317 treatment [297], more than half of the downregulated genes (61.1%) and 43.9% of the upregulated genes had LXR binding sites. In short, the majority of the differentially expressed genes in LXRDKO livers had LXR binding detected by ChIP-Seq. However, only a small fraction of the genes associated with LXR liver ChIP-Seq peaks were differentially expressed in LXRDKO livers (7.1% of the vehicle treated and 4.6% of the T0901317-treated ChIP-Seq sites, SI Appendix Fig. 3-S5A). Among genes with LXR binding sites, genes that were differentially expressed between WT and

LXRDKO mice tended to have higher number of LXR binding sites compared to genes whose expression did not change in LXRDKO liver (SI Appendix Fig. 3-S5B). This suggests that only a small subset of LXR binding sites in liver is functionally required for hepatic gene expression.

The overall accessibility across LXR binding sites was reduced in LXRDKO livers; 71.57% of LXR binding sites lost some accessibility (Fig. 3-2B and SI Appendix Fig. 3-S5C). A majority of the ATAC peaks at LXR binding sites located at intergenic, and intronic regions in LXRDKO liver showed a decrease in accessibility, but that trend was not observed for peaks located at promoter regions (SI Appendix Fig. 3-S5D). Thus, the degree to which LXR binding sites changed in accessibility in LXRDKO liver was influenced by their locations in relation to individual genes.

Integrating the expression, binding, and chromatin accessibility data, LXR binding sites associated with downregulated genes were less accessible in LXRDKO liver than those associated with genes whose expression did not change or were upregulated (Fig. 3-2C). For instance, one context where LXR binding is known to be functionally important is at the *Srebf1* locus [353]. The regulatory regions of *Srebf1* contain multiple LXR binding sites (Fig. 3-2D), including one at the alternative promoter for *Srebf1c* (left panel). All of the LXR binding sites at this gene lost some accessibility in the LXRDKO samples compared to controls, accompanying the downregulation of the gene.

Loss of LXR affects accessibility at binding sites for other transcription factors.

Changes in chromatin accessibility at transcription factor binding sites may reflect a change in transcription factor activity. To analyze these trends across the genome, we ranked all of our ATAC-Seq peaks based on changes in accessibility between LXRDKO and WT samples

and binned them into equal sized bins (~1000 peaks each). We performed motif enrichment analysis for known binding motifs (see Methods for details) for all of the bins. We then displayed the enrichment of each of the transcription factor motifs across all bins in a heatmap (Fig. 3-3A). This method allowed us to visualize the difference in enrichment of each motif both across bins and compared to other motifs. The results showed a gradual increase in enrichment of binding motifs in relation to changes in chromatin accessibility in LXRDKO liver. We identified several transcription factors whose binding motif became less accessible in LXRDKO liver. Motifs predicted to bind CTCF/CTCFL, the nuclear receptor family, HNF1/HNF1B, HNF6/CUX2, the FOX family, and the ATF4/CHOP family showed the strongest enrichment in peaks that lost accessibility in LXRDKO liver. Among nuclear receptor motifs, the DR1 motif (bound by PPARα, HNF4α, and RXR) was the most strongly enriched, but the DR4 motif (bound by LXR and TR) and the nuclear receptor half-site motif (recognized by ERRs, Coup-TFII and others) were also enriched. Many of these transcription factor motifs are primarily present in intergenic and intronic regions. Even among intergenic and intronic peaks, these motifs were enriched in peaks that were specifically losing accessibility in LXRDKO liver (SI Appendix Fig. 3-S6A).

We further examined the transcription factor motifs associated with the top 1000 ATAC peaks that lost accessibility in LXRDKO liver (Fig. 3-3B). A number of peaks associated with CTCF motifs lost almost all signal in LXRDKO liver, indicating largely inaccessible CTCF binding sites. In comparison, peaks associated with PPAR motifs and FOXA2 motifs showed strong reductions in ATAC signal intensity but still retained some accessibility (Fig. 3-3B, SI Appendix Fig. 3-S6B). This result implies that loss of CTCF binding may lead to the closing of these peaks. To ensure that the motifs we identified were independently changing, we examined

the peaks among the top bins that lost accessibility in LXRDKO liver with these motifs. Each family motif was present on a unique set of peaks with some overlap with other transcription factor families (SI Appendix Fig. 3-S6C left). This suggests that there is specificity to the reduction of motif accessibility for each these transcription factor families, and that the reduction of accessibility of one transcription family was not completely dependent on another transcription factor family. With the exception of a modest decrease in PPARα and modest increase in Foxa2 expression in the LXR DKO samples, the expression of most of these transcription factors themselves was not different between groups, suggesting that the changes in their motif accessibility were not likely to be due to differences in transcription factor abundance (SI Appendix Fig. 3-S6D).

We further assessed changes in accessibility some of the motifs via footprinting [357]. This approach measures transcription factor binding activity by quantifying the protection of the binding site from sequencing. The accessibility of predicted binding sites for HNF1B and HNF6A were reduced across the LXRDKO liver genome compared to control (SI Appendix Fig. 3-S7A, B). Although this method was not as sensitive, it nevertheless provided independent validation of some of the observations shown in Fig. 3-3A.

To address how the loss of LXR affected the activity of other transcription factors specifically at its target genes, we performed a similar analysis on the top bins of ATAC peaks proximal to a putative LXR-binding gene that lost accessibility in LXRDKO liver. When we clustered genes associated with each transcription factor motif, we observed patterns of motif co-occurrence across different families (SI Appendix Fig. 3-S5C, right). This suggests that a number of transcription factors were collectively losing accessibility in LXR target genes. As an example, the *Insig2* locus has a number of LXR binding sites that became less accessible in

LXRDKO liver. Based on available liver ChIP-Seq datasets, each of the peaks associated with LXR binding was also predicted to bind to combinations of other transcription factors, including CTCF, PPAR, RXR, HNF4A, FOXA2, HNF6 and HNF1 (Fig. 3-3C), exemplifying how the loss of LXR could impact the potential binding of other transcription factors to the same gene. Our analysis revealed instances of independent and collective loss of activity of these transcription factors on LXR-binding genes.

NF-Y motifs are more accessible in the absence of LXRs.

Fewer transcription factor motifs were enriched in ATAC peaks that gained accessibility in LXRDKO liver (Fig. 3-4A). Interestingly, many of these binding sites share a core ETS motif and are known to appear frequently in promoter regions. Peaks in promoter regions were overrepresented among those that gained accessibility in the absence of LXRs (Fig. 3-1B). Among the promoter peaks, the NFY motif was particularly prevalent among those that gained accessibility in LXRDKO liver (Fig. 3-4A, B). By contrast, ETS family motifs were enriched across promoter regions without a preference for sites that gained accessibility upon loss of LXR. Footprinting analysis validated this finding (Fig. 3-4C). The NFY footprint was more accessible across the LXRDKO liver ATAC-Seq sample compared to control. Peaks at which NFY motifs gained accessibility were already accessible in WT samples, but became even more accessible in LXRDKO samples (Fig. 3-4D).

A majority of genes with increased NFY accessibility had an LXR binding site (either basal or with agonist treatment (Fig. 3-4E). Moreover, the NFY motif was enriched among the LXR-binding promoter peaks that were increased in accessibility. This could indicate that the absence of LXR could be leading to compensatory increased NFY binding at these LXR target genes. Genes proximal to NFY motifs that gained accessibility in LXRDKO liver were enriched

for pathways related to cell cycle, NF-kB signaling, and cholesterol synthesis (SI Appendix Fig. 3-S7C), and included SREBP2 targets such as *Hmgcr*, *Hmgcs1*, *Sqle*, and *Fdps*. For instance, the *Hmgcr* promoter was on average more accessible in LXRDKO liver (Fig. 3-5F). The peak in this region overlaps with an SREBP2 binding site and contains 4 NFY binding motifs. Interestingly, among genes with increased NFY accessibility, only a small proportion was differentially expressed between WT and LXR DKO liver (3.36%, accounting for 15.8% of all upregulated genes in LXR DKO) (SI Appendix Fig. 3-S7D). As an example, *Got1* was upregulated and its promoter (with 4 NFY motifs) was on average more accessible in LXRDKO liver (Fig. 3-4F).

Distinct modes of LXR transcriptional regulation in liver

Many studies on LXRs have focused on their functions as ligand-activated transcription factors, using pharmacological tools such as the potent synthetic agonists GW3965 and T0901317 [346,358,359]. Our analysis of global accessibility changes induced by loss of LXR supported this major mode of LXR action, but also revealed additional mechanisms. We integrated datasets for genes differentially expressed in liver in response to T0901317 treatment with LXR ChIP-Seq data and our RNA-seq data [352]. We found that the expression of a majority of the differentially expressed genes in WT vs LXRDKO liver was not altered by agonist treatment (Fig. 3-5A). This was true even for those genes predicted to have LXR binding by ChIP-Seq. This observation suggests distinct basal and pharmacological ligand-dependent functions for LXRs at individual genes.

We next focused on genes that were regulated both by synthetic agonist and the presence or absence of LXRα/β. A majority of these genes was regulated in opposite directions by agonist treatment and LXR deletion (Fig. 3-5A). We identified 32 genes that were downregulated in LXRDKO liver and induced by agonist treatment in WT liver (Fig. 3-5A). This set was enriched

for classical LXR targets mostly involved in fatty acid metabolism, including *Srebf1*, *Scd1*, *Acaca, Fasn, and Lpcat3*. ATAC peaks at these LXR binding sites were enriched for DR1 and DR4 nuclear receptor motifs. Additionally, LXR binding sites for these pharmacological ligand-activated genes were more likely to be located in promoter regions in comparison to pharmacological ligand-unresponsive genes downregulated in LXRDKO liver (SI Appendix Fig. 3-8A).

By contrast, a substantial subset of genes downregulated in LXRDKO liver with putative LXR binding but no transcriptional response to agonist were enriched for canonical PPARα targets such as *Acox1*, *Acsl5,* and *Fabp1* (Fig. 3-5A, SI Appendix Fig. 3-S8B). The LXR binding sites for these genes were enriched for the nuclear receptor DR1 motif (Fig. 3-5A). This observation suggests that LXR may associate widely with DR1 nuclear receptor motif sites and thereby contribute to the expression of canonical PPARα genes that do not respond to pharmacologic LXR agonist.

The LXRE/DR4 motif was enriched among the set of intergenic and intronic ATAC peaks with putative LXR-binding sites that showed the largest loss of accessibility in LXRDKO liver (SI Appendix Fig. 3-S8C). The DR1 motif was enriched across all intergenic and intronic LXR binding sites regardless of their change in accessibility in LXRDKO livers. Thus, the DR4/LXRE motif is strongly associated with classical LXR targets that are upregulated by agonist treatment and downregulated in the LXRα/β knockout, and with LXR binding sites that lose accessibility with the loss of LXR. The data further suggest that, outside of these canonical LXR targets, LXR can bind to nuclear receptor motifs more broadly, including at DR1 motifs.

We also identified 14 genes that were upregulated in the absence of LXRs, downregulated with agonist treatment, and had putative LXR binding sites by ChIP-seq (Fig. 3-5A). These genes

represent potential targets for direct ligand-dependent repression by LXRs. This mode of regulation is known to occur with certain other nuclear receptors, such as TR, but has not been rigorously documented for LXRs. LXR binding sites for these ligand-repressed genes were more likely to be located in promoter regions (SI Appendix Fig. 3-8A). These LXR-repressed genes were involved in various cellular functions not focused on lipid metabolism. Interestingly, ATAC peaks associated with the LXR binding sites in these repressed genes were enriched for the FOXA and C/EBP motifs. Overall accessibility of these LXR binding sites were decreased in LXRDKO liver (SI Appendix Fig. 3-8D). As an example, *Slc25a15* and *Lurap1l* had increased expression in LXRDKO liver and decreased expression with LXR agonist treatment. Their loci have LXR binding sites that were on average reduced in accessibility in LXRDKO livers and have putative binding sites for FOXA2, C/EBP and other nuclear receptors such as HNF4a and PPARα (Fig. 3-5B). Public ChIP-Seq data provided additional support for the presence of FOXA2 and C/EBP binding at these sites (Fig. 3-5B). By comparison, genes upregulated in LXRDKO liver that lack the transcriptional response to the agonist included genes involved in cysteine and methionine metabolism and genes encoding for transcription factors such as *Foxa2* and *Hnf4a* (Fig. 3-5A). These finding suggests that FOXA1/2 binding could be important for LXR ligand-dependent repressor function. In accordance with our findings, published data suggest that loss of hepatic *Foxa2* abolishes the downregulation of some of these genes (*Cxcl*, *Etnppl*, *Got1*, *Nnmt*, *Slc25a15*, *Tbc1d8*, *Tymp*) by LXR agonist (GSE149075) [352].

To further validate the ability of LXR agonists to repress gene expression through direct LXR binding, we treated WT mice with GW3965 and measured gene expression by qPCR (Fig. 3-5C). Out of the 14 genes tested, 8 were reduced by GW3965 treatment, and 4 trended down (p

value < 0.1). Independent confirmation of the downregulation of these predicted targets supports the conclusion that LXRs are capable of acting as ligand-dependent repressors.

Discussion

In this study, we assessed the implications of loss of LXR expression in mouse liver for gene expression, chromatin accessibility and transcription factor activity. Unlike fork head factors, LXRs are not known to be pioneer factors that play key roles in establishing regions of open chromatin. Accordingly, the changes in chromatin accessibility we observed with loss of these nuclear receptors, especially on LXR binding sites, were rarely dramatic; i.e., complete closing of an existing peak or opening of a new peak. A majority of the genes differentially expressed between WT and LXRDKO liver had LXR binding sites, suggesting the change in their expression was likely to be a direct consequence of loss of LXR binding. At the same time, a majority of the genes differentially expressed between WT and LXRDKO liver did not change in WT mice treated with synthetic LXR agonist. This finding suggests that many LXR binding sites do not transduce ligand-dependent signals, or are active with basal levels of endogenous ligands. Such LXR binding sites appear necessary to maintain expression of their target genes but do not respond to pharmacological activation, perhaps due to specific coactivator requirements. A similar disconnect between basal nuclear receptor activity and synthetic ligand response has been previously observed in macrophages [347]. It would be interesting to determine if challenging mice with high-cholesterol diet, which would provide a higher concentration of endogenous sterol ligands, would alter the pattern of gene responses.

An important limitation of our study is the use of whole liver tissue. Our RNA expression and chromatin accessibility experiments incorporate signals from hepatocytes and non-parenchymal cells such as Kupffer cells, liver sinusoidal endothelial cells, stellate cells, and other cell types. Changes in gene expression in these non-parenchymal cells and/or shifts in the proportion of these cells present in LXRDKO liver may contribute to the results of the RNA-Seq

and ATAC-Seq analyses. In particular, LXRα is known to be crucial for Kupffer cell identity [334,335], and LXR-deficient liver has been reported to display an altered profile of immune cells, especially in the context of inflammation [360,361]. In agreement with these prior findings, genes highly expressed in Kupffer cells such as *Cd5l* and *Clec4f* showed reduced expression in LXRDKO liver. LXRs have also been reported to affect the capillarization of sinusoidal endothelial cells and the ability of stellate cells to contribute to fibrosis in response to injury [362,363]. Further dissection of the contributions of different cell types to the overall phenotype of LXR-deficient livers will require addition studies, including single-cell RNA-Seq and single-cell ATAC-Seq.

Genes downregulated in response to LXR deletion in our study were enriched for classical LXR targets related to fatty acid metabolism, including *Srebf1*. Thus, the presence of LXRs on the regulatory regions of these genes appears to be required for their basal expression. Interestingly, however, LXR target genes related to cholesterol metabolism and efflux (such as *Abca1*, *Abcg5*, *Abcg8,* and *ApoA1*) were generally not differentially expressed between WT and LXRDKO liver. Although LXR binding is not required for the basal expression of these genes, prior studies have shown that LXRs mediate induction of these genes in liver in response to synthetic LXR ligand or cholesterol diet challenge [294,295,328]. This separation is consistent with a primary role for hepatic LXRs in the basal state in fatty acid metabolism and roles in both fatty acid and cholesterol metabolism for LXR in the setting of high ligand concentration [343].

Among genes that responded to both synthetic agonist treatment and LXR deletion in our analysis, most responded in opposite directions. Classical LXR target genes had one or more LXR binding sites associated with a DR4 or DR1 motif, were reduced in expression with the loss of LXR, and were increased in expression with LXR agonist treatment. Unexpectedly, we also

identified a small set of genes that were repressed by LXR in the basal state and in response to synthetic agonist. These genes had putative LXR binding sites by ChIP [297], showed increased expression in LXRDKO liver, and showed decreased expression with LXR agonist treatment of WT mice [352]. Such a direct ligand-dependent repressor function for LXR has not been demonstrated in liver previously. Analysis of the ATAC peaks associated with LXR binding revealed that the FOXA motif was common to these genes repressed by LXR agonist. Our ATAC-Seq results showed decreased FOXA motif accessibility across the genome in LXRDKO liver, despite increased expression of the *Foxa2* gene. For half of the candidate direct ligand-dependent repressor target genes we identified, the pharmacological repression by LXR agonist was dependent on the presence of *Foxa2* [352]. Kain et al. [352] demonstrated the importance of FOXA2 for synthetic ligand-dependent activation of LXR. Our data suggest an additional role for FOXA2 in the ligand-dependent repressor function of LXR.

Our data also provide evidence that the loss of LXRs from the liver affects the activity of other transcription factors. Undoubtedly, alterations in lipid metabolism upon loss of LXRs contributes to some of the gene expression changes observed, such as the reduction in fatty acid synthesis due to loss of *Srebf1* expression [296]. Reduced availability of fatty acids would be expected to reduce ligand activation of PPARα. At the same time, we also found evidence of cooperation between LXR and other transcription factors on the regulatory regions of individual genes. One of the most prominent factors whose motif lost accessibility in our LXRDKO dataset was PPARα. Interestingly, the expression of both PPARα target genes and *Ppara* itself was reduced in LXRDKO liver. This finding argues against a competition between PPARα and LXR, and indicates that the presence of LXR is necessary for PPARα signaling. Ducheix et al. have noted that the impact of the PPARα agonist fenofibrate on PPARα target genes was decreased in

LXRDKO liver [342]. Many genes share LXR and PPARα binding sites [297], suggesting direct cooperation of LXR and PPARα in their regulation. Many ATAC peaks associated with LXR binding are also associated with binding of other transcription factors such as FOXA2 and HNF6 (Fig. 3-4F). Such regions resemble previously described transcription factor hotspots, which function as super-enhancers [364]. The reduced accessibility of these sites in LXRDKO liver supports idea of cooperation between LXRs and other factors thereon.

Other global changes in the LXRDKO liver included increased accessibility of promoter regions, and decreased accessibility of intergenic and intronic regions, suggesting a reduction in enhancer activity. This pattern was particularly evident for the intergenic and intronic regions of genes whose expression was downregulated and for the promoter regions of those upregulated in LXRDKO liver. The CTCF motif was enriched among the intergenic and intronic regions that lost accessibility in LXRDKO liver. In a recent paper, ATAC-Seq of hearts from CTCF knockout mice showed decreased accessibility in intergenic and intronic regions and increased accessibility in promoter regions [365]. A reduction in CTCF activity could thus contribute to the changes in the intergenic and intronic accessibility in the absence of LXRs.

Loss of LXR also appeared to provoke compensatory responses at promoters. In particular, NF-Y motifs broadly increased in accessibility in LXRDKO liver compared to WT. This motif was enriched among promoters already accessible in WT liver that became more accessible in LXRDKO liver. NF-Y is known for its role in maintaining the accessibility of promoter regions and protecting them from nucleosomes [366]. A majority of the sites with increased NF-Y accessibility occurred in LXR binding genes. More directed studies are needed to explore the mechanistic relationships between LXR and NF-Y.

Prior studies have documented instances of squelching, in which an activated transcription factor represses a target gene without binding to its location by competing for cofactors [367–370]. However, our study was not designed to test this mode of regulation for LXRs, as we did not perform ATAC-seq in the presence of synthetic LXR agonist treatment. For genes upregulated in LXRDKO liver that have no direct LXR binding, we observed an enrichment of the CTCF motif in peaks that lost accessibility and NFY motif in peaks that gained accessibility. This finding suggests that changes in CTCF and NFY may contribute to the ability of LXR to repress genes without direct binding. The mechanism whereby loss of LXR alters CTCF and NFY activity on LXR-binding and non-binding genes requires further investigation.

Acknowledgements

Funding for this project was provided by grants to PT from the National Institutes of Health (HL136618, DK126779, DK063491). The authors would like to thank the staff at the UCLA Technology Center for Genomics and Bioinformatics for their assistance with this work.

Conflict of Interest Statement

The authors declare they have no financial interest related to this work.

Data Sharing Plan

ATAC-Seq and RNA-seq data have been deposited to the GEO database (GSE191030).

.

Methods

Mice

*Lxr*α−/− and *Lxr*β−/− mice originally provided by David Mangelsdorf (UT Southwestern Medical Center, Dallas) were backcrossed more than 10 generation to the C57/Bl6 background. Animals were housed in a 25 °C temperature-controlled room under a 12-hour light / 12-hour dark cycle under pathogen-free conditions. Mice had *ad lib* access to water and standard chow (Harlan NIH-31, 3.1 kcal/g, 23% calories from protein, 18% from fat, and 59% from carbohydrate). Mice were sacrificed at 8 weeks of age. All animal experiments were approved by the Institutional Animal Care and Research Advisory Committee of the University of California, Los Angeles.

RNA-Seq sample preparation

RNA from frozen tissue was extracted through TRIzol (Invitrogen) and Qiagen RNeasy Mini Kit. Total RNA libraries were made with KAPA Stranded kit with mRNA capture. Libraries were sequenced as single-end (50bp) on an Illumina HiSeq3000.

RNA-Seq data processing and analysis

Data quality analysis was performed via FastQC [371]. The reads were aligned to the mm10 genome using STAR (v2.6.0c, [308]). Alignments were visualized using samtools [310] and the IGV browser (v2.9.4) [315]. Differential expression analysis was performed with DESeq2 (v1.32.0)[372], and genes were classified as significantly regulated if adjusted P value < 0.05. Genes were annotated using *biomaRt* package (v2.48.3) in R (1v4.1.0)[373]. Plots and heatmaps were created in R using *pheatmap* (v1.0.12) and *EnhancedVolcano* (v1.10.0)and the *ClustVis* web tool [316,374]. Gene sets were

enriched for pathways using *BioPlanet* 2019 and ChIP-seq targets using ChIP Enrichment Analysis (ChEA) 2016 through *Enrichr* [317,375,376].

ATAC-Seq sample preparation

ATAC-Seq from tissue was conducted as previously published [377] with some modifications. Approximately 50 -100 mg of fresh tissue was homogenized via dounce homogenizer in 1 ml of nuclear isolation buffer (20 mM Tris-HCl, 50 mM EDTA, 5 mM Spermidine, 0.15 mM Spermine, 0.1% mercaptoethanol, 40% glycerol, 1mM EGTA, 60 mM KCl, 1% IGEPAL pH 7.5) and filtered through a 40 μM nylon filter. Samples were centrifuged at 4 °C at 1000 × g for 10 min and the pellet was resuspended with 1 ml cold resuspension buffer (RSB) (10 mM Tris-HCl, 10 mM NaCl, 3 mM MgCl2, pH 7.4). Approximately 50,000 nuclei from these samples were removed and centrifuged at 4 °C at 500 × g for 5 min. Supernatant was removed and the transposase reaction was performed immediately as described [306]. DNA was purified using Qiagen MinElute Kit and libraries were prepared as described [306]. Size selection was done with AMPure XP magnetic beads. Libraries were quantified by qPCR using NEBNext Library Quant Kit for Illumina and were sequenced on Illumina HiSeq 4000 as single-end 50 bp at the UCLA Broad Stem Cell Research Center Sequencing core.

ATAC-Seq data processing and analysis

Samples were demultiplexed and quality control was done using FastQC [371]. Cutadapt [378] was used to trim adapters and trimmed sequences were aligned to the mm10 mouse genome assembly using bowtie2 (v2.3.3)[309]. Mitochondrial, unmapped, multi-mapped and duplicate reads were removed using *samtools* [310] and in-house scripts. Peaks were called using MACS2 [311] and quantitated across samples using Seqmonk (v1.38.2) [379] and normalized to million reads per

sample and peak length (RPKM). Peaks were annotated to genomic features and nearest promoter via Homer (v4.10)[314] *annotate* function. *Bedgraphs* were created using Homer and converted to .tdf files for visualization in the IGV browser [315]. tSNE plots were created using Seqmonk (v1.38.2). For ranked analysis, peaks that had less than 10 counts across all 4 samples were removed. We ran the Irreproducible Discovery Rate (IDR) software (v2.0.3) for quality control [356]. The filtering improved the percentage of peaks that met the 1e-6 threshold in the IDR software. The reads from replicates for each peak were averaged and the peaks were ranked based on the difference between the average counts among conditions. The *pheatmap* R package was used to plot the top 1000 peaks heatmap. ChIP-Seeker (v1.28.3) was used to plot the distribution of peaks relative to TSS [380]. Merged bam files were created using *samtools* (v1.6) merge function. deepTools2 (v3.5.1) was employed to profile the signal intensity across defined peaks using the merged replicates [319].

Motif analysis to infer transcription factor (TF) binding was done through the *findMotifGenome* and *findMotifs* functions in Homer using known motifs. Ranked peaks were binned into equal sized bins and known motif analysis was run for each bin. The p-value for each motif was plotted across all bins. Non-enriched and not-changing motifs were filtered out. Motifs with high similarity (>.90) within the same TF family were combined. Footprinting was done with HINT-ATAC using the bam files and the JASPAR motif database as input [357,381].

Additional ChIP-Seq and RNA-Seq datasets

Additional data was downloaded from the Gene Expression Omnibus and processed as above: LXR Liver ChIP-Seq data (GSE35262), LXR vehicle-ChIP-Seq data (GSM864670), LXR T09 peaks (GSM864669). Differentially expressed genes in response to LXR agonist treatment were obtained from GSE149075. Hepatic SREBP-2 peaks were obtained from GSE28082. The ChIP-

Atlas was used to provide a summarized ChIP-Seq experiments from mouse liver or hepatocytes or liver derived cell lines [382].

Validation with LXR Agonist

9-week-old mice on mixed background 129X1/SvJ and C57BL/6 were gavaged with 40 mg/kg GW3965[324] first 17 hrs before and second 8 hrs before sacrificing. Mice were 4hrs fasted before sacrificing. GW3965 was gavaged in canola oil. DMSO was used as vehicle control. RNA was extracted using TRIzol. The differences between gene expression were determined via qPCR using Taq Universal SYBR Green Supermix (BIO-RAD) using primers that are provided in SI Appendix Table 1.

Figures and Tables

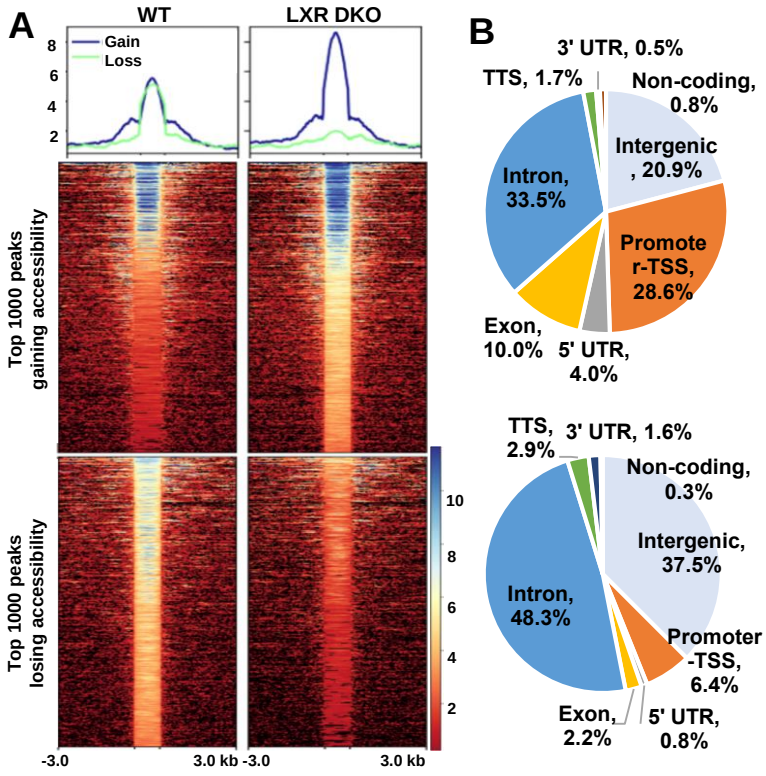

Figure 3-1:Global chromatin accessibility changes in LXRDKO liver.

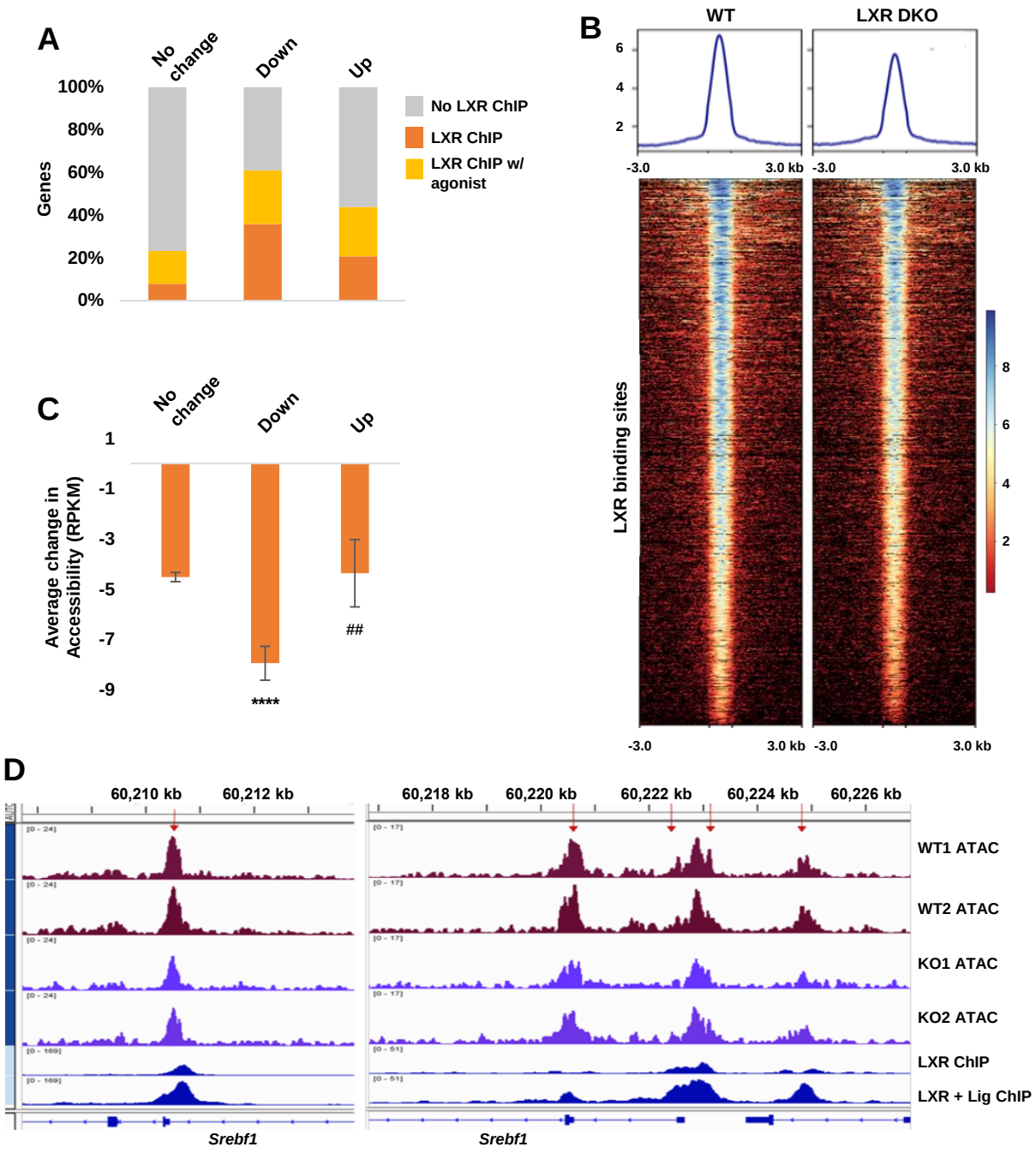

Figure 3-2: Correlation of LXR binding, gene expression, and chromatin accessibility.

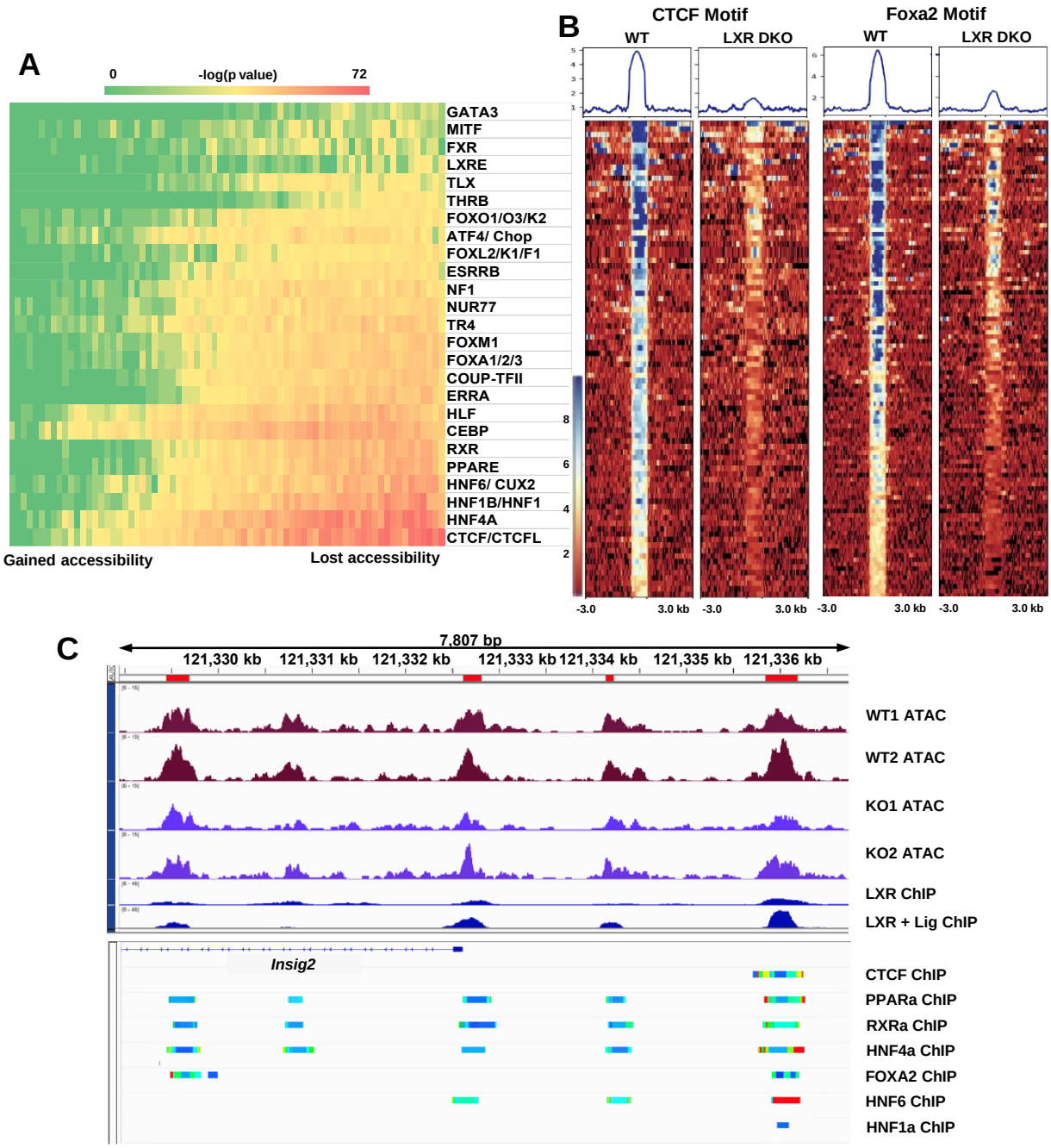

Figure 3-3: Loss of LXR affects chromatin accessibility at other transcription factor binding sites.

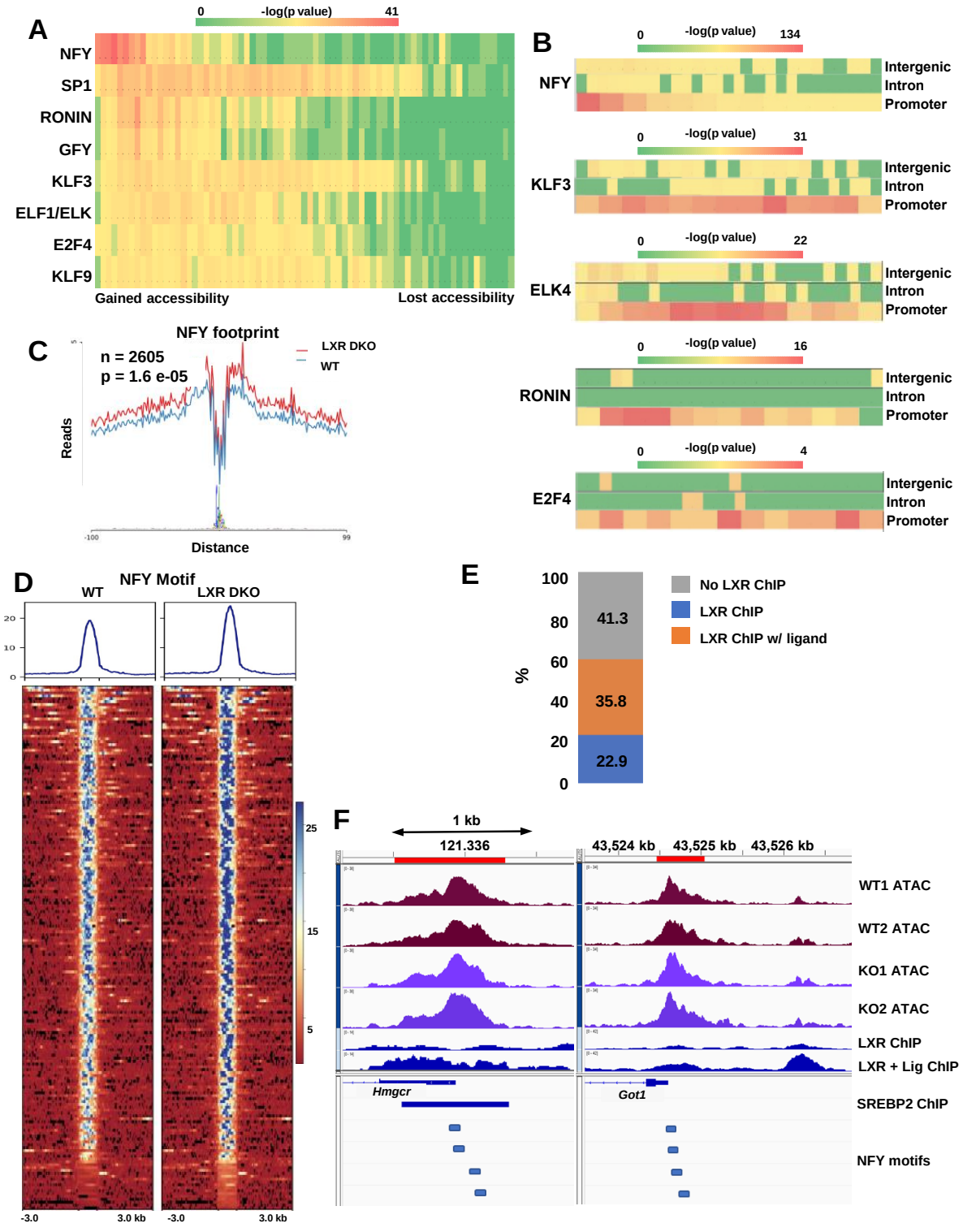

Figure 3-4: Increased accessibility of NFY motifs in LXR-deficient liver.

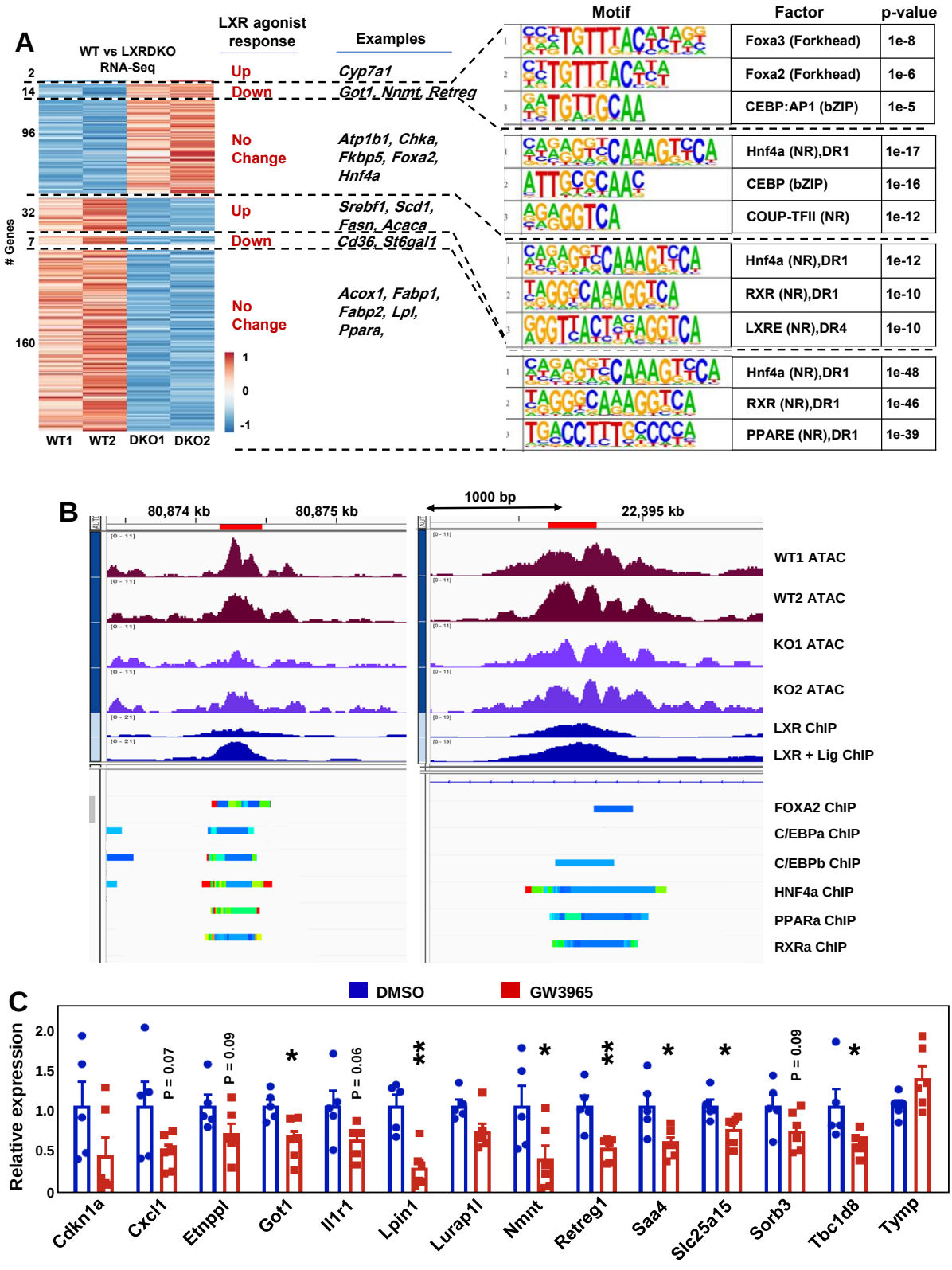

Figure 3-5:LXR can act as a ligand-dependent and -independent repressor.

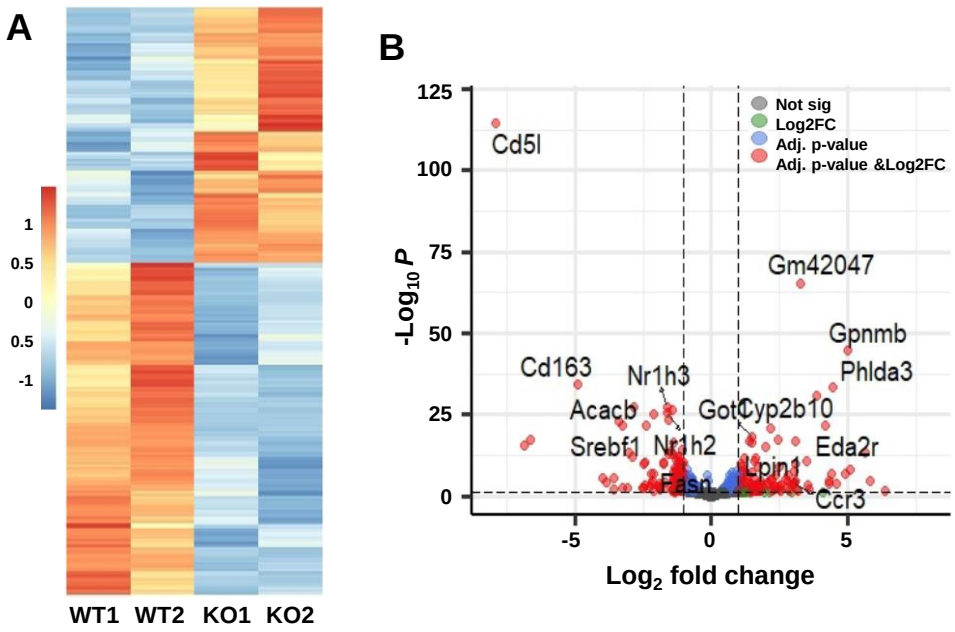

C

Top 10 Downregulated Genes

Name	Adj. p value	Fold Change	Type
Cd5l	2.05E-115	0.0040	protein coding
Cd163	4.39E-35	0.0335	protein coding
Clec4f	3.45E-28	0.1402	protein coding
Nr1h3	3.45E-28	0.3239	protein coding
Ces1e	2.66E-27	0.3733	protein coding
Nr1h2	3.87E-26	0.3219	protein coding
Acacb	5.26E-26	0.2306	protein coding
1810008I18Rik	3.91E-24	0.3331	lincRNA
Hamp2	9.02E-24	0.0939	protein coding
Srebf1	1.84E-22	0.1875	protein coding

Top 10 Upregulated Genes

Name	Adj. p value	Fold Change	Type
Gm42047	4.36E-66	9.6148	lincRNA
Gpnmb	1.44E-45	32.1408	protein coding
Phlda3	3.49E-34	21.7534	protein coding
Sult2a7	1.15E-31	14.4144	protein coding
Eda2r	2.66E-22	18.0955	protein coding
Cyp2b10	2.70E-21	4.4866	protein coding
Got1	1.20E-18	2.8311	protein coding
Cplane1	4.55E-18	5.3950	protein coding
Gm48199	9.53E-18	8.6393	lincRNA
Fkbp5	9.54E-18	2.6513	protein coding

Figure 3-S1:Transcriptional changes in LXR-deficient liver.

A

Downregulated Pathwaysz	Adjusted p-value	Genes
PPAR signaling pathway	3.92E-08	*Acsl5, Lpl, Nr1h3, Dbi, Sorbs1, Fabp1, Fads2, Fabp2, Fabp5, Acox1, Me1, Cd36, Ppara*
Lipid and lipoprotein metabolism	2.11E-06	*Slc44a1, Mttp, Lpl, Sgms2, Acacb, Acaca, Mtm1, Helz2, Fads2, Me1, Cd36, Arsa, Srebf1, Stard4, Hsd3b2, Elovl5, Srd5a1, Slc10a2, Elovl2, Acsl5, Fabp1, Gpam, Acox1, Fasn, Lpcat3, Ppara, Mgll, Abcg1*
Fatty acid, triacylglycerol, and ketone body metabolism	1.70E-04	*Srebf1, Elovl5, Elovl2, Acsl5, Acacb, Acaca, Helz2, Fabp1, Gpam, Acox1, Fasn, Me1, Cd36, Ppara*

Upregulated Pathways	Adjusted P-value	Genes
Cysteine and methionine metabolism	0.001861	*Sds, Got1, Tat, Cth, Mat1a, Cdo1*
p53 activity regulation	0.004402	*Cdkn1a, Zmat3, Igfbp3, Sesn2, Ccng1, Mdm2, Tnfrsf10b, Bax, Gtse1*
MicroRNA regulation of DNA damage response	0.004582	*Cdkn1a, Myc, Ccng1, Mdm2, Tnfrsf10b, Bax, Brca1*

B

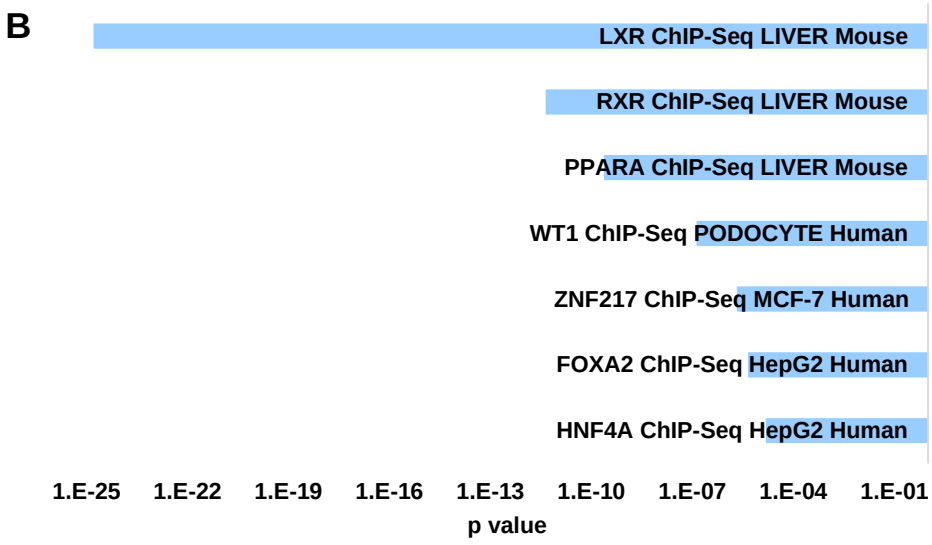

Figure 3-S2: Expression profiles of LXRDKO livers.

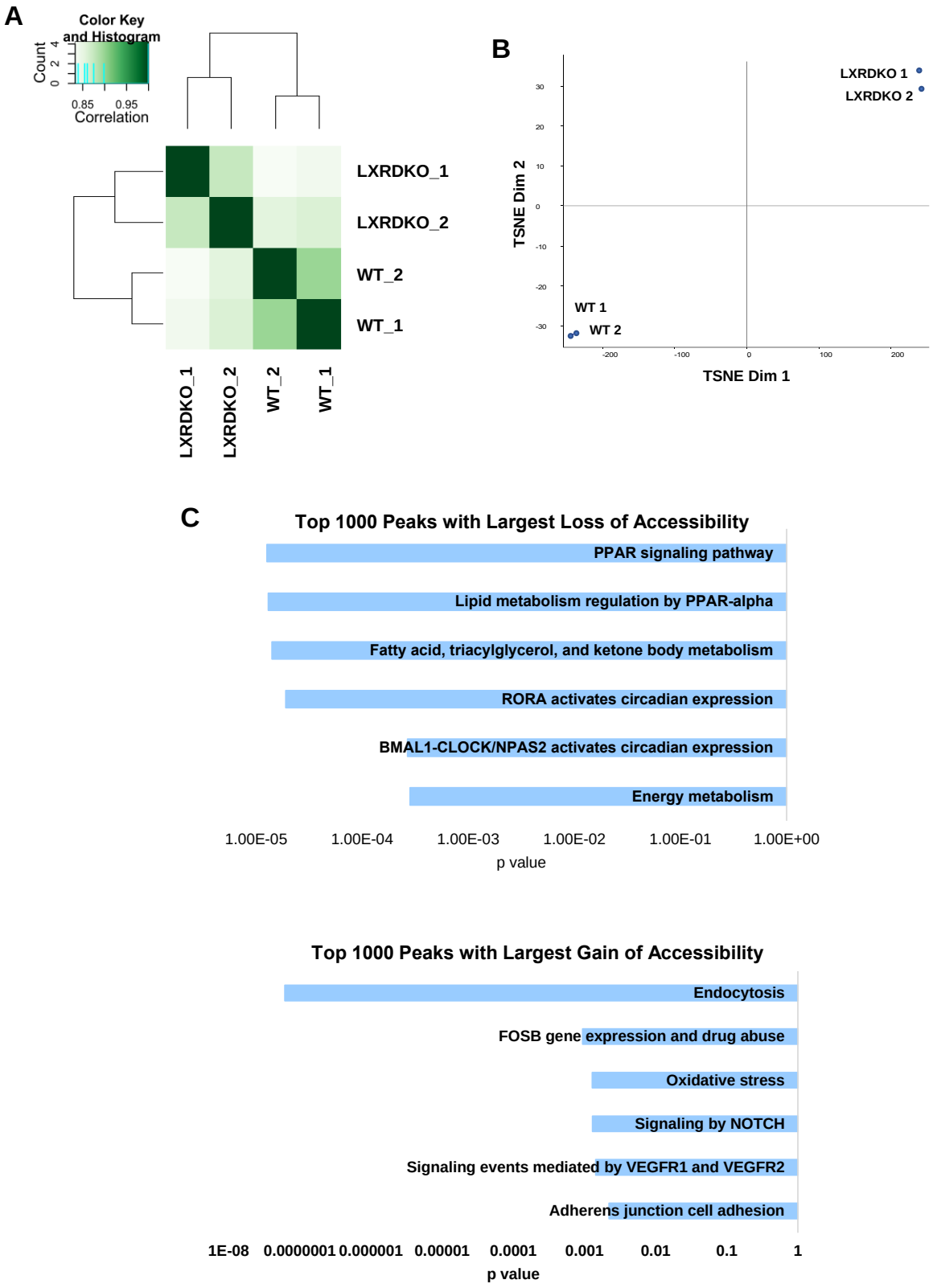

Figure 3-S3: Chromatin accessibility profiles of LXRDKO livers

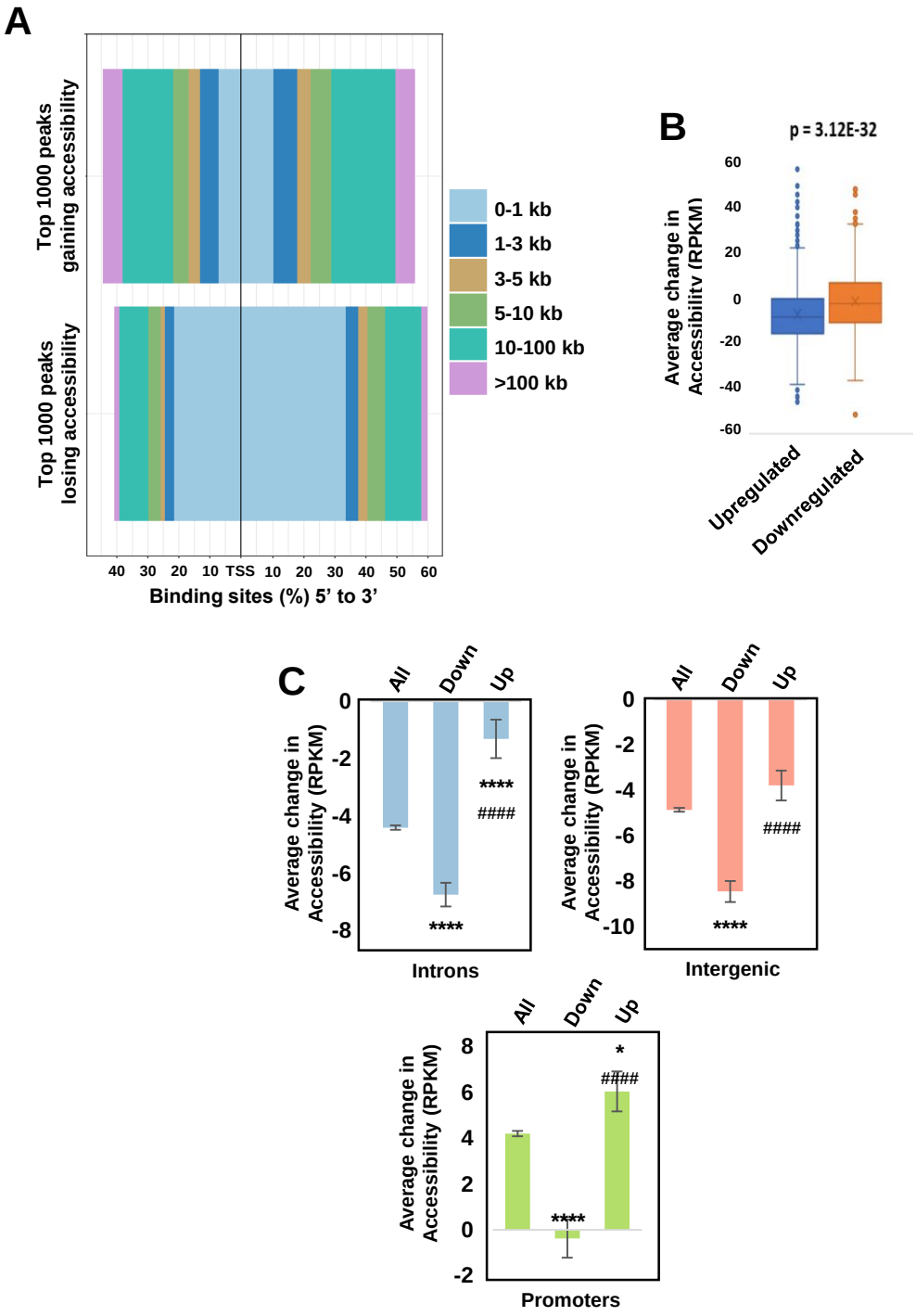

Figure 3-S4:Pathway enrichment.

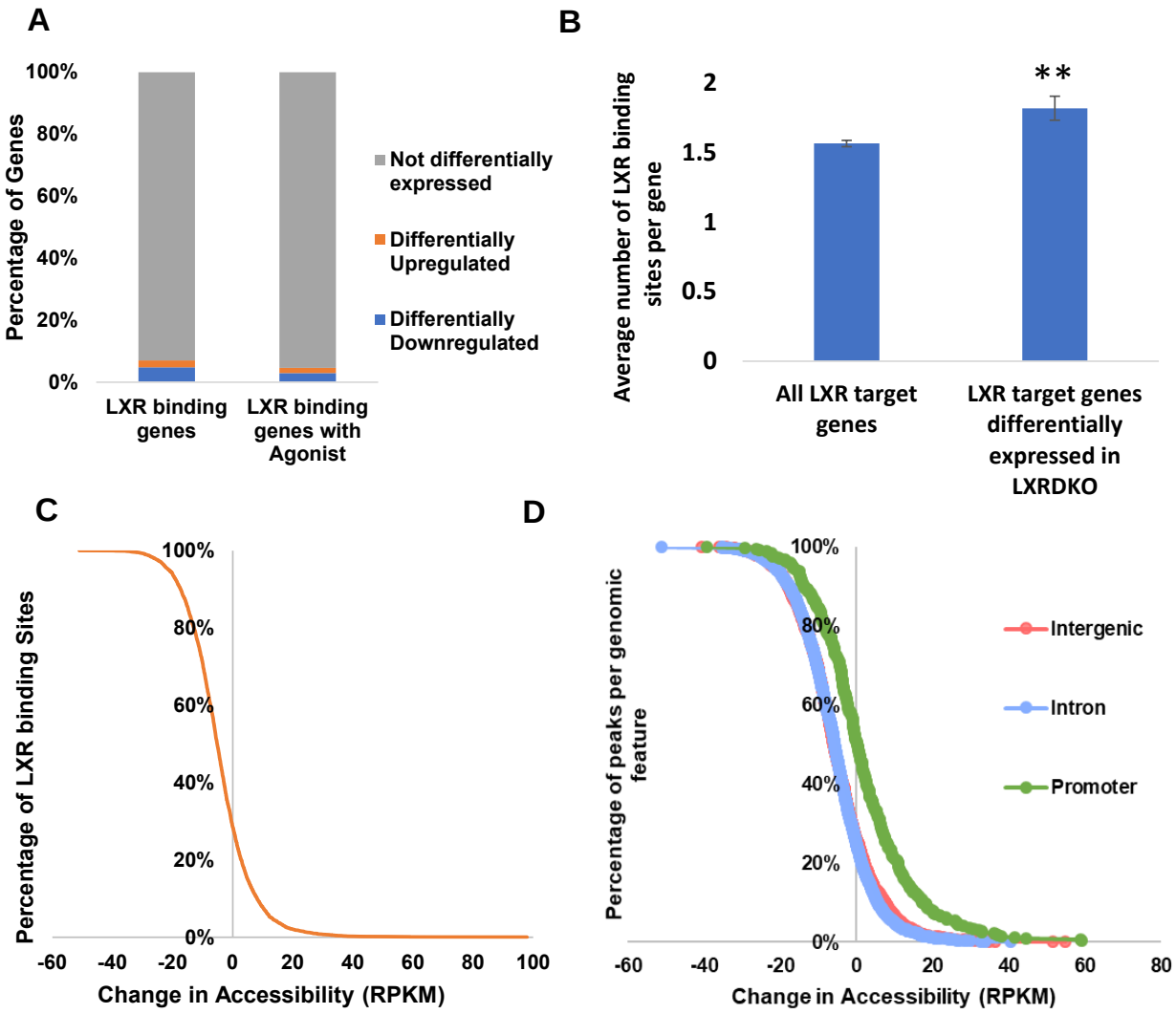

Figure 3-S5:Changes to LXR binding sites in LXRDKO livers.

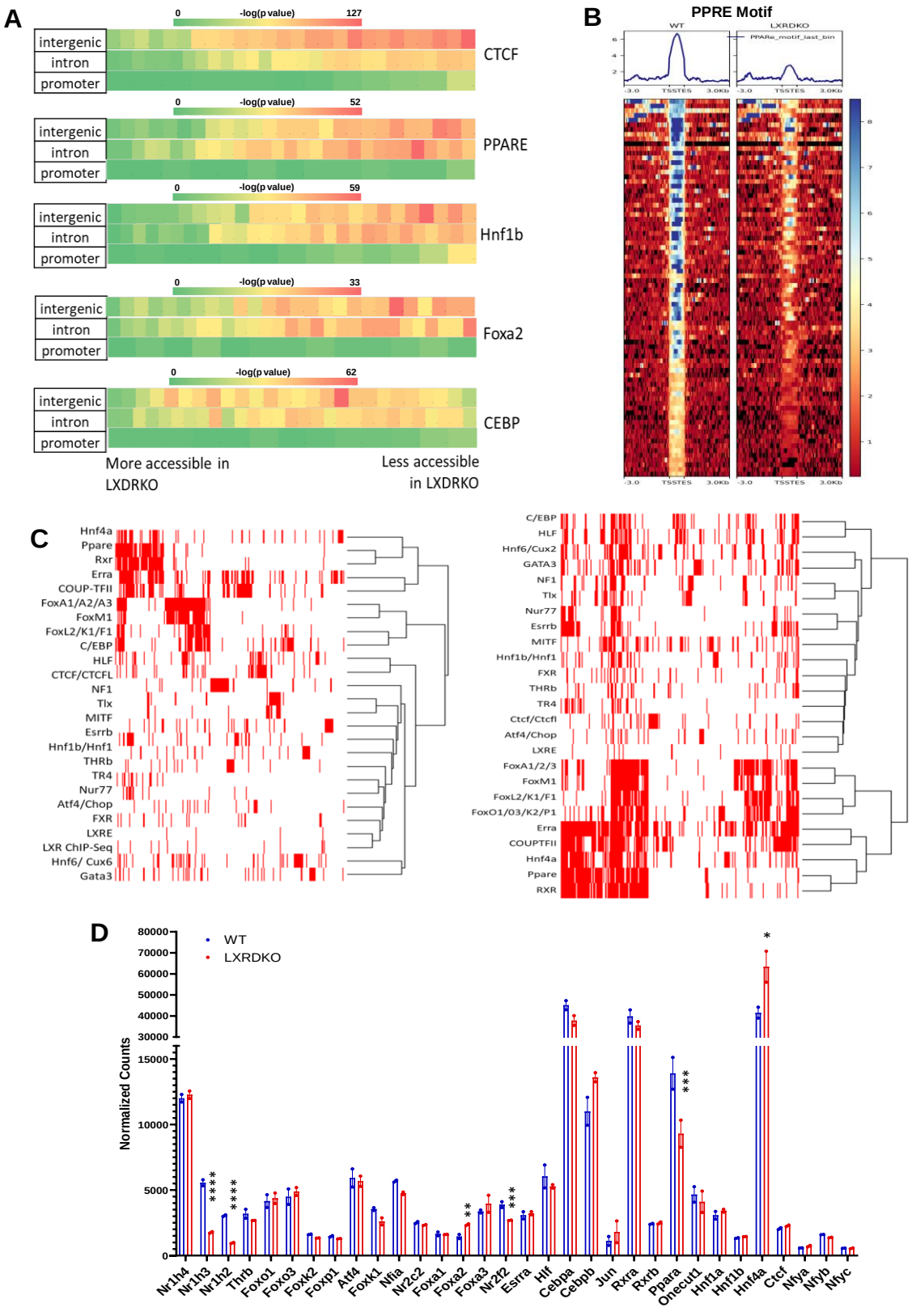

Figure 3-S3-6: Loss of LXRs reduces motif accessibility of other transcription factors.

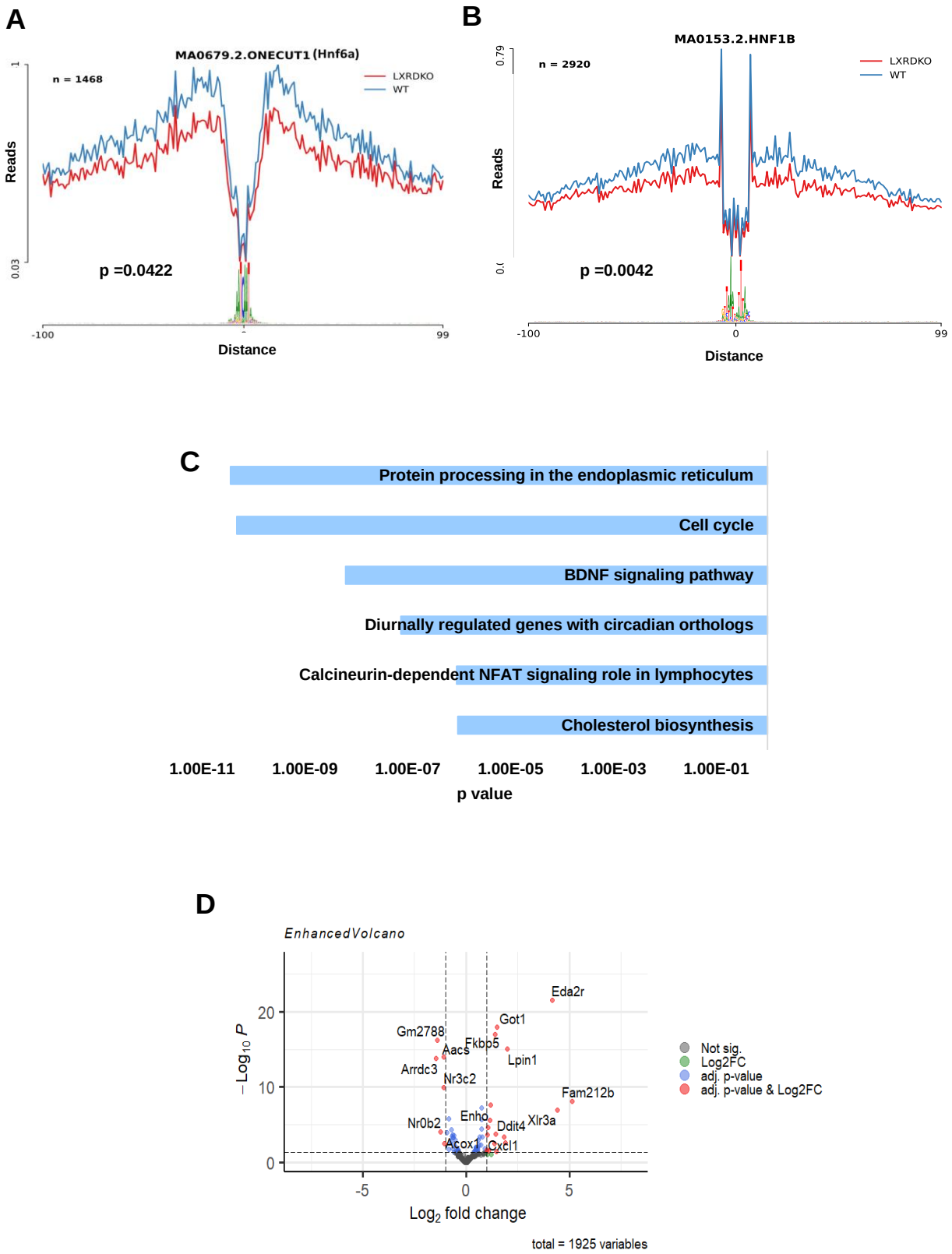

Figure 3-S3-7: Impact of the loss of LXR on other transcription factor motif activity.

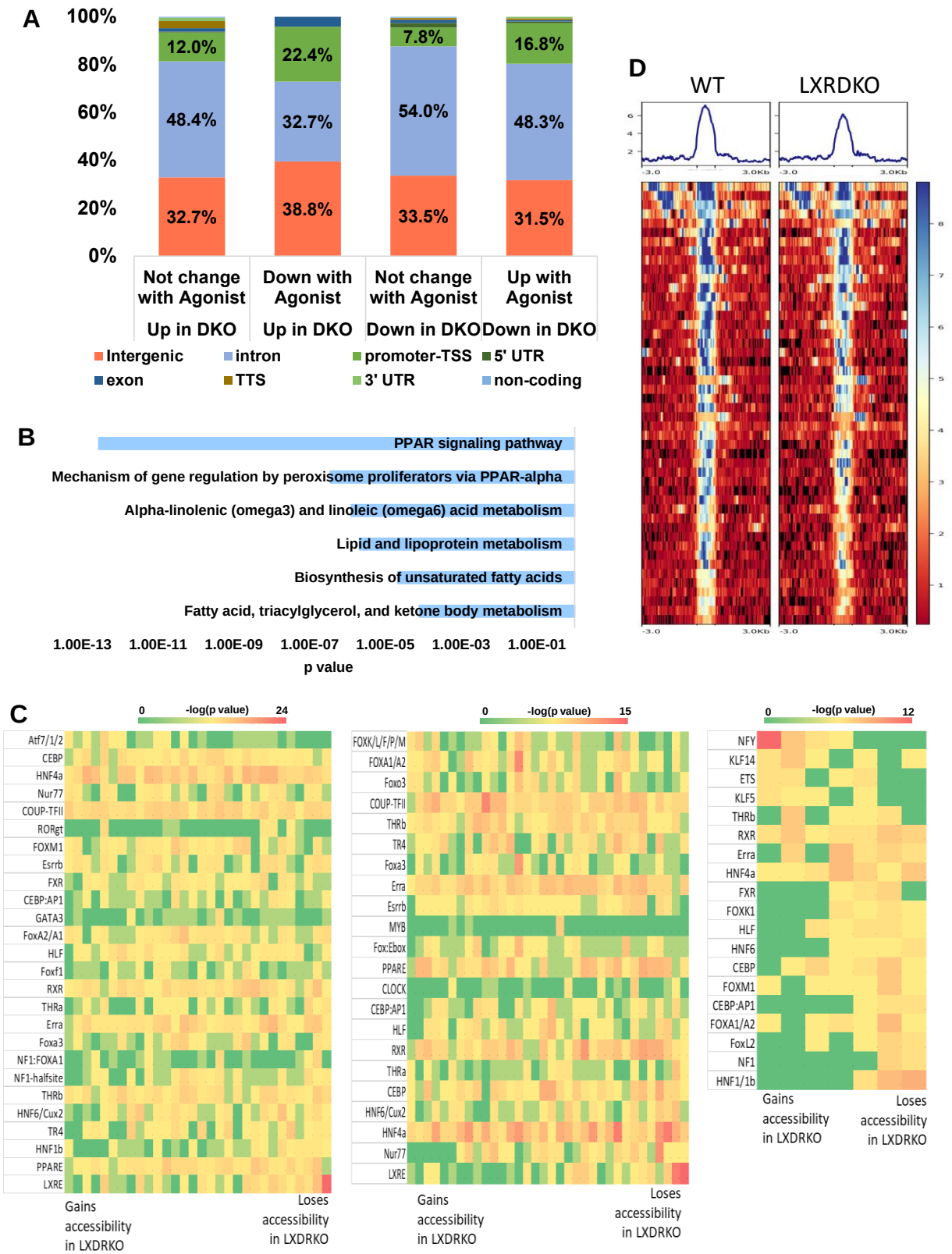

Figure 3-8: Change in accessibility and genomic features at the LXR binding sites in relation to different modes of LXR action.

Table 3-S1: Primers for RT-qPCR

Primer name (m for mouse)	Sequence
mLpin1_F	CATGCTTCGGAAAGTCCTTCA
mLpin1_R	GGTTATTCTTTGGCGTCAACCT
mCxcl1_F	CTGGGATTCACCTCAAGAACATC
mCxcl1_R	CAGGGTCAAGGCAAGCCTC
mSaa4_F	CTCTGTTCTTTGTTCCTGGGAG
mSaa4_R	CTAGGTTGTCCCGATAGGCTC
mSlc25a15_F	GCTGCCTCAAGACCTACTCC
mSlc25a15_R	CCGTAACACATGAACAGCACC
mSorbs3_F	TTCAGCTTCGTCTTTGAACAACA
mSorbs3_R	CTTGGGTCAAGGTTGGAGGA
mNnmt_F	TGTGCAGAAAACGAGATCCTC
mNnmt_R	AGTTCTCCTTTTACAGCACCCA
mCdkn1a_F	CCTGGTGATGTCCGACCTG
mCdkn1a_R	CCATGAGCGCATCGCAATC
mTbc1d8_F	AGCCTAGCCAGATCACAAAGA
mTbc1d8_R	CGTCCAGAGGGAACAGTCT
mTymp_F	CGCGGTGATAGATGGAAGAGC
mTymp_R	CACACCTCCTGTGGAGTGTT
mGot1_F	GCGCCTCCATCAGTCTTTG
mGot1_R	ATTCATCTGTGCGGTACGCTC
mEtnppl_F	GCTCTCCGTTTGCTACTTCAC

mEtnppl_R	CCCTCTTGACATCTTTGCCCTT
mIl1r1_F	CGAACCGTGAACAACACAAA
mIl1r1_R	CAGAGGCACCATGAGACAAA
mLurap1l_F	TCTCTTGGGTCTCTCGGTATAA
mLurap1l_R	TCCACAGCCAGCAAGATTAG
mRetreg1_F	GCCATCAAAGACCAGCTAGAA
mRetreg1_R	GTCCCAGCTCACTCTCAATTT

Figure Legends

Figure 3-1: Global chromatin accessibility changes in LXRDKO liver.

A. Top: Average normalized ATAC-Seq signal intensity for top 1000-ranked peaks changing in accessibility in WT and LXRDKO samples. Bottom: Heatmap of signal distribution around ATAC-Seq peak summits, for the same peaks. B. Pie charts showing distribution of genomic features among the top 1000 peaks with largest loss and gain in LXRDKO liver.

Figure 3-2: Correlation of LXR binding, gene expression, and chromatin accessibility.

A. Comparison of the proportion of genes with LXR Liver ChIP-Seq and LXR Liver + T0901317 ChIP-Seq binding [297] among genes whose expression is downregulated, upregulated, and unchanged in LXRDKO liver. B. ATAC-Seq signal intensity across LXR (basal) binding sites in WT and LXRDKO samples. Average signal profile is plotted on top. C. Average change in LXR binding site accessibility for peaks proximal to genes whose expression is downregulated, upregulated or unchanged in LXRDKO liver in comparison to WT. D. Example of ATAC-Seq signal on LXR binding sites in the alternative first exon (left) and promoter (right)

of the *Srebf1* locus. Peaks that on average lost accessibility for at least 10 RPKM in LXRDKO compared to WT are indicated with red arrows. Publicly available LXR Liver ChIP-Seq data are aligned alongside the ATAC-Seq tracks [297].

Figure 3-3: Loss of LXR affects chromatin accessibility at other transcription factor binding sites.

A. Heatmap of motif accessibility across all ATAC-Seq peaks ranked and binned based on the accessibility difference between LXRDKO and WT samples. Shown are 73 bins each containing approximately 1000 peaks. The heatmaps represent the enrichment p-value obtained after known motif analysis. Transcription factors are grouped based on motif similarity (>90%). Only motifs that were enriched in peaks that lost accessibility in LXRDKO liver are shown. B. ATAC-Seq signal intensity heatmap and profiles across peaks associated with CTCF (left), and FoxA2 (right) motifs, among the top 1000 peaks losing accessibility in LXRDKO livers. C. Browser view of *Insig2* locus showing WT and LXRDKO ATAC-Seq normalized signal alongside LXR ChIP-Seq data [297]. Below the reference gene are ChIP-Atlas tracks presenting aggregate liver ChIP-Seq data for selected transcription factors [382].

Figure 3-4. Increased accessibility of NFY motifs in LXR-deficient liver.

A. Heatmap of motif accessibility across all ATAC-Seq peaks ranked and binned based on differences between LXRDKO and WT. Shown are 73 bins each containing approximately 1000 peaks. The heatmaps represents the enrichment p-value obtained after known motif analysis. Transcription factors are grouped based on motif similarity (>90%). Only motifs that were enriched in peaks that gained accessibility in LXRDKO liver are shown. B. Heatmaps of motif enrichment of selected overrepresented transcription factors across binned intergenic, intronic

and promoter ATAC-Seq peaks based on change in accessibility. C. Footprint of the NFYA motif in WT and LXRDKO ATAC-Seq samples using HINT-ATAC. D. ATAC-Seq signal intensity heatmap and profile of peaks with NFY motif among the top 1000 peaks with the largest gains of accessibility. E Within top 1000 peaks that gained accessibility in LXRDKO, proportion of genes with increased NFY motif accessibility that also have LXR binding. F. Browser view of peaks with increased NFY motif accessibility, including the promoter regions of *Hmcgr* (left) and *Got1* (right). Publicly available SREBP2 Liver ChIP-Seq and NFY motif locations are aligned below the gene annotation [383].

Figure 3-5: LXR can act as a ligand-dependent and -independent repressor.

A. Heatmap of normalized counts of differentially expressed genes with an LXR ChIP-Seq binding site. Unit variance scaling was used for scaling rows. Genes are arranged in according to their behavior in response to agonist treatment (combining publicly available GW3965 and T0901317 treatment results). Highlighted are selected genes in each segment. Top 3 results from known motif analysis for each segment are shown in the following order: 1) Upregulated in LXRDKO samples and downregulated by agonist, 2) Upregulated in LXRDKO and not changed by agonist, 3) Downregulated in LXRDKO and upregulated by agonist 4) Downregulated in LXRDKO and not changed by agonist. B. Example regions in which peaks with LXR binding motifs were on average less accessible in LXRDKO liver, for genes where LXR was acting as a repressor. Intergenic region associated with the Lurap1l gene (left) and intronic region associated with Slc25a15 (right). D. Independent validation of 14 ligand-repressed genes by qPCR assessment from livers of acute GW3965 treated mice (n=5-6).

SI Appendix Figure 3-S1: Transcriptional changes in LXR-deficient liver.

A. Differential expression analysis of the LXRDKO liver RNA-Seq results showed 246 upregulated and 321 downregulated genes. B. Volcano plot showing differential gene expression between WT and LXRDKO samples. Genes are color-coded based on their fold change and adjusted p value. C. Top 10 downregulated (left) and upregulated (right) genes from LXRDKO liver RNA-Seq based on adjusted p value.

SI Appendix Figure 3-S2: Expression profiles of LXRDKO livers.

A. Pathway enrichment results for downregulated (top) and upregulated (bottom) genes in LXRDKO liver. B. Transcription Factor ChIP-Seq enrichment analysis (ChEA) for downregulated genes in LXRDKO liver. Publicly available ChIP-Seq data were used to estimate enrichment of transcription factor binding in the promoters of genes downregulated in LXRDKO liver.

SI Appendix Figure 3-S3: Chromatin accessibility profiles of LXRDKO livers

A. Correlation heatmap of ATAC-Seq samples using all peaks. B. t-SNE plot of ATAC-Seq samples. C. Distribution of top 1000 peaks with largest loss and gain in LXRDKO liver based on relative distance to closest TSS. D. Average change in accessibility of peaks associated with differentially expressed genes in LXRDKO liver. E. Average change in accessibility in intronic (left), intergenic (right), and promoter (bottom) regions for all genes (All) and those whose expression was reduced (Down) or increased (Up) in LXRDKO livers. * comparison to all genes; # comparison between downregulated and upregulated genes.

SI Appendix Figure 3-S4: Pathway enrichment.

Pathway enrichment analysis of the top 1000 peaks that lost (top) and gained (bottom) accessibility.

SI Appendix Figure 3-S5: Changes to LXR binding sites in LXRDKO livers.

A. Proportion of LXR basal or agonist induced binding genes among genes differentially expressed in LXRDKO livers. B. Average number of (basal) LXR binding sites per gene for all LXR target genes and genes that are differentially expressed in LXRDKO liver. C. Changes in accessibility across LXR binding sites in LXRDKO liver compared to WT. D. Proportion of LXR binding sites within intergenic, intronic and promoter regions plotted as a function of the change in accessibility in LXRDKO liver.

SI Appendix Figure 3-S6: Loss of LXRs reduces motif accessibility of other transcription factors.

A. Heatmaps of motif enrichment of selected transcription factors from Figure 3-4A across binned intergenic, intronic and promoter ATAC-Seq peaks based on the change in accessibility. B. ATAC-Seq signal intensity heatmap and profile across peaks with PPARE motif, among the top 1000 peaks losing accessibility in LXRDKO livers. C. (Left) Hierarchical clustering heatmap for transcription factor motif co-occurrence among the least accessible 10 bins from Figure 3-4A. Eachcolumn represents a peak and red indicates presence of the corresponding motif in that peak. (Right) Hierarchical clustering heatmap for transcription factor motif co-occurrence among LXR binding genes that are associated with the least accessible 10 bins in LXRDKO livers. Each column represents a gene and red indicates presence of the corresponding motif in the peaks associated with the same gene. D. Normalized counts for the expression of transcription factors identified in Figure 3-4A. (* is used to indicate the FDR < 0.05)

SI Appendix Figure 3-S7: Impact of the loss of LXR on other transcription factor motif activity.

Footprint profile of HNF6 (A) and HNF1B (B) using the ATAC-Seq samples for LXRDKO and WT with merged replicates. C. Pathway enrichment analysis of genes associated with increased accessibility of the NFY motif (top 10 bin from Figure 3-5A). D. Volcano plot of the expression profile of genes with NFY motif containing peaks within the top 10 bins that gain accessibility (from Figure 3-5A).

SI Appendix Figure 3-S8: Change in accessibility and genomic features at the LXR binding sites in relation to different modes of LXR action.

A. Proportions of genomic annotations for LXR binding peaks that are associated with genes that are differentially upregulated or downregulated in LXRDKO and either downregulated, upregulated or not changing in response to either GW3965 and T0901317 treatment are plotted. B. Pathway enrichment analysis of genes that were downregulated in LXRDKO and have an LXR ChIP-Seq peak but did not change in expression in response to agonist treatment. C. LXR ChIP-Seq (basal) sites are segregated based on their genomic feature and ranked and binned based on their change in accessibility in LXRDKO livers. Motif analysis was performed for each of the bins across the accessibility and genomic features. Similar motifs were combined (>.90 Similarity) and motif with low enrichment were not displayed. Transcription factor motifs enriched in the LXR binding intergenic (left), intron (middle) and promoter (right) regions are displayed. D. Signal intensity heatmap and profiles of ATAC peaks at LXR binding sites proximal to ligand-dependent repressed genes.

Chapter 4 : Conclusions

Hepatic metabolism is flexible and responds to changes in nutrient availability. Levels of lipids, glucose, amino acids and other metabolites in the liver are regulated in an interdependent flux. Transcriptional networks coordinate many of these responses. Recent tools using high-throughput sequencing have revealed not only changes in global expression patterns, but also the regulatory changes in the genome that lead to the changes in expression. Multiomic approaches that can integrate these and other modes of profiling, have enhanced our understanding of the inner dynamics of metabolic tissues. The studies discussed in this dissertation used the power of multiomics to reveal new nodes in the hepatic lipid metabolism network.

In Chapter 2 of the thesis, I profiled chromatin accessibility via ATAC-Seq in liver as a strategy to identify transcriptional regulators that were previously not known to be involved in particular physiological processes. Integrating ATAC-Seq, RNA-Seq, and ChIP data revealed that GATA4 is activated by feeding. Feeding-specific targets of GATA4 contribute to fatty acid, phospholipid, ceramide and glucose metabolism. These processes are derailed in liver of Gata4LKO mice in the fed state.

Loss of GATA4 led to a decrease in plasma HDL cholesterol and the accumulation of liver triglycerides, factors relevant to the pathogenesis of atherosclerosis and fatty liver disease, respectively. The gene expression signature in Gata4LKO livers suggested a reduction in cholesterol efflux and triglyceride hydrolysis, and an upregulation of lipid uptake as potential contributors to these phenotypes. However, future studies are needed to verify these mechanisms.

Our studies further uncovered widespread collaboration between LXR and GATA4. GATA4 colocalized with LXR in the genome, especially on genes involved in cholesterol efflux.

Loss of GATA4 expression from mouse liver impeded LXR activity. It remains possible that GATA4 may collaborate with additional transcription factors in the regulation of its other targets.

In chapter 3 of the thesis, I used ATAC-Seq and RNA-Seq experiments to reveal that loss of LXR impacts the hepatic transcriptional landscape broadly. Loss of LXRs in liver resulted in reduced expression of classical LXR targets and PPARa targets in fatty acid metabolism pathways and had increased expression of genes involved with amino acid metabolism and DNA repair pathways. Chromatin regions in losing accessibility in LXRDKO livers enriched for intergenic regions. In contrast, those that are gaining accessibility disproportionately enriched for promoters, indicating a shift from enhancer to promoter control. Moreover, while binding sites for many transcription factors in enhancers including nuclear receptors, CTCF and FOXA lost accessibility and activity, those in promoters such as NFY gained them. Loss of LXR activity impacted the activity of a broad set of prominent liver transcription factor families.

Integrating data from our LXRα/β knockout model with data from wild-type mice treated with LXR agonist revealed different modes of LXR action. Basal versus agonist-driven LXRs largely induced a different set of genes. Presence of LXR is needed for SREBP1c and PPARα target gene expression. However, activation of LXR only induces SREBP1c targets but not PPARα targets. Agonist treatment also induces cholesterol transport genes, while they are unaffected in basal loss of LXRs. In addition, this analysis revealed that LXRs can also function as repressors on certain genes not involved in lipid metabolism.

Briefly, the contribution of LXR to chromatin landscape exceeded its canonical roles in lipid metabolism. LXRs support activity of other transcription factors by maintaining the

accessibility of enhancers. They suppress genes involved in amino acid metabolism and other processes.

In conclusion, these studies revealed a new role for GATA4 and expanded our understanding of LXRs in hepatic lipid metabolism. Additionally, they highlighted the importance of interplay between transcription factors in regulation of gene expression.

References

1. Trefts, E., Gannon, M. & Wasserman, D. H. The liver. *Curr Biol* **27**, R1147–R1151 (2017).
2. Sutherland, E. W. & Cori, C. F. EFFECT OF HYPERGLYCEMIC-GLYCOGENOLYTIC FACTOR AND EPINEPHRINE ON LIVER PHOSPHORYLASE. *Journal of Biological Chemistry* **188**, 531–543 (1951).
3. Fine, M. B. & Williams, R. H. Effect of fasting, epinephrine and glucose and insulin on hepatic uptake of nonesterified fatty acids. *American Journal of Physiology-Legacy Content* **199**, 403–406 (1960).
4. Berg, J. M., Tymoczko, J. L. & Stryer, L. Food Intake and Starvation Induce Metabolic Changes. *Biochemistry. 5th edition* (2002).
5. Rui, L. Energy Metabolism in the Liver. in *Comprehensive Physiology* 177–197 (American Cancer Society, 2014). doi:10.1002/cphy.c130024.
6. Alves-Bezerra, M. & Cohen, D. E. Triglyceride metabolism in the liver. *Compr Physiol* **8**, 1–8 (2017).
7. Kersten, S. *et al.* Peroxisome proliferator–activated receptor α mediates the adaptive response to fasting. *J Clin Invest* **103**, 1489–1498 (1999).
8. Leone, T. C., Weinheimer, C. J. & Kelly, D. P. A critical role for the peroxisome proliferator-activated receptor α (PPARα) in the cellular fasting response: The PPARα-null mouse as a model of fatty acid oxidation disorders. *PNAS* **96**, 7473–7478 (1999).
9. Cheon, Y. *et al.* Induction of overlapping genes by fasting and a peroxisome proliferator in pigs: evidence of functional PPARα in nonproliferating species. *American Journal of Physiology-Regulatory, Integrative and Comparative Physiology* **288**, R1525–R1535 (2005).
10. Lee, G. Y., Kim, N. H., Zhao, Z.-S., Cha, B. S. & Kim, Y. S. Peroxisomal-proliferator-activated receptor alpha activates transcription of the rat hepatic malonyl-CoA decarboxylase gene: a key regulation of malonyl-CoA level. *Biochem J* **378**, 983–990 (2004).

11. Régnier, M. *et al.* Insights into the role of hepatocyte PPARα activity in response to fasting. *Molecular and Cellular Endocrinology* **471**, 75–88 (2018).

12. Potthoff, M. J. *et al.* FGF21 induces PGC-1α and regulates carbohydrate and fatty acid metabolism during the adaptive starvation response. *PNAS* **106**, 10853–10858 (2009).

13. Rhee, J. *et al.* Regulation of hepatic fasting response by PPARγ coactivator-1α (PGC-1): Requirement for hepatocyte nuclear factor 4α in gluconeogenesis. *PNAS* **100**, 4012–4017 (2003).

14. Keller, H. *et al.* Fatty acids and retinoids control lipid metabolism through activation of peroxisome proliferator-activated receptor-retinoid X receptor heterodimers. *PNAS* **90**, 2160–2164 (1993).

15. Kliewer, S. A. *et al.* Fatty acids and eicosanoids regulate gene expression through direct interactions with peroxisome proliferator-activated receptors α and γ. *PNAS* **94**, 4318–4323 (1997).

16. Forman, B. M., Chen, J. & Evans, R. M. Hypolipidemic drugs, polyunsaturated fatty acids, and eicosanoids are ligands for peroxisome proliferator-activated receptors α and δ. *PNAS* **94**, 4312–4317 (1997).

17. Montagner, A. *et al.* Liver PPARα is crucial for whole-body fatty acid homeostasis and is protective against NAFLD. *Gut* **65**, 1202–1214 (2016).

18. Sanderson, L. M., Boekschoten, M. V., Desvergne, B., Müller, M. & Kersten, S. Transcriptional profiling reveals divergent roles of PPARα and PPARβ/δ in regulation of gene expression in mouse liver. *Physiological Genomics* **41**, 42–52 (2009).

19. Chakravarthy, M. V. *et al.* "New" hepatic fat activates PPARα to maintain glucose, lipid, and cholesterol homeostasis. *Cell Metabolism* **1**, 309–322 (2005).

20. Ong, K. T., Mashek, M. T., Bu, S. Y., Greenberg, A. S. & Mashek, D. G. Adipose triglyceride lipase is a major hepatic lipase that regulates triacylglycerol turnover and fatty acid signaling and partitioning. *Hepatology* **53**, 116–126 (2011).

21. Longuet, C. *et al.* The Glucagon Receptor Is Required for the Adaptive Metabolic Response to Fasting. *Cell Metabolism* **8**, 359–371 (2008).

22. Purushotham, A. *et al.* Hepatocyte-Specific Deletion of SIRT1 Alters Fatty Acid Metabolism and Results in Hepatic Steatosis and Inflammation. *Cell Metabolism* **9**, 327–338 (2009).

23. Vega, R. B., Huss, J. M. & Kelly, D. P. The Coactivator PGC-1 Cooperates with Peroxisome Proliferator-Activated Receptor α in Transcriptional Control of Nuclear Genes Encoding Mitochondrial Fatty Acid Oxidation Enzymes. *Molecular and Cellular Biology* **20**, 1868–1876 (2000).

24. Goldstein, I. *et al.* Transcription factor assisted loading and enhancer dynamics dictate the hepatic fasting response. *Genome Res.* **27**, 427–439 (2017).

25. Sengupta, S., Peterson, T. R., Laplante, M., Oh, S. & Sabatini, D. M. mTORC1 controls fasting-induced ketogenesis and its modulation by ageing. *Nature* **468**, 1100–1104 (2010).

26. Rommelaere, S. *et al.* Sox17 Regulates Liver Lipid Metabolism and Adaptation to Fasting. *PLOS ONE* **9**, e104925 (2014).

27. Lopez-Guadamillas, E. *et al.* p21 Cip1 plays a critical role in the physiological adaptation to fasting through activation of PPARα. *Scientific Reports* **6**, 34542 (2016).

28. Guan, G., Dai, P. H., Osborne, T. F., Kim, J. B. & Shechter, I. Multiple sequence elements are involved in the transcriptional regulation of the human squalene synthase gene. *J Biol Chem* **272**, 10295–10302 (1997).

29. Brown, M. S. & Goldstein, J. L. A proteolytic pathway that controls the cholesterol content of membranes, cells, and blood. *PNAS* **96**, 11041–11048 (1999).

30. Matsuzaka, T. *et al.* Cloning and characterization of a mammalian fatty acyl-CoA elongase as a lipogenic enzyme regulated by SREBPs. *J. Lipid Res.* **43**, 911–920 (2002).

31. Shimano, H. *et al.* Sterol Regulatory Element-binding Protein-1 as a Key Transcription Factor for Nutritional Induction of Lipogenic Enzyme Genes. *J. Biol. Chem.* **274**, 35832–35839 (1999).

32. Huang, Y. *et al.* A feed-forward loop amplifies nutritional regulation of PNPLA3. *PNAS* **107**, 7892–7897 (2010).

33. Liang, G. *et al.* Diminished hepatic response to fasting/refeeding and liver X receptor agonists in mice with selective deficiency of sterol regulatory element-binding protein-1c. *J. Biol. Chem.* **277**, 9520–9528 (2002).

34. Horton, J. D., Bashmakov, Y., Shimomura, I. & Shimano, H. Regulation of sterol regulatory element binding proteins in livers of fasted and refed mice. *PNAS* **95**, 5987–5992 (1998).

35. Foretz, M. *et al.* ADD1/SREBP-1c Is Required in the Activation of Hepatic Lipogenic Gene Expression by Glucose. *Molecular and Cellular Biology* **19**, 3760–3768 (1999).

36. Matsuda, M. *et al.* SREBP cleavage-activating protein (SCAP) is required for increased lipid synthesis in liver induced by cholesterol deprivation and insulin elevation. *Genes Dev.* **15**, 1206–1216 (2001).

37. Yamamoto, T. *et al.* Protein kinase Cbeta mediates hepatic induction of sterol-regulatory element binding protein-1c by insulin. *J. Lipid Res.* **51**, 1859–1870 (2010).

38. Matsumoto, M. *et al.* PKCλ in liver mediates insulin-induced SREBP-1c expression and determines both hepatic lipid content and overall insulin sensitivity. *J Clin Invest* **112**, 935–944 (2003).

39. Chen, G., Liang, G., Ou, J., Goldstein, J. L. & Brown, M. S. Central role for liver X receptor in insulin-mediated activation of Srebp-1c transcription and stimulation of fatty acid synthesis in liver. *PNAS* **101**, 11245–11250 (2004).

40. Tian, J., Goldstein, J. L. & Brown, M. S. Insulin induction of SREBP-1c in rodent liver requires LXRα-C/EBPβ complex. *PNAS* **113**, 8182–8187 (2016).

41. Berthier, A. *et al.* Combinatorial regulation of hepatic cytoplasmic signaling and nuclear transcriptional events by the OGT/REV-ERBα complex. *PNAS* **115**, E11033–E11042 (2018).

42. Amemiya-Kudo, M. *et al.* Promoter Analysis of the Mouse Sterol Regulatory Element-binding Protein-1c Gene. *J. Biol. Chem.* **275**, 31078–31085 (2000).

43. Yellaturu, C. R. *et al.* Insulin Enhances Post-translational Processing of Nascent SREBP-1c by Promoting Its Phosphorylation and Association with COPII Vesicles. *J. Biol. Chem.* **284**, 7518–7532 (2009).

44. Owen, J. L. *et al.* Insulin stimulation of SREBP-1c processing in transgenic rat hepatocytes requires p70 S6-kinase. *Proc. Natl. Acad. Sci. U.S.A.* **109**, 16184–16189 (2012).

45. Lu, M. & Shyy, J. Y.-J. Sterol regulatory element-binding protein 1 is negatively modulated by PKA phosphorylation. *Am. J. Physiol., Cell Physiol.* **290**, C1477-1486 (2006).

46. Ponugoti, B. *et al.* SIRT1 deacetylates and inhibits SREBP-1C activity in regulation of hepatic lipid metabolism. *J. Biol. Chem.* **285**, 33959–33970 (2010).

47. Tong, X. *et al.* E4BP4 is an insulin-induced stabilizer of nuclear SREBP-1c and promotes SREBP-1c-mediated lipogenesis. *J. Lipid Res.* **57**, 1219–1230 (2016).

48. Yabe, D., Komuro, R., Liang, G., Goldstein, J. L. & Brown, M. S. Liver-specific mRNA for Insig-2 down-regulated by insulin: Implications for fatty acid synthesis. *PNAS* **100**, 3155–3160 (2003).

49. Yahagi, N. *et al.* A crucial role of sterol regulatory element-binding protein-1 in the regulation of lipogenic gene expression by polyunsaturated fatty acids. *J. Biol. Chem.* **274**, 35840–35844 (1999).

50. Xu, J., Teran-Garcia, M., Park, J. H., Nakamura, M. T. & Clarke, S. D. Polyunsaturated fatty acids suppress hepatic sterol regulatory element-binding protein-1 expression by accelerating transcript decay. *J. Biol. Chem.* **276**, 9800–9807 (2001).

51. Kim, C.-W. *et al.* Acetyl CoA Carboxylase Inhibition Reduces Hepatic Steatosis but Elevates Plasma Triglycerides in Mice and Humans: A Bedside to Bench Investigation. *Cell Metabolism* **26**, 394-406.e6 (2017).

52. Rong, X. *et al.* ER phospholipid composition modulates lipogenesis during feeding and in obesity. *J Clin Invest* **127**, 3640–3651 (2017).

53. Janowski, B. A. *et al.* Structural requirements of ligands for the oxysterol liver X receptors LXRα and LXRβ. *Proc Natl Acad Sci U S A* **96**, 266–271 (1999).

54. Repa, J. J. *et al.* Regulation of mouse sterol regulatory element-binding protein-1c gene (SREBP-1c) by oxysterol receptors, LXRα and LXRβ. *Genes Dev.* **14**, 2819–2830 (2000).

55. Anthonisen, E. H. *et al.* Nuclear Receptor Liver X Receptor Is O-GlcNAc-modified in Response to Glucose. *J. Biol. Chem.* **285**, 1607–1615 (2010).

56. Beaven, S. W. *et al.* Reciprocal regulation of hepatic and adipose lipogenesis by liver X receptors in obesity and insulin resistance. *Cell Metab* **18**, 106–117 (2013).

57. Wong, R. H. F. *et al.* USF functions as a molecular switch during fasting/feeding to regulate lipogenesis. The role of DNA-PK. *Cell* **136**, 1056–1072 (2009).

58. Griffin, M. J., Wong, R. H. F., Pandya, N. & Sul, H. S. Direct Interaction between USF and SREBP-1c Mediates Synergistic Activation of the Fatty-acid Synthase Promoter. *J. Biol. Chem.* **282**, 5453–5467 (2007).

59. Jerkins, A. A., Liu, W. R., Lee, S. & Sul, H. S. Characterization of the Murine Mitochondrial Glycerol-3-phosphate Acyltransferase Promoter. *J. Biol. Chem.* **270**, 1416–1421 (1995).

60. Stoeckman, A. K., Ma, L. & Towle, H. C. Mlx Is the Functional Heteromeric Partner of the Carbohydrate Response Element-binding Protein in Glucose Regulation of Lipogenic Enzyme Genes. *J. Biol. Chem.* **279**, 15662–15669 (2004).

61. Iizuka, K., Bruick, R. K., Liang, G., Horton, J. D. & Uyeda, K. Deficiency of carbohydrate response element-binding protein (ChREBP) reduces lipogenesis as well as glycolysis. *PNAS* **101**, 7281–7286 (2004).

62. Adamson, A. W. *et al.* Hepatocyte nuclear factor-4α contributes to carbohydrate-induced transcriptional activation of hepatic fatty acid synthase. *Biochem J* **399**, 285–295 (2006).

63. Linden, A. G. *et al.* Interplay between ChREBP and SREBP-1c coordinates postprandial glycolysis and lipogenesis in livers of mice. *J. Lipid Res.* **59**, 475–487 (2018).

64. Iizuka, K. Recent progress on the role of ChREBP in glucose and lipid metabolism [Review]. *Endocrine Journal* **60**, 543–555 (2013).

65. Fan, Q. *et al.* LXRα Regulates Hepatic ChREBPα Activity and Lipogenesis upon Glucose, but Not Fructose Feeding in Mice. *Nutrients* **9**, 678 (2017).

66. Kawaguchi, T., Osatomi, K., Yamashita, H., Kabashima, T. & Uyeda, K. Mechanism for fatty acid 'sparing' effect on glucose-induced transcription: regulation of carbohydrate-responsive element-binding protein by AMP-activated protein kinase. *J. Biol. Chem.* **277**, 3829–3835 (2002).

67. Kawaguchi, T., Takenoshita, M., Kabashima, T. & Uyeda, K. Glucose and cAMP regulate the L-type pyruvate kinase gene by phosphorylation/dephosphorylation of the carbohydrate response element binding protein. *Proc. Natl. Acad. Sci. U.S.A.* **98**, 13710–13715 (2001).

68. Kabashima, T., Kawaguchi, T., Wadzinski, B. E. & Uyeda, K. Xylulose 5-phosphate mediates glucose-induced lipogenesis by xylulose 5-phosphate-activated protein phosphatase in rat liver. *Proc. Natl. Acad. Sci. U.S.A.* **100**, 5107–5112 (2003).

69. Guinez, C. *et al.* O-GlcNAcylation Increases ChREBP Protein Content and Transcriptional Activity in the Liver. *Diabetes* **60**, 1399–1413 (2011).

70. Sakiyama, H. *et al.* The role of O-linked GlcNAc modification on the glucose response of ChREBP. *Biochemical and Biophysical Research Communications* **402**, 784–789 (2010).

71. Tao, R., Xiong, X., DePinho, R. A., Deng, C.-X. & Dong, X. C. Hepatic SREBP-2 and cholesterol biosynthesis are regulated by FoxO3 and Sirt6. *J Lipid Res* **54**, 2745–2753 (2013).

72. Seyer, P. *et al.* Hepatic glucose sensing is required to preserve β cell glucose competence. *J Clin Invest* **123**, 1662–1676 (2013).

73. Lu, X.-Y. *et al.* Feeding induces cholesterol biosynthesis via the mTORC1–USP20–HMGCR axis. *Nature* **588**, 479–484 (2020).

74. Zhang, M., Sun, W., Qian, J. & Tang, Y. Fasting exacerbates hepatic growth differentiation factor 15 to promote fatty acid β-oxidation and ketogenesis via activating XBP1 signaling in liver. *Redox Biology* **16**, 87–96 (2018).

75. Pfaffenbach, K. T. *et al.* Rapamycin Inhibits Postprandial-Mediated X-Box-Binding Protein-1 Splicing in Rat Liver. *The Journal of Nutrition* **140**, 879–884 (2010).

76. Liu, J. S., Park, E. A., Gurney, A. L., Roesler, W. J. & Hanson, R. W. Cyclic AMP induction of phosphoenolpyruvate carboxykinase (GTP) gene transcription is mediated by multiple promoter elements. *J. Biol. Chem.* **266**, 19095–19102 (1991).

77. Quinn, P. G. & Granner, D. K. Cyclic AMP-dependent protein kinase regulates transcription of the phosphoenolpyruvate carboxykinase gene but not binding of nuclear factors to the cyclic AMP regulatory element. *Molecular and Cellular Biology* **10**, 3357–3364 (1990).

78. Herzig, S. *et al.* CREB regulates hepatic gluconeogenesis through the coactivator PGC-1. *Nature* **413**, 179–183 (2001).

79. Lee, M.-W. *et al.* Regulation of Hepatic Gluconeogenesis by an ER-Bound Transcription Factor, CREBH. *Cell Metabolism* **11**, 331–339 (2010).

80. Pei, L. *et al.* NR4A orphan nuclear receptors are transcriptional regulators of hepatic glucose metabolism. *Nature Medicine* **12**, 1048–1055 (2006).

81. Seok, S. *et al.* Transcriptional regulation of autophagy by an FXR–CREB axis. *Nature* **516**, 108–111 (2014).

82. Lu, Y. *et al.* Yin Yang 1 Promotes Hepatic Gluconeogenesis Through Upregulation of Glucocorticoid Receptor. *Diabetes* **62**, 1064–1073 (2013).

83. Altarejos, J. Y. & Montminy, M. CREB and the CRTC co-activators: sensors for hormonal and metabolic signals. *Nature Reviews Molecular Cell Biology* **12**, 141–151 (2011).

84. Liu, Y. *et al.* A fasting inducible switch modulates gluconeogenesis via activator/coactivator exchange. *Nature* **456**, 269–273 (2008).

85. Koo, S.-H. *et al.* The CREB coactivator TORC2 is a key regulator of fasting glucose metabolism. *Nature* **437**, 1109–1114 (2005).

86. He, L. *et al.* Metformin and insulin suppress hepatic gluconeogenesis through phosphorylation of CREB binding protein. *Cell* **137**, 635–646 (2009).

87. Dentin, R. *et al.* Insulin modulates gluconeogenesis by inhibition of the coactivator TORC2. *Nature* **449**, 366–369 (2007).

88. Wang, Y., Vera, L., Fischer, W. H. & Montminy, M. The CREB coactivator CRTC2 links hepatic ER stress and fasting gluconeogenesis. *Nature* **460**, 534–537 (2009).

89. Haeusler, R. A., Kaestner, K. H. & Accili, D. FoxOs Function Synergistically to Promote Glucose Production. *J Biol Chem* **285**, 35245–35248 (2010).

90. Wu, Z. *et al.* MAPK phosphatase–3 promotes hepatic gluconeogenesis through dephosphorylation of forkhead box O1 in mice. *J Clin Invest* **120**, 3901–3911 (2010).

91. Nakae, J., Park, B.-C. & Accili, D. Insulin Stimulates Phosphorylation of the Forkhead Transcription Factor FKHR on Serine 253 through a Wortmannin-sensitive Pathway. *J. Biol. Chem.* **274**, 15982–15985 (1999).

92. Dong, X. C. *et al.* Inactivation of Hepatic Foxo1 by Insulin Signaling Is Required for Adaptive Nutrient Homeostasis and Endocrine Growth Regulation. *Cell Metabolism* **8**, 65–76 (2008).

93. Matsuzaki, H. *et al.* Acetylation of Foxo1 alters its DNA-binding ability and sensitivity to phosphorylation. *PNAS* **102**, 11278–11283 (2005).

94. Frescas, D., Valenti, L. & Accili, D. Nuclear Trapping of the Forkhead Transcription Factor FoxO1 via Sirt-dependent Deacetylation Promotes Expression of Glucogenetic Genes. *J. Biol. Chem.* **280**, 20589–20595 (2005).

95. Mihaylova, M. M. *et al.* Class IIa Histone Deacetylases Are Hormone-Activated Regulators of FOXO and Mammalian Glucose Homeostasis. *Cell* **145**, 607–621 (2011).

96. Choi, W.-I. *et al.* Zbtb7c is a critical gluconeogenic transcription factor that induces glucose-6-phosphatase and phosphoenylpyruvate carboxykinase 1 genes expression during mice fasting. *Biochim Biophys Acta Gene Regul Mech* **1862**, 643–656 (2019).

97. Zhang, W. *et al.* FoxO1 Regulates Multiple Metabolic Pathways in the Liver: *EFFECTS ON GLUCONEOGENIC, GLYCOLYTIC, AND LIPOGENIC GENE EXPRESSION*. *J. Biol. Chem.* **281**, 10105–10117 (2006).

98. Matsumoto, M., Pocai, A., Rossetti, L., DePinho, R. A. & Accili, D. Impaired Regulation of Hepatic Glucose Production in Mice Lacking the Forkhead Transcription Factor Foxo1 in Liver. *Cell Metabolism* **6**, 208–216 (2007).

99. Puigserver, P. *et al.* Insulin-regulated hepatic gluconeogenesis through FOXO1–PGC-1α interaction. *Nature* **423**, 550–555 (2003).

100. Kim, D. H. *et al.* FoxO6 Integrates Insulin Signaling With Gluconeogenesis in the Liver. *Diabetes* **60**, 2763–2774 (2011).

101. Liu, H. *et al.* Wnt Signaling Regulates Hepatic Metabolism. *Sci. Signal.* **4**, ra6–ra6 (2011).

102. Oh, K.-J. *et al.* TCF7L2 Modulates Glucose Homeostasis by Regulating CREB- and FoxO1-Dependent Transcriptional Pathway in the Liver. *PLOS Genetics* **8**, e1002986 (2012).

103. Wei, D., Tao, R., Zhang, Y., White, M. F. & Dong, X. C. Feedback regulation of hepatic gluconeogenesis through modulation of SHP/Nr0b2 gene expression by Sirt1 and FoxO1. *American Journal of Physiology-Endocrinology and Metabolism* **300**, E312–E320 (2010).

104. Hirota, K. *et al.* A Combination of HNF-4 and Foxo1 Is Required for Reciprocal Transcriptional Regulation of Glucokinase and Glucose-6-phosphatase Genes in Response to Fasting and Feeding. *J. Biol. Chem.* **283**, 32432–32441 (2008).

105. Yoon, J. C. *et al.* Control of hepatic gluconeogenesis through the transcriptional coactivator PGC-1. *Nature* **413**, 131–138 (2001).

106. Estall, J. L. *et al.* PGC-1α negatively regulates hepatic FGF21 expression by modulating the heme/Rev-Erbα axis. *PNAS* **106**, 22510–22515 (2009).

107. Lustig, Y. *et al.* Separation of the gluconeogenic and mitochondrial functions of PGC-1α through S6 kinase. *Genes & Development* **25**, 1232 (2011).

108. Li, X., Monks, B., Ge, Q. & Birnbaum, M. J. Akt/PKB regulates hepatic metabolism by directly inhibiting PGC-1α transcription coactivator. *Nature* **447**, 1012–1016 (2007).

109. Lerin, C. *et al.* GCN5 acetyltransferase complex controls glucose metabolism through transcriptional repression of PGC-1α. *Cell Metabolism* **3**, 429–438 (2006).

110. Rodgers, J. T. *et al.* Nutrient control of glucose homeostasis through a complex of PGC-1α and SIRT1. *Nature* **434**, 113–118 (2005).

111. Burgess, S. C. *et al.* Diminished Hepatic Gluconeogenesis via Defects in Tricarboxylic Acid Cycle Flux in Peroxisome Proliferator-activated Receptor γ Coactivator-1α (PGC-1α)-deficient Mice. *J. Biol. Chem.* **281**, 19000–19008 (2006).

112. Estall, J. L. *et al.* Sensitivity of Lipid Metabolism and Insulin Signaling to Genetic Alterations in Hepatic Peroxisome Proliferator–Activated Receptor-γ Coactivator-1α Expression. *Diabetes* **58**, 1499–1508 (2009).

113. Morris, E. M. *et al.* PGC-1α overexpression results in increased hepatic fatty acid oxidation with reduced triacylglycerol accumulation and secretion. *American Journal of Physiology-Gastrointestinal and Liver Physiology* **303**, G979–G992 (2012).

114. Liang, H. *et al.* Whole body overexpression of PGC-1alpha has opposite effects on hepatic and muscle insulin sensitivity. *Am J Physiol Endocrinol Metab* **296**, E945-954 (2009).

115. Besse-Patin, A. *et al.* PGC1A regulates the IRS1:IRS2 ratio during fasting to influence hepatic metabolism downstream of insulin. *PNAS* **116**, 4285–4290 (2019).

116. Koo, S.-H. *et al.* PGC-1 promotes insulin resistance in liver through PPAR-α-dependent induction of TRB-3. *Nature Medicine* **10**, 530–534 (2004).

117. Leone, T. C. *et al.* PGC-1α Deficiency Causes Multi-System Energy Metabolic Derangements: Muscle Dysfunction, Abnormal Weight Control and Hepatic Steatosis. *PLOS Biology* **3**, e101 (2005).

118. Lee, J.-M. *et al.* Insulin-Inducible SMILE Inhibits Hepatic Gluconeogenesis. *Diabetes* **65**, 62–73 (2016).

119. Opherk, C. *et al.* Inactivation of the Glucocorticoid Receptor in Hepatocytes Leads to Fasting Hypoglycemia and Ameliorates Hyperglycemia in Streptozotocin-Induced Diabetes Mellitus. *Mol Endocrinol* **18**, 1346–1353 (2004).

120. McCallum, R. E., Seale, T. W. & Stith, R. D. Influence of endotoxin treatment on dexamethasone induction of hepatic phosphoenolpyruvate carboxykinase. *Infect Immun* **39**, 213–219 (1983).

121. Cassuto, H. *et al.* Glucocorticoids Regulate Transcription of the Gene for Phosphoenolpyruvate Carboxykinase in the Liver via an Extended Glucocorticoid Regulatory Unit. *J. Biol. Chem.* **280**, 33873–33884 (2005).

122. Zhang, W.-S. *et al.* Inactivation of NF-κB2 (p52) restrains hepatic glucagon response via preserving PDE4B induction. *Nature Communications* **10**, 4303 (2019).

123. Zhang, Y. *et al.* Regulation of hepatic gluconeogenesis by nuclear factor Y transcription factor in mice. *J. Biol. Chem.* **293**, 7894–7904 (2018).

124. Ploton, M. *et al.* The nuclear bile acid receptor FXR is a PKA- and FOXA2-sensitive activator of fasting hepatic gluconeogenesis. *Journal of Hepatology* **69**, 1099–1109 (2018).

125. Massafra, V. & van Mil, S. W. C. Farnesoid X receptor: A "homeostat" for hepatic nutrient metabolism. *Biochimica et Biophysica Acta (BBA) - Molecular Basis of Disease* **1864**, 45–59 (2018).

126. Kersten, S. Integrated physiology and systems biology of PPARα. *Molecular Metabolism* **3**, 354–371 (2014).

127. Bandsma, R. H. J. *et al.* Hepatic de Novo Synthesis of Glucose 6-Phosphate Is Not Affected in Peroxisome Proliferator-activated Receptor α-Deficient Mice but Is Preferentially Directed toward Hepatic Glycogen Stores after a Short Term Fast. *J. Biol. Chem.* **279**, 8930–8937 (2004).

128. Rufo, C. *et al.* Involvement of a Unique Carbohydrate-responsive Factor in the Glucose Regulation of Rat Liver Fatty-acid Synthase Gene Transcription. *J. Biol. Chem.* **276**, 21969–21975 (2001).

129. Stamatikos, A. D. *et al.* Tissue Specific Effects of Dietary Carbohydrates and Obesity on ChREBPα and ChREBPβ Expression. *Lipids* **51**, 95–104 (2016).

130. Zhou, Y. *et al.* Regulation of glucose homeostasis through a XBP-1–FoxO1 interaction. *Nature Medicine* **17**, 356–365 (2011).

131. Inoue, H. *et al.* Role of hepatic STAT3 in brain-insulin action on hepatic glucose production. *Cell Metabolism* **3**, 267–275 (2006).

132. Stanya, K. J. *et al.* Direct control of hepatic glucose production by interleukin-13 in mice. *J Clin Invest* **123**, 261–271 (2013).

133. Ramadoss, P., Unger-Smith, N. E., Lam, F. S. & Hollenberg, A. N. STAT3 Targets the Regulatory Regions of Gluconeogenic Genes in Vivo. *Mol Endocrinol* **23**, 827–837 (2009).

134. Nie, Y. *et al.* STAT3 inhibition of gluconeogenesis is downregulated by SirT1. *Nat Cell Biol* **11**, 492–500 (2009).

135. Ramakrishnan, S. K. *et al.* HIF2 α Is an Essential Molecular Brake for Postprandial Hepatic Glucagon Response Independent of Insulin Signaling. *Cell Metabolism* **23**, 505–516 (2016).

136. Scott, C. H. *et al.* Hepatic Aryl hydrocarbon Receptor Nuclear Translocator (ARNT) regulates metabolism in mice. *PLOS ONE* **12**, e0186543 (2017).

137. Oosterveer, M. H. *et al.* LRH-1–dependent glucose sensing determines intermediary metabolism in liver. *J Clin Invest* **122**, 2817–2826 (2012).

138. Brosnan, M. E. & Brosnan, J. T. Hepatic glutamate metabolism: a tale of 2 hepatocytes. *The American Journal of Clinical Nutrition* **90**, 857S-861S (2009).

139. Sokolović, M. *et al.* The transcriptomic signature of fasting murine liver. *BMC Genomics* **9**, 528 (2008).

140. Mosoni, L., Malmezat, T., Valluy, M. C., Houlier, M. L. & Mirand, P. P. Muscle and liver protein synthesis adapt efficiently to food deprivation and refeeding in 12-month-old rats. *J Nutr* **126**, 516–522 (1996).

141. Kimball, S. R. *et al.* Feeding stimulates protein synthesis in muscle and liver of neonatal pigs through an mTOR-dependent process. *Am J Physiol Endocrinol Metab* **279**, E1080-1087 (2000).

142. Louet, J.-F. *et al.* The Coactivator SRC-1 is an Essential Coordinator of Hepatic Glucose Production. *Cell Metab* **12**, 606–618 (2010).

143. Kimura, T. *et al.* Hypoglycemia-associated Hyperammonemia Caused by Impaired Expression of Ornithine Cycle Enzyme Genes in C/EBPα Knockout Mice. *J. Biol. Chem.* **273**, 27505–27510 (1998).

144. Prokesch, A. *et al.* Liver p53 is stabilized upon starvation and required for amino acid catabolism and gluconeogenesis. *The FASEB Journal* **31**, 732–742 (2016).

145. Teshigawara, K. *et al.* Role of Krüppel-like factor 15 in PEPCK gene expression in the liver. *Biochemical and Biophysical Research Communications* **327**, 920–926 (2005).

146. Gray, S. *et al.* Regulation of gluconeogenesis by Krüppel-like factor 15. *Cell Metab.* **5**, 305–312 (2007).

147. de Aguiar Vallim, T. Q. *et al.* MAFG Is a Transcriptional Repressor of Bile Acid Synthesis and Metabolism. *Cell Metabolism* **21**, 298–311 (2015).

148. Kong, B. *et al.* Mechanism of Tissue-specific Farnesoid X Receptor in Suppressing the Expression of Genes in Bile-acid Synthesis in Mice. *Hepatology* **56**, 1034–1043 (2012).

149. Duran-Sandoval, D. *et al.* The Farnesoid X Receptor Modulates Hepatic Carbohydrate Metabolism during the Fasting-Refeeding Transition. *J. Biol. Chem.* **280**, 29971–29979 (2005).

150. Claudel, T. *et al.* Farnesoid X receptor agonists suppress hepatic apolipoprotein CIII expression. *Gastroenterology* **125**, 544–555 (2003).

151. Watanabe, M. *et al.* Bile acids lower triglyceride levels via a pathway involving FXR, SHP, and SREBP-1c. *J Clin Invest* **113**, 1408–1418 (2004).

152. Vecchi, C. *et al.* Gluconeogenic Signals Regulate Iron Homeostasis via Hepcidin in Mice. *Gastroenterology* **146**, 1060-1069.e3 (2014).

153. Handschin, C. *et al.* Nutritional Regulation of Hepatic Heme Biosynthesis and Porphyria through PGC-1α. *Cell* **122**, 505–515 (2005).

154. Kallin, A. *et al.* SREBP-1 regulates the expression of heme oxygenase 1 and the phosphatidylinositol-3 kinase regulatory subunit p55γ. *J. Lipid Res.* **48**, 1628–1636 (2007).

155. Renaud, H. J., Cui, J. Y., Lu, H. & Klaassen, C. D. Effect of Diet on Expression of Genes Involved in Lipid Metabolism, Oxidative Stress, and Inflammation in Mouse Liver–Insights into Mechanisms of Hepatic Steatosis. *PLoS One* **9**, (2014).

156. Örd, T., Örd, D. & Örd, T. TRIB3 limits FGF21 induction during in vitro and in vivo nutrient deficiencies by inhibiting C/EBP–ATF response elements in the Fgf21 promoter. *Biochimica et Biophysica Acta (BBA) - Gene Regulatory Mechanisms* **1861**, 271–281 (2018).

157. Maruyama, R. *et al.* FGF21 Alleviates Hepatic Endoplasmic Reticulum Stress under Physiological Conditions. *Journal of Nutritional Science and Vitaminology* **64**, 200–208 (2018).

158. Scheffler, K. *et al.* 8-oxoguanine DNA glycosylase (Ogg1) controls hepatic gluconeogenesis. *DNA Repair* **61**, 56–62 (2018).

159. van der Vos, K. E. *et al.* Modulation of glutamine metabolism by the PI(3)K–PKB–FOXO network regulates autophagy. *Nature Cell Biology* **14**, 829–837 (2012).

160. Zhao, Y. *et al.* Cytosolic FoxO1 is essential for the induction of autophagy and tumour suppressor activity. *Nature Cell Biology* **12**, 665–675 (2010).

161. Robertson, D. G. *et al.* Metabolomic and Transcriptomic Changes Induced by Overnight (16 h) Fasting in Male and Female Sprague−Dawley Rats. *Chem. Res. Toxicol.* **24**, 481–487 (2011).

162. Morgan, K. T. *et al.* The Hepatic Transcriptome as a Window on Whole-Body Physiology and Pathophysiology. *Toxicol Pathol* **33**, 136–145 (2005).

163. Zhang, F., Xu, X., Zhou, B., He, Z. & Zhai, Q. Gene Expression Profile Change and Associated Physiological and Pathological Effects in Mouse Liver Induced by Fasting and Refeeding. *PLOS ONE* **6**, e27553 (2011).

164. Hakvoort, T. B. M. *et al.* Interorgan Coordination of the Murine Adaptive Response to Fasting. *J. Biol. Chem.* **286**, 16332–16343 (2011).

165. Geisler, C. E., Hepler, C., Higgins, M. R. & Renquist, B. J. Hepatic adaptations to maintain metabolic homeostasis in response to fasting and refeeding in mice. *Nutrition & Metabolism* **13**, 62 (2016).

166. Hellerstein, M. K. *et al.* Hepatic gluconeogenic fluxes and glycogen turnover during fasting in humans. A stable isotope study. *J Clin Invest* **100**, 1305–1319 (1997).

167. Chi, Y. *et al.* Regulation of gene expression during the fasting-feeding cycle of the liver displays mouse strain specificity. *J. Biol. Chem.* **295**, 4809–4821 (2020).

168. Schupp, M. *et al.* Metabolite and transcriptome analysis during fasting suggest a role for the p53-Ddit4 axis in major metabolic tissues. *BMC Genomics* **14**, 758 (2013).

169. Hui, S. *et al.* Glucose feeds the TCA cycle via circulating lactate. *Nature* **551**, 115–118 (2017).

170. Kinouchi, K. *et al.* Fasting Imparts a Switch to Alternative Daily Pathways in Liver and Muscle. *Cell Reports* **25**, 3299-3314.e6 (2018).

171. Rennert, C. *et al.* The Diurnal Timing of Starvation Differently Impacts Murine Hepatic Gene Expression and Lipid Metabolism – A Systems Biology Analysis Using Self-Organizing Maps. *Front. Physiol.* **9**, (2018).

172. Sano, T. *et al.* Selective control of up-regulated and down-regulated genes by temporal patterns and doses of insulin. *Sci. Signal.* **9**, ra112–ra112 (2016).

173. Li, S. *et al.* Genome-wide Coactivation Analysis of PGC-1α Identifies BAF60a as a Regulator of Hepatic Lipid Metabolism. *Cell Metabolism* **8**, 105–117 (2008).

174. Wang, Y. *et al.* Phosphorylation and Recruitment of BAF60c in Chromatin Remodeling for Lipogenesis in Response to Insulin. *Mol Cell* **49**, 283–297 (2013).

175. Bitterman, K. J., Anderson, R. M., Cohen, H. Y., Latorre-Esteves, M. & Sinclair, D. A. Inhibition of Silencing and Accelerated Aging by Nicotinamide, a Putative Negative Regulator of Yeast Sir2 and Human SIRT1. *J. Biol. Chem.* **277**, 45099–45107 (2002).

176. Noriega, L. G. *et al.* CREB and ChREBP oppositely regulate SIRT1 expression in response to energy availability. *EMBO reports* **12**, 1069–1076 (2011).

177. Gerhart-Hines, Z. *et al.* The cAMP/PKA Pathway Rapidly Activates SIRT1 to Promote Fatty Acid Oxidation Independently of Changes in NAD+. *Molecular Cell* **44**, 851–863 (2011).

178. Seok, S. *et al.* Fasting-induced JMJD3 histone demethylase epigenetically activates mitochondrial fatty acid **β**-oxidation. *J Clin Invest* **128**, 3144–3159 (2018).

179. Chattopadhyay, T. *et al.* Spatiotemporal gating of SIRT1 functions by O-GlcNAcylation is essential for liver metabolic switching and prevents hyperglycemia. *PNAS* **117**, 6890–6900 (2020).

180. Li, Y. *et al.* Hepatic overexpression of SIRT1 in mice attenuates endoplasmic reticulum stress and insulin resistance in the liver. *The FASEB Journal* **25**, 1664–1679 (2011).

181. Sakai, M. *et al.* The GCN5-CITED2-PKA signalling module controls hepatic glucose metabolism through a cAMP-induced substrate switch. *Nature Communications* **7**, 13147 (2016).

182. Sakai, M. *et al.* CITED2 links hormonal signaling to PGC-1α acetylation in the regulation of gluconeogenesis. *Nature Medicine* **18**, 612–617 (2012).

183. Da Li *et al.* Hepatic TET3 contributes to type-2 diabetes by inducing the HNF4α fetal isoform. *Nature Communications* **11**, 342 (2020).

184. Roqueta-Rivera, M. *et al.* SETDB2 Links Glucocorticoid to Lipid Metabolism through Insig2a Regulation. *Cell Metabolism* **24**, 474–484 (2016).

185. Maniyadath, B. *et al.* Loss of Hepatic Oscillatory Fed microRNAs Abrogates Refed Transition and Causes Liver Dysfunctions. *Cell Reports* **26**, 2212-2226.e7 (2019).

186. Batista, T. M. *et al.* Multi-dimensional Transcriptional Remodeling by Physiological Insulin In Vivo. *Cell Rep* **26**, 3429-3443.e3 (2019).

187. Zhang, N. *et al.* Elevated hepatic expression of H19 long noncoding RNA contributes to diabetic hyperglycemia. *JCI Insight* **3**, (2018).

188. Aguilo, F. *et al.* Deposition of 5-Methylcytosine on Enhancer RNAs Enables the Coactivator Function of PGC-1α. *Cell Reports* **14**, 479–492 (2016).

189. Everett, L. J. *et al.* Integrative genomic analysis of CREB defines a critical role for transcription factor networks in mediating the fed/fasted switch in liver. *BMC Genomics* **14**, 337 (2013).

190. He, L. *et al.* Transcriptional Co-activator p300 Maintains Basal Hepatic Gluconeogenesis. *J. Biol. Chem.* **287**, 32069–32077 (2012).

191. Shimizu, Y. I. *et al.* Fasting induced up-regulation of activating transcription factor 5 in mouse liver. *Life Sciences* **84**, 894–902 (2009).

192. He, L. *et al.* Activation of Basal Gluconeogenesis by Coactivator p300 Maintains Hepatic Glycogen Storage. *Mol Endocrinol* **27**, 1322–1332 (2013).

193. Caron, S. *et al.* Farnesoid X Receptor Inhibits the Transcriptional Activity of Carbohydrate Response Element Binding Protein in Human Hepatocytes. *Molecular and Cellular Biology* **33**, 2202–2211 (2013).

194. Bennett, M. K., Seo, Y.-K., Datta, S., Shin, D.-J. & Osborne, T. F. Selective Binding of Sterol Regulatory Element-binding Protein Isoforms and Co-regulatory Proteins to Promoters for Lipid Metabolic Genes in Liver. *J Biol Chem* **283**, 15628–15637 (2008).

195. Joseph, S. B. *et al.* Direct and Indirect Mechanisms for Regulation of Fatty Acid Synthase Gene Expression by Liver X Receptors. *J. Biol. Chem.* **277**, 11019–11025 (2002).

196. Talukdar, S. & Hillgartner, F. B. The mechanism mediating the activation of acetyl-coenzyme A carboxylase-α gene transcription by the liver X receptor agonist T0-901317. *J. Lipid Res.* **47**, 2451–2461 (2006).

197. Sommars, M. A. *et al.* Dynamic repression by BCL6 controls the genome-wide liver response to fasting and steatosis. *eLife* **8**, e43922 (2019).

198. Byun, S. *et al.* Fasting-induced FGF21 signaling activates hepatic autophagy and lipid degradation via JMJD3 histone demethylase. *Nature Communications* **11**, 807 (2020).

199. Lee, J. M. *et al.* Nutrient-sensing nuclear receptors coordinate autophagy. *Nature* **516**, 112–115 (2014).

200. Byun, S. *et al.* A postprandial FGF19-SHP-LSD1 regulatory axis mediates epigenetic repression of hepatic autophagy. *The EMBO Journal* **36**, 1755–1769 (2017).

201. Ide, T. *et al.* SREBPs suppress IRS-2-mediated insulin signalling in the liver. *Nature Cell Biology* **6**, 351–357 (2004).

202. Titchenell, P. M., Lazar, M. A. & Birnbaum, M. J. Unraveling the Regulation of Hepatic Metabolism by Insulin. *Trends in Endocrinology & Metabolism* **28**, 497–505 (2017).

203. Titchenell, P. M. *et al.* Direct Hepatocyte Insulin Signaling Is Required for Lipogenesis but Is Dispensable for the Suppression of Glucose Production. *Cell Metabolism* **23**, 1154–1166 (2016).

204. Boden, G. *et al.* Comparison of In Vivo Effects of Insulin on SREBP-1c Activation and INSIG-1/2 in Rat Liver and Human and Rat Adipose Tissue. *Obesity (Silver Spring)* **21**, 1208–1214 (2013).

205. Michael, M. D. *et al.* Loss of Insulin Signaling in Hepatocytes Leads to Severe Insulin Resistance and Progressive Hepatic Dysfunction. *Molecular Cell* **6**, 87–97 (2000).

206. Lu, M. *et al.* Insulin regulates liver metabolism in vivo in the absence of hepatic Akt and Foxo1. *Nature Medicine* **18**, 388–395 (2012).

207. Capuani, B. *et al.* Liver protein profiles in insulin receptor-knockout mice reveal novel molecules involved in the diabetes pathophysiology. *Am. J. Physiol. Endocrinol. Metab.* **308**, E744-755 (2015).

208. Tsuchida, A. *et al.* Insulin/Foxo1 Pathway Regulates Expression Levels of Adiponectin Receptors and Adiponectin Sensitivity. *J. Biol. Chem.* **279**, 30817–30822 (2004).

209. Kubota, N. *et al.* Differential hepatic distribution of insulin receptor substrates causes selective insulin resistance in diabetes and obesity. *Nat Commun* **7**, 12977 (2016).

210. Markan, K. R. *et al.* Circulating FGF21 Is Liver Derived and Enhances Glucose Uptake During Refeeding and Overfeeding. *Diabetes* **63**, 4057–4063 (2014).

211. Panda, S. *et al.* Coordinated transcription of key pathways in the mouse by the circadian clock. *Cell* **109**, 307–320 (2002).

212. Storch, K.-F. *et al.* Extensive and divergent circadian gene expression in liver and heart. *Nature* **417**, 78–83 (2002).

213. Li, H. *et al.* Endogenous circadian time genes expressions in the liver of mice under constant darkness. *BMC Genomics* **21**, 224 (2020).

214. Menet, J. S., Pescatore, S. & Rosbash, M. CLOCK:BMAL1 is a pioneer-like transcription factor. *Genes Dev* **28**, 8–13 (2014).

215. Lee, Y. J., Han, D. H., Pak, Y. K. & Cho, S. H. Circadian regulation of low density lipoprotein receptor promoter activity by CLOCK/BMAL1, Hes1 and Hes6. *Exp. Mol. Med.* **44**, 642–652 (2012).

216. Doi, R., Oishi, K. & Ishida, N. CLOCK regulates circadian rhythms of hepatic glycogen synthesis through transcriptional activation of Gys2. *J. Biol. Chem.* **285**, 22114–22121 (2010).

217. Dang, F. *et al.* Insulin post-transcriptionally modulates Bmal1 protein to affect the hepatic circadian clock. *Nat Commun* **7**, 12696 (2016).

218. Sun, X. *et al.* Glucagon-CREB/CRTC2 signaling cascade regulates hepatic BMAL1 protein. *J. Biol. Chem.* **290**, 2189–2197 (2015).

219. Kinouchi, K. *et al.* Fasting Imparts a Switch to Alternative Daily Pathways in Liver and Muscle. *Cell Reports* **25**, 3299-3314.e6 (2018).

220. Zani, F. *et al.* PER2 promotes glucose storage to liver glycogen during feeding and acute fasting by inducing Gys2 PTG and G L expression. *Mol Metab* **2**, 292–305 (2013).

221. Carvas, J. M. *et al.* Period2 gene mutant mice show compromised insulin-mediated endothelial nitric oxide release and altered glucose homeostasis. *Front Physiol* **3**, 337 (2012).

222. Tong, X. *et al.* DDB1-Mediated CRY1 Degradation Promotes FOXO1-Driven Gluconeogenesis in Liver. *Diabetes* **66**, 2571–2582 (2017).

223. Hirota, T. *et al.* Identification of small molecule activators of cryptochrome. *Science* **337**, 1094–1097 (2012).

224. Machicao, F. *et al.* Glucose-Raising Polymorphisms in the Human Clock Gene Cryptochrome 2 (CRY2) Affect Hepatic Lipid Content. *PLoS One* **11**, e0145563 (2016).

225. Lamia, K. A. *et al.* Cryptochromes mediate rhythmic repression of the glucocorticoid receptor. *Nature* **480**, 552–556 (2011).

226. Guillaumond, F., Dardente, H., Giguère, V. & Cermakian, N. Differential control of Bmal1 circadian transcription by REV-ERB and ROR nuclear receptors. *J Biol Rhythms* **20**, 391–403 (2005).

227. Takeda, Y., Jothi, R., Birault, V. & Jetten, A. M. RORγ directly regulates the circadian expression of clock genes and downstream targets in vivo. *Nucleic Acids Res* **40**, 8519–8535 (2012).

228. Feng, D. *et al.* A circadian rhythm orchestrated by histone deacetylase 3 controls hepatic lipid metabolism. *Science* **331**, 1315–1319 (2011).

229. Yin, L. & Lazar, M. A. The orphan nuclear receptor Rev-erbalpha recruits the N-CoR/histone deacetylase 3 corepressor to regulate the circadian Bmal1 gene. *Mol Endocrinol* **19**, 1452–1459 (2005).

230. Cho, H. *et al.* Regulation of circadian behaviour and metabolism by REV-ERB-α and REV-ERB-β. *Nature* **485**, 123–127 (2012).

231. Zhang, Y. *et al.* The hepatic circadian clock fine-tunes the lipogenic response to feeding through RORα/γ. *Genes Dev.* **31**, 1202–1211 (2017).

232. Kim, H., Zheng, Z., Walker, P. D., Kapatos, G. & Zhang, K. CREBH Maintains Circadian Glucose Homeostasis by Regulating Hepatic Glycogenolysis and Gluconeogenesis. *Mol. Cell. Biol.* **37**, (2017).

233. Yang, X. *et al.* Nuclear receptor expression links the circadian clock to metabolism. *Cell* **126**, 801–810 (2006).

234. Kohsaka, A. *et al.* High-fat diet disrupts behavioral and molecular circadian rhythms in mice. *Cell Metab* **6**, 414–421 (2007).

235. Damiola, F. *et al.* Restricted feeding uncouples circadian oscillators in peripheral tissues from the central pacemaker in the suprachiasmatic nucleus. *Genes Dev* **14**, 2950–2961 (2000).

236. Vollmers, C. *et al.* Time of feeding and the intrinsic circadian clock drive rhythms in hepatic gene expression. *Proc. Natl. Acad. Sci. U.S.A.* **106**, 21453–21458 (2009).

237. Tahara, Y. & Shibata, S. Circadian rhythms of liver physiology and disease: experimental and clinical evidence. *Nat Rev Gastroenterol Hepatol* **13**, 217–226 (2016).

238. Hatori, M. *et al.* Time-restricted feeding without reducing caloric intake prevents metabolic diseases in mice fed a high-fat diet. *Cell Metab.* **15**, 848–860 (2012).

239. Sherman, H. *et al.* Timed high-fat diet resets circadian metabolism and prevents obesity. *FASEB J* **26**, 3493–3502 (2012).

240. Chaix, A., Zarrinpar, A., Miu, P. & Panda, S. Time-restricted feeding is a preventative and therapeutic intervention against diverse nutritional challenges. *Cell Metab* **20**, 991–1005 (2014).

241. Chaix, A., Lin, T., Le, H. D., Chang, M. W. & Panda, S. Time-Restricted Feeding Prevents Obesity and Metabolic Syndrome in Mice Lacking a Circadian Clock. *Cell Metabolism* **29**, 303-319.e4 (2019).

242. Wilkinson, M. J. *et al.* Ten-Hour Time-Restricted Eating Reduces Weight, Blood Pressure, and Atherogenic Lipids in Patients with Metabolic Syndrome. *Cell Metab* **31**, 92-104.e5 (2020).

243. Sánchez, J., Palou, A. & Picó, C. Response to Carbohydrate and Fat Refeeding in the Expression of Genes Involved in Nutrient Partitioning and Metabolism: Striking Effects on Fibroblast Growth Factor-21 Induction. *Endocrinology* **150**, 5341–5350 (2009).

244. Suchankova, G. *et al.* Dietary polyunsaturated fatty acids enhance hepatic AMP-activated protein kinase activity in rats. *Biochemical and Biophysical Research Communications* **326**, 851–858 (2005).

245. Castro, H., Pomar, C. A., Picó, C., Sánchez, J. & Palou, A. Cafeteria diet overfeeding in young male rats impairs the adaptive response to fed/fasted conditions and increases adiposity independent of body weight. *International Journal of Obesity* **39**, 430–437 (2015).

246. Fiebig, R. *et al.* Exercise Training Down-Regulates Hepatic Lipogenic Enzymes in Meal-Fed Rats: Fructose versus Complex-Carbohydrate Diets. *J Nutr* **128**, 810–817 (1998).

247. Matsuzaka, T. *et al.* Insulin-Independent Induction of Sterol Regulatory Element-Binding Protein-1c Expression in the Livers of Streptozotocin-Treated Mice. *Diabetes* **53**, 560–569 (2004).

248. Wei, Y., Wang, D., Topczewski, F. & Pagliassotti, M. J. Fructose-mediated stress signaling in the liver: implications for hepatic insulin resistance. *The Journal of Nutritional Biochemistry* **18**, 1–9 (2007).

249. Oarada, M. *et al.* Refeeding with glucose rather than fructose elicits greater hepatic inflammatory gene expression in mice. *Nutrition* **31**, 757–765 (2015).

250. Oarada, M. *et al.* Refeeding with a high-protein diet after a 48 h fast causes acute hepatocellular injury in mice. *British Journal of Nutrition* **107**, 1435–1444 (2012).

251. Wan, X. *et al.* Dietary protein-induced hepatic IGF-1 secretion mediated by PPARγ activation. *PLOS ONE* **12**, e0173174 (2017).

252. Carraro, V. *et al.* Amino Acid Availability Controls TRB3 Transcription in Liver through the GCN2/eIF2α/ATF4 Pathway. *PLOS ONE* **5**, e15716 (2010).

253. Soltis, A. R. *et al.* Hyper- and hypo- nutrition studies of the hepatic transcriptome and epigenome suggest that PPARα regulates anaerobic glycolysis. *Scientific Reports* **7**, 174 (2017).

254. Harten, S. van *et al.* Gene expression of regulatory enzymes involved in the intermediate metabolism of sheep subjected to feed restriction. *animal* **7**, 439–445 (2013).

255. Xu, J. *et al.* The less weight loss due to modest food restriction drove more fat accumulation in striped hamsters refed with high–fat diet. *Hormones and Behavior* **110**, 19–28 (2019).

256. Stelmanska, E., Korczynska, J. & Swierczynski, J. Tissue-specific effect of refeeding after short- and long-term caloric restriction on malic enzyme gene expression in rat tissues. *Acta Biochim. Pol.* **51**, 805–814 (2004).

257. Chen, D. *et al.* Tissue-specific regulation of SIRT1 by calorie restriction. *Genes Dev* **22**, 1753–1757 (2008).

258. Cuthbertson, D. J. *et al.* Dissociation between exercise-induced reduction in liver fat and changes in hepatic and peripheral glucose homoeostasis in obese patients with non-alcoholic fatty liver disease. *Clin Sci (Lond)* **130**, 93–104 (2016).

259. Cho, J. *et al.* Effect of aerobic exercise training on non-alcoholic fatty liver disease induced by a high fat diet in C57BL/6 mice. *J Exerc Nutrition Biochem* **18**, 339–346 (2014).

260. Hu, X. *et al.* Proteomic profile of carbonylated proteins in rat liver: Exercise attenuated oxidative stress may be involved in fatty liver improvement. *PROTEOMICS* **13**, 1755–1764 (2013).

261. Gehrke, N. *et al.* Voluntary exercise in mice fed an obesogenic diet alters the hepatic immune phenotype and improves metabolic parameters – an animal model of life style intervention in NAFLD. *Scientific Reports* **9**, 4007 (2019).

262. Tu, G., Dai, C., Qu, H., Wang, Y. & Liao, B. Role of exercise and rapamycin on the expression of energy metabolism genes in liver tissues of rats fed a high-fat diet. *Molecular Medicine Reports* **22**, 2932–2940 (2020).

263. Alex, S., Boss, A., Heerschap, A. & Kersten, S. Exercise training improves liver steatosis in mice. *Nutr Metab (Lond)* **12**, (2015).

264. Bazhan, N. *et al.* Sex Differences in Liver, Adipose Tissue, and Muscle Transcriptional Response to Fasting and Refeeding in Mice. *Cells* **8**, 1529 (2019).

265. Gustavsson, C. *et al.* Sex-different hepatic glycogen content and glucose output in rats. *BMC Biochemistry* **11**, 38 (2010).

266. Jansson, J. O., Edén, S. & Isaksson, O. Sexual dimorphism in the control of growth hormone secretion. *Endocr Rev* **6**, 128–150 (1985).

267. Zhang, Y., Laz, E. V. & Waxman, D. J. Dynamic, Sex-Differential STAT5 and BCL6 Binding to Sex-Biased, Growth Hormone-Regulated Genes in Adult Mouse Liver. *Molecular and Cellular Biology* **32**, 880–896 (2012).

268. Ellacott, K. L. J., Morton, G. J., Woods, S. C., Tso, P. & Schwartz, M. W. Assessment of feeding behavior in laboratory mice. *Cell Metab* **12**, 10–17 (2010).

269. Ayala, J. E. *et al.* Standard operating procedures for describing and performing metabolic tests of glucose homeostasis in mice. *Dis Model Mech* **3**, 525–534 (2010).

270. Ayala, J. E., Bracy, D. P., McGuinness, O. P. & Wasserman, D. H. Considerations in the design of hyperinsulinemic-euglycemic clamps in the conscious mouse. *Diabetes* **55**, 390–397 (2006).

271. Goldstein, J. L. & Brown, M. S. A Century of Cholesterol and Coronaries: From Plaques to Genes to Statins. *Cell* **161**, 161–172 (2015).

272. Duell, P. B. *et al.* Nonalcoholic Fatty Liver Disease and Cardiovascular Risk: A Scientific Statement From the American Heart Association. *Arteriosclerosis, Thrombosis, and Vascular Biology* **42**, e168–e185 (2022).

273. Lentjes, M. H. *et al.* The emerging role of GATA transcription factors in development and disease. *Expert Reviews in Molecular Medicine* **18**, (2016).

274. Molkentin, J. D., Lin, Q., Duncan, S. A. & Olson, E. N. Requirement of the transcription factor GATA4 for heart tube formation and ventral morphogenesis. *Genes Dev.* **11**, 1061–1072 (1997).

275. Oka, T. *et al.* Cardiac-Specific Deletion of Gata4 Reveals Its Requirement for Hypertrophy, Compensation, and Myocyte Viability. *Circulation Research* **98**, 837–845 (2006).

276. Watt, A. J., Zhao, R., Li, J. & Duncan, S. A. Development of the mammalian liver and ventral pancreas is dependent on GATA4. *BMC Dev Biol* **7**, 37 (2007).

277. Enane, F. O. *et al.* GATA4 loss of function in liver cancer impedes precursor to hepatocyte transition. *J Clin Invest* **127**, 3527–3542 (2017).

278. Arroyo, N. *et al.* GATA4 induces liver fibrosis regression by deactivating hepatic stellate cells. *JCI Insight* **6**, e150059 (2021).

279. Zheng, R. *et al.* Function of GATA Factors in the Adult Mouse Liver. *PLoS One* **8**, e83723 (2013).

280. Winkler, M. *et al.* Endothelial GATA4 controls liver fibrosis and regeneration by preventing a pathogenic switch in angiocrine signaling. *J Hepatol* **74**, 380–393 (2021).

281. Romano, O. & Miccio, A. GATA factor transcriptional activity: Insights from genome-wide binding profiles. *IUBMB Life* **72**, 10–26 (2020).

282. He, A. *et al.* Dynamic GATA4 enhancers shape the chromatin landscape central to heart development and disease. *Nat Commun* **5**, 4907 (2014).

283. Lamina, C., Coassin, S., Illig, T. & Kronenberg, F. Look beyond one's own nose: combination of information from publicly available sources reveals an association of GATA4 polymorphisms with plasma triglycerides. *Atherosclerosis* **219**, 698–703 (2011).

284. Ding, L. *et al.* Identification and functional study of GATA4 gene regulatory variants in type 2 diabetes mellitus. *BMC Endocrine Disorders* **21**, 73 (2021).

285. Chou, W.-C., Chen, W.-T. & Shen, C.-Y. A common variant in 11q23.3 associated with hyperlipidemia is mediated by the binding and regulation of GATA4. *npj Genom. Med.* **7**, 1–10 (2022).

286. Asselbergs, F. W. *et al.* Large-Scale Gene-Centric Meta-analysis across 32 Studies Identifies Multiple Lipid Loci. *The American Journal of Human Genetics* **91**, 823–838 (2012).

287. Bergeron, F., Nadeau, G. & Viger, R. S. GATA4 knockdown in MA-10 Leydig cells identifies multiple target genes in the steroidogenic pathway. *Reproduction* **149**, 245–257 (2015).

288. Schrade, A. *et al.* GATA4 Is a Key Regulator of Steroidogenesis and Glycolysis in Mouse Leydig Cells. *Endocrinology* **156**, 1860–1872 (2015).

289. Patankar, J. V. *et al.* Loss of intestinal GATA4 prevents diet-induced obesity and promotes insulin sensitivity in mice. *Am J Physiol Endocrinol Metab* **300**, E478–E488 (2011).

290. Bideyan, L., Nagari, R. & Tontonoz, P. Hepatic transcriptional responses to fasting and feeding. *Genes Dev.* (2021) doi:10.1101/gad.348340.121.

291. Yang, T. *et al.* Crucial Step in Cholesterol Homeostasis: Sterols Promote Binding of SCAP to INSIG-1, a Membrane Protein that Facilitates Retention of SREBPs in ER. *Cell* **110**, 489–500 (2002).

292. Creyghton, M. P. *et al.* Histone H3K27ac separates active from poised enhancers and predicts developmental state. *Proceedings of the National Academy of Sciences* **107**, 21931–21936 (2010).

293. Repa, J. J. *et al.* Regulation of mouse sterol regulatory element-binding protein-1c gene (SREBP-1c) by oxysterol receptors, LXRα and LXRβ. *Genes Dev.* **14**, 2819–2830 (2000).

294. Repa, J. J. *et al.* Regulation of ATP-binding cassette sterol transporters ABCG5 and ABCG8 by the liver X receptors alpha and beta. *J Biol Chem* **277**, 18793–18800 (2002).

295. Repa, J. J. *et al.* Regulation of Absorption and ABC1-Mediated Efflux of Cholesterol by RXR Heterodimers. *Science* **289**, 1524–1529 (2000).

296. Joseph, S. B. *et al.* Direct and indirect mechanisms for regulation of fatty acid synthase gene expression by liver X receptors. *J Biol Chem* **277**, 11019–11025 (2002).

297. Boergesen, M. *et al.* Genome-Wide Profiling of Liver X Receptor, Retinoid X Receptor, and Peroxisome Proliferator-Activated Receptor α in Mouse Liver Reveals Extensive Sharing of Binding Sites. *Molecular and Cellular Biology* **32**, 852–867 (2012).

298. Francis, G. A. Chapter 15 - High-Density Lipoproteins: Metabolism and Protective Roles Against Atherosclerosis. in *Biochemistry of Lipids, Lipoproteins and Membranes (Sixth Edition)* (eds. Ridgway, N. D. & McLeod, R. S.) 437–457 (Elsevier, 2016). doi:10.1016/B978-0-444-63438-2.00015-8.

299. Venkateswaran, A. *et al.* Control of cellular cholesterol efflux by the nuclear oxysterol receptor LXRα. *Proceedings of the National Academy of Sciences* **97**, 12097–12102 (2000).

300. Battle, M. A. *et al.* GATA4 Is Essential for Jejunal Function in Mice. *Gastroenterology* **135**, 1676-1686.e1 (2008).

301. Lian, J., Nelson, R. & Lehner, R. Carboxylesterases in lipid metabolism: from mouse to human. *Protein Cell* **9**, 178–195 (2018).

302. Back, S. S. *et al.* Cooperative transcriptional activation of ATP-binding cassette sterol transporters ABCG5 and ABCG8 genes by nuclear receptors including Liver-X-Receptor. *BMB Rep* **46**, 322–327 (2013).

303. Sumi, K. *et al.* Cooperative Interaction between Hepatocyte Nuclear Factor 4α and GATA Transcription Factors Regulates ATP-Binding Cassette Sterol Transporters ABCG5 and ABCG8. *Mol Cell Biol* **27**, 4248–4260 (2007).

304. Watt, A. J., Battle, M. A., Li, J. & Duncan, S. A. GATA4 is essential for formation of the proepicardium and regulates cardiogenesis. *Proceedings of the National Academy of Sciences* **101**, 12573–12578 (2004).

305. Bideyan, L. *et al.* Integrative analysis reveals multiple modes of LXR transcriptional regulation in liver. *PNAS* **119**, (2022).

306. Buenrostro, J. D., Wu, B., Chang, H. Y. & Greenleaf, W. J. ATAC-seq: A Method for Assaying Chromatin Accessibility Genome-Wide. *Current Protocols in Molecular Biology* **109**, 21.29.1-21.29.9 (2015).

307. Ferrari, A. *et al.* HDAC3 is a molecular brake of the metabolic switch supporting white adipose tissue browning. *Nat Commun* **8**, 93 (2017).

308. Dobin, A. *et al.* STAR: ultrafast universal RNA-seq aligner. *Bioinformatics* **29**, 15–21 (2013).

309. Langmead, B. & Salzberg, S. L. Fast gapped-read alignment with Bowtie 2. *Nat Methods* **9**, 357–359 (2012).

310. Li, H. *et al.* The Sequence Alignment/Map format and SAMtools. *Bioinformatics* **25**, 2078–2079 (2009).

311. Zhang, Y. *et al.* Model-based analysis of ChIP-Seq (MACS). *Genome Biol* **9**, R137 (2008).

312. Robinson, M. D., McCarthy, D. J. & Smyth, G. K. edgeR: a Bioconductor package for differential expression analysis of digital gene expression data. *Bioinformatics* **26**, 139–140 (2010).

313. Ross-Innes, C. S. *et al.* Differential oestrogen receptor binding is associated with clinical outcome in breast cancer. *Nature* **481**, 389–393 (2012).

314. Heinz, S. *et al.* Simple combinations of lineage-determining transcription factors prime cis-regulatory elements required for macrophage and B cell identities. *Mol Cell* **38**, 576–589 (2010).

315. Robinson, J. T. *et al.* Integrative genomics viewer. *Nat Biotechnol* **29**, 24–26 (2011).

316. Metsalu, T. & Vilo, J. ClustVis: a web tool for visualizing clustering of multivariate data using Principal Component Analysis and heatmap. *Nucleic Acids Res* **43**, W566–W570 (2015).

317. Chen, E. Y. *et al.* Enrichr: interactive and collaborative HTML5 gene list enrichment analysis tool. *BMC Bioinformatics* **14**, 128 (2013).

318. Subramanian, A. *et al.* Gene set enrichment analysis: A knowledge-based approach for interpreting genome-wide expression profiles. *Proceedings of the National Academy of Sciences* **102**, 15545–15550 (2005).

319. Ramírez, F. *et al.* deepTools2: a next generation web server for deep-sequencing data analysis. *Nucleic Acids Research* **44**, W160–W165 (2016).

320. Bligh, E. G. & Dyer, W. J. A rapid method of total lipid extraction and purification. *Can J Biochem Physiol* **37**, 911–917 (1959).

321. Priest, C. *et al.* Brap regulates liver morphology and hepatocyte turnover via modulation of the Hippo pathway. *Proceedings of the National Academy of Sciences* **119**, e2201859119 (2022).

322. Mehlem, A., Hagberg, C. E., Muhl, L., Eriksson, U. & Falkevall, A. Imaging of neutral lipids by oil red O for analyzing the metabolic status in health and disease. *Nat Protoc* **8**, 1149–1154 (2013).

323. Willecke, F., Scerbo, D., Nagareddy, P., Obunike, J. C. & Barrett, T. J. Hepatic VLDL secretion assay. *protocols.io* https://www.protocols.io/view/hepatic-vldl-secretion-assay-izxcf7n (2017).

324. Collins, J. L. *et al.* Identification of a nonsteroidal liver X receptor agonist through parallel array synthesis of tertiary amines. *J Med Chem* **45**, 1963–1966 (2002).

325. Demeure, O. *et al.* Regulation of LPCAT3 by LXR. *Gene* **470**, 7–11 (2011).

326. Rong, X. *et al.* LXRs regulate ER stress and inflammation through dynamic modulation of membrane phospholipid composition. *Cell Metab* **18**, 685–697 (2013).

327. Zelcer, N., Hong, C., Boyadjian, R. & Tontonoz, P. LXR regulates cholesterol uptake through Idol-dependent ubiquitination of the LDL receptor. *Science* **325**, 100–104 (2009).

328. Venkateswaran, A. *et al.* Control of cellular cholesterol efflux by the nuclear oxysterol receptor LXR alpha. *Proc Natl Acad Sci U S A* **97**, 12097–12102 (2000).

329. Chiang, J. Y., Kimmel, R. & Stroup, D. Regulation of cholesterol 7alpha-hydroxylase gene (CYP7A1) transcription by the liver orphan receptor (LXRalpha). *Gene* **262**, 257–265 (2001).

330. Joseph, S. B. *et al.* LXR-Dependent Gene Expression Is Important for Macrophage Survival and the Innate Immune Response. *Cell* **119**, 299–309 (2004).

331. Shibata, N. & Glass, C. K. Macrophages, oxysterols and atherosclerosis. *Circ J* **74**, 2045–2051 (2010).

332. Zelcer, N. & Tontonoz, P. Liver X receptors as integrators of metabolic and inflammatory signaling. *J Clin Invest* **116**, 607–614 (2006).

333. Endo-Umeda, K. & Makishima, M. Liver X Receptors Regulate Cholesterol Metabolism and Immunity in Hepatic Nonparenchymal Cells. *Int J Mol Sci* **20**, E5045 (2019).

334. Scott, C. L. *et al.* The Transcription Factor ZEB2 Is Required to Maintain the Tissue-Specific Identities of Macrophages. *Immunity* **49**, 312-325.e5 (2018).

335. Sakai, M. *et al.* Liver-Derived Signals Sequentially Reprogram Myeloid Enhancers to Initiate and Maintain Kupffer Cell Identity. *Immunity* **51**, 655-670.e8 (2019).

336. Janowski, B. A., Willy, P. J., Devi, T. R., Falck, J. R. & Mangelsdorf, D. J. An oxysterol signalling pathway mediated by the nuclear receptor LXRα. *Nature* **383**, 728–731 (1996).

337. Moldavski, O. *et al.* 4β-Hydroxycholesterol is a prolipogenic factor that promotes SREBP1c expression and activity through the liver X receptor. *J Lipid Res* **62**, 100051 (2021).

338. Yang, C. *et al.* Sterol Intermediates from Cholesterol Biosynthetic Pathway as Liver X Receptor Ligands *. *Journal of Biological Chemistry* **281**, 27816–27826 (2006).

339. Fu, X. *et al.* 27-hydroxycholesterol is an endogenous ligand for liver X receptor in cholesterol-loaded cells. *J Biol Chem* **276**, 38378–38387 (2001).

340. Peet, D. J. *et al.* Cholesterol and Bile Acid Metabolism Are Impaired in Mice Lacking the Nuclear Oxysterol Receptor LXRα. *Cell* **93**, 693–704 (1998).

341. Zhang, Y. *et al.* Liver LXRα expression is crucial for whole body cholesterol homeostasis and reverse cholesterol transport in mice. *J Clin Invest* **122**, 1688–1699 (2012).

342. Ducheix, S. *et al.* A systems biology approach to the hepatic role of the oxysterol receptor LXR in the regulation of lipogenesis highlights a cross-talk with PPARα. *Biochimie* **95**, 556–567 (2013).

343. Russo-Savage, L. & Schulman, I. G. Liver X receptors and liver physiology. *Biochimica et Biophysica Acta (BBA) - Molecular Basis of Disease* **1867**, 166121 (2021).

344. Joseph, S. B. *et al.* Synthetic LXR ligand inhibits the development of atherosclerosis in mice. *Proc Natl Acad Sci U S A* **99**, 7604–7609 (2002).

345. Laffitte, B. A. *et al.* Activation of liver X receptor improves glucose tolerance through coordinate regulation of glucose metabolism in liver and adipose tissue. *Proc Natl Acad Sci U S A* **100**, 5419–5424 (2003).

346. Schultz, J. R. *et al.* Role of LXRs in control of lipogenesis. *Genes Dev.* **14**, 2831–2838 (2000).

347. Ramón-Vázquez, A. *et al.* Common and Differential Transcriptional Actions of Nuclear Receptors Liver X Receptors α and β in Macrophages. *Molecular and Cellular Biology* **39**, e00376-18.

348. Willy, P. J. *et al.* LXR, a nuclear receptor that defines a distinct retinoid response pathway. *Genes Dev.* **9**, 1033–1045 (1995).

349. Nagy, G. & Nagy, L. Motif grammar: The basis of the language of gene expression. *Computational and Structural Biotechnology Journal* **18**, 2026–2032 (2020).

350. Feldmann, R. *et al.* Genome-wide analysis of LXRα activation reveals new transcriptional networks in human atherosclerotic foam cells. *Nucleic Acids Research* **41**, 3518–3531 (2013).

351. Yan, F., Powell, D. R., Curtis, D. J. & Wong, N. C. From reads to insight: a hitchhiker's guide to ATAC-seq data analysis. *Genome Biology* **21**, 22 (2020).

352. Kain, J. *et al.* Pioneer factor Foxa2 enables ligand-dependent activation of type II nuclear receptors FXR and LXRα. *Molecular Metabolism* **53**, 101291 (2021).

353. Yoshikawa, T. *et al.* Identification of Liver X Receptor-Retinoid X Receptor as an Activator of the Sterol Regulatory Element-Binding Protein 1c Gene Promoter. *Mol Cell Biol* **21**, 2991–3000 (2001).

354. Chapski, D. J., Rosa-Garrido, M., Hua, N., Alber, F. & Vondriska, T. M. Spatial Principles of Chromatin Architecture Associated With Organ-Specific Gene Regulation. *Front Cardiovasc Med* **5**, 186 (2019).

355. Salisbury, D. A. *et al.* Transcriptional regulation of N6-methyladenosine orchestrates sex-dimorphic metabolic traits. *Nat Metab* **3**, 940–953 (2021).

356. Li, Q., Brown, J. B., Huang, H. & Bickel, P. J. Measuring reproducibility of high-throughput experiments. *The Annals of Applied Statistics* **5**, 1752–1779 (2011).

357. Li, Z. *et al.* Identification of transcription factor binding sites using ATAC-seq. *Genome Biology* **20**, 45 (2019).

358. Naik, S. U. *et al.* Pharmacological Activation of Liver X Receptors Promotes Reverse Cholesterol Transport In Vivo. *Circulation* **113**, 90–97 (2006).

359. Lee, S. D. & Tontonoz, P. Liver X receptors at the intersection of lipid metabolism and atherogenesis. *Atherosclerosis* **242**, 29–36 (2015).

360. Endo-Umeda, K., Nakashima, H., Umeda, N., Seki, S. & Makishima, M. Dysregulation of Kupffer Cells/Macrophages and Natural Killer T Cells in Steatohepatitis in LXRα Knockout Male Mice. *Endocrinology* **159**, 1419–1432 (2018).

361. Endo-Umeda, K. *et al.* Liver X receptors regulate hepatic F4/80 + CD11b+ Kupffer cells/macrophages and innate immune responses in mice. *Sci Rep* **8**, 9281 (2018).

362. Xing, Y., Zhao, T., Gao, X. & Wu, Y. Liver X receptor α is essential for the capillarization of liver sinusoidal endothelial cells in liver injury. *Sci Rep* **6**, 21309 (2016).

363. Beaven, S. W. *et al.* Liver X Receptor Signaling Is a Determinant of Stellate Cell Activation and Susceptibility to Fibrotic Liver Disease. *Gastroenterology* **140**, 1052–1062 (2011).

364. Siersbæk, R. *et al.* Transcription Factor Cooperativity in Early Adipogenic Hotspots and Super-Enhancers. *Cell Reports* **7**, 1443–1455 (2014).

365. Chapski, D. J. *et al.* Early adaptive chromatin remodeling events precede pathologic phenotypes and are reinforced in the failing heart. *Journal of Molecular and Cellular Cardiology* **160**, 73–86 (2021).

366. Oldfield, A. J. *et al.* Histone-Fold Domain Protein NF-Y Promotes Chromatin Accessibility for Cell Type-Specific Master Transcription Factors. *Molecular Cell* **55**, 708–722 (2014).

367. Schmidt, S. F. *et al.* Acute TNF-induced repression of cell identity genes is mediated by NFκB-directed redistribution of cofactors from super-enhancers. *Genome Res* **25**, 1281–1294 (2015).

368. Step, S. E. *et al.* Anti-diabetic rosiglitazone remodels the adipocyte transcriptome by redistributing transcription to PPARγ-driven enhancers. *Genes Dev* **28**, 1018–1028 (2014).

369. Guertin, M. J., Zhang, X., Coonrod, S. A. & Hager, G. L. Transient estrogen receptor binding and p300 redistribution support a squelching mechanism for estradiol-repressed genes. *Mol Endocrinol* **28**, 1522–1533 (2014).

370. Schmidt, S. F., Larsen, B. D., Loft, A. & Mandrup, S. Cofactor squelching: Artifact or fact? *BioEssays* **38**, 618–626 (2016).

371. Andrew, S. Babraham Bioinformatics - FastQC A Quality Control tool for High Throughput Sequence Data. (2010).

372. Love, M. I., Huber, W. & Anders, S. Moderated estimation of fold change and dispersion for RNA-seq data with DESeq2. *Genome Biology* **15**, 550 (2014).

373. R Core Team. R: A language and environment for statistical computing. (2021).

374. Durinck, S., Spellman, P. T., Birney, E. & Huber, W. Mapping identifiers for the integration of genomic datasets with the R/Bioconductor package biomaRt. *Nat Protoc* **4**, 1184–1191 (2009).

375. Huang, R. *et al.* The NCATS BioPlanet – An Integrated Platform for Exploring the Universe of Cellular Signaling Pathways for Toxicology, Systems Biology, and Chemical Genomics. *Frontiers in Pharmacology* **10**, 445 (2019).

376. Lachmann, A. *et al.* ChEA: transcription factor regulation inferred from integrating genome-wide ChIP-X experiments. *Bioinformatics* **26**, 2438–2444 (2010).

377. Bryois, J. *et al.* Evaluation of chromatin accessibility in prefrontal cortex of individuals with schizophrenia. *Nat Commun* **9**, 3121 (2018).

378. Martin, M. Cutadapt removes adapter sequences from high-throughput sequencing reads. *EMBnet.journal* **17**, 10–12 (2011).

379. SeqMonk Mapped Sequence Analysis Tool.

380. Yu, G., Wang, L.-G. & He, Q.-Y. ChIPseeker: an R/Bioconductor package for ChIP peak annotation, comparison and visualization. *Bioinformatics* **31**, 2382–2383 (2015).

381. Castro-Mondragon, J. A. *et al.* JASPAR 2022: the 9th release of the open-access database of transcription factor binding profiles. *Nucleic Acids Research* gkab1113 (2021) doi:10.1093/nar/gkab1113.

382. Oki, S. *et al.* ChIP-Atlas: a data-mining suite powered by full integration of public ChIP-seq data. *EMBO Rep* **19**, e46255 (2018).

383. Seo, Y.-K. *et al.* Genome-wide localization of SREBP-2 in hepatic chromatin predicts a role in autophagy. *Cell Metab* **13**, 367–375 (2011).